5-2014

A Qualitative Experimental Study of Drag Reduction Devices for Tractor Trailers with Ground Effects

Nicolas Robert Reed
University of Tennessee - Knoxville, nreed3@utk.edu

To the Graduate Council:

I am submitting herewith a thesis written by Nicolas Robert Reed entitled "A Qualitative Experimental Study of Drag Reduction Devices for Tractor Trailers with Ground Effects." I have examined the final electronic copy of this thesis for form and content and recommend that it be accepted in partial fulfillment of the requirements for the degree of Master of Science, with a major in Mechanical Engineering.

Ahmad Vakili, Major Professor

We have read this thesis and recommend its acceptance:

Trevor Moeller, Reza Abeda

Accepted for the Council:
Carolyn R. Hodges

Vice Provost and Dean of the Graduate School

(Original signatures are on file with official student records.)

A Qualitative Experimental Study of Drag Reduction Devices for Tractor Trailers with Ground Effects

A Thesis Presented for the
Master of Science
Degree
The University of Tennessee, Knoxville

Nicolas Robert Reed
May 2014

ABSTRACT

This is an experimental qualitative study of how drag reduction devices affect air flow around a tractor trailer. A 1/32 scale detail model of a truck with its trailer was used for testing in a 20"x14" low speed wind tunnel at the University of Tennessee Space Institute. Major modifications were made to the wind tunnel so that it would include a moving bed (floor) section for ground effect simulation. This was done to accurately simulate relative ground movement with the truck being held stationary in the tunnel flow.

Drag reduction devices were designed based on aerodynamic fundamental understanding for streamlining the various zones of the truck readily available for flow path modifications or flow management around the truck. The drag reduction devices were fabricated using a desktop 3D printer. Flow visualization was performed using sewing (twisted) string as tufts to validate if there were any flow improvement effectiveness as a result the flow management devices. A total of 102 tests were performed. This was done using 24 unique drag reduction devices, which were tested in 28 different configurations. Wind tunnel speed was in the range of 55 to 70 PMH at a corresponding tunnel unit Reynolds number of 5.6*10^5 to 7.12*10^5. Observations show that each device affects the flow, locally, and that an overall change in aerodynamic efficiency (drag reduction) can be achieved by the addition of a number of these devices.

Test results from this investigation showed that the addition of drag reduction devices did change flow paths under the tractor trailer and did provide methods for managing flow under the trailer. A possible novel method for addressing the wake zone behind the tractor trailer, by addition of drag reduction devices installed under the trailer, was also investigated.

Quantitative measurements are needed to determine the overall and individual contributions, and to select the best configuration of a number of configurations for maximum level of drag reduction.

TABLE OF CONTENTS

LIST OF TABLES

LIST OF FIGURES

CHAPTER I
INTRODUCTION AND GENERAL INFORMATION

Introduction

The majority of commercial freight shipping in the US is performed by tractor trailers. In 2002 11.7 million tons of a total 18.9 million tons of freight were shipped by truck [table 1 – Commercial Freight activity in the United States]. The cost of diesel fuel has a direct effect on the cost effectiveness of this mode of transportation. The aerodynamic drag effects on the tractor trailer directly affect the fuel economy of this mode of transportation.

In 2011 heavy trucks (tractor trailers) traveled 163.7 billion miles, and used 28.2 billion gallons of fuel with an average fuel economy of 5.8 miles per gallon. [table 5.2 Transportation Energy Data Book Edition 32]. Sixty-five percent of energy used by a truck is used to overcome aerodynamic drag, when traveling at 70 miles per hour [Seifert, 2008 and Doyle, 2008]. A modest decrease in tractor trailer aerodynamic drag of 10% would have an annual fuel savings 1.8 billion gallons.

Beyond the economy of improving fuel efficiency, other incentives exist to implement these improvements. Specifically the state of California Air Advisory Board has dictated that drag reduction devices that result in a fuel savings of 5% be installed on tractor trailers operating in the state of California (http://www.arb.ca.gov/cc/hdghg/technologies.htm). Because California has the largest volume of freight shipments in the U.S., 11.5% of the national total [RITA – State Transportation Facts], this requirement more or less makes the installation of drag reduction devices required for the majority of interstate trucking tractor trailers.

Purpose

The purpose of this study is to discover possible drag reduction devices for tractor trailers. The specific area of interest is under the trailer of the truck.

Approach

Testing was conducted at the UTSI 20”x14” wind tunnel. In order to accurately simulate the effects of driving over a road, this wind tunnel was modified to include a moving bed. A 1/32 scale model of a tractor trailer was modified and placed in the wind tunnel. A Makerbot Replicator desktop 3D printer was used to fabricate a variety of the different drag reduction devices. Tufts where installed on the model and the drag reduction devices to provide flow visualization. Comparisons were made between photographs of the model with the drag reduction devices installed and the unmodified model to determine which devices are useful in reducing drag.

CHAPTER II
LITERATURE REVIEW

Literature Review of Moving Ground

The area of concern for this study is the area under the trailer. For vehicle wind tunnel testing Hoerner in **Fluid-Dynamic Drag** states that;

"The most perfect reproduction of the road surface in a wind tunnel is through the use of a belt, moving at proper distance (close to the wheels) under the model, in the same direction and with the same speed as the artificial flow." [Horerner, 1965]

Stone from **Automotive Engineering Fundamentals** states;

"Any tests that are designed to reveal the true drag and lift forces must take into account the ground effect, and the only way that this can be modeled properly is by having a moving ground plane." [Stone, 2004]

In order to provide an accurate and realistic simulation of tractor trailer driving over a road, a moving belt would need to be installed in the UTSI wind tunnel.

The majority of wind tunnel testing of drag reduction devices used models installed on the floor of a wind tunnel. A few generic studies have incorporated a moving belt in to the analysis of wheel wells and areas under a vehicle. However these studies were for a general vehicle features and not for a tractor trailer. Buckley has shown that wind tunnel results of a drag reduction device do not exactly correlate to full scale testing a device installed on a tractor trailer being driven on a highway [Buckley, 1978]. Several explanations can be given for this, including variable operating speeds, changes in local wind speeds, and changes in terrain grade. One issue that could be addressed in the wind tunnel is the effect of a vehicle traveling over a road. By installing a moving belt underneath the model two situations can be studied. The first is the elimination of the boundary layer that develops at the tunnel floor. The second is the wheel of the model can be made to rotate by being in contact with the moving belt.

One of the major concerns of this testing is addressing the interaction of the vehicle boundary layer and the road. A boundary layer is defined as a layer of fluid in vicinity of a bounding surface; eg, layer of air surrounding a body moving through the atmosphere [Gunston, 2009]. When a truck drives down a road, only one boundary layer is present, originating at the truck. In a wind tunnel with solid walls, boundary layers will be present at all of the wind tunnel surfaces, and at the model.

For the elimination of the boundary layer originating from the tunnel floor see figure 1. The figure shows that two sets of boundary layers will be present in the wind tunnel, those originating from the tunnel walls and those originating from the model. The specific boundary layers labeled “model lower boundary layer” and “tunnel floor boundary layer” will interfere with each other and form a confluence. This will occur in the area of study, under the trailer.

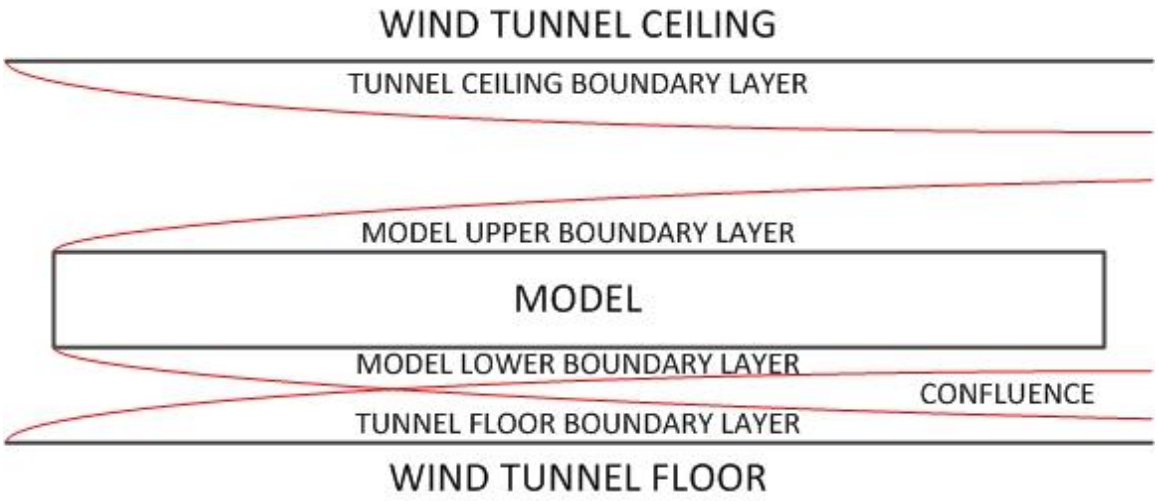

Figure 1: Boundary layers with a stationary floor.

To eliminate the tunnel floor boundary layer, a moving belt was installed in place of the tunnel floor. Assuming the belt is moving at the same speed as the air velocity, a boundary layer at the tunnel floor cannot form. This will effectively result in the conditions seen in figure 2. In addition to the boundary layer effect, the moving floor also forces the wheels to rotate which help generate the wheel flow effects. However, this is normally done separately, as the scaling factors are complicated to be mixed, if combined with the main truck body flow field.

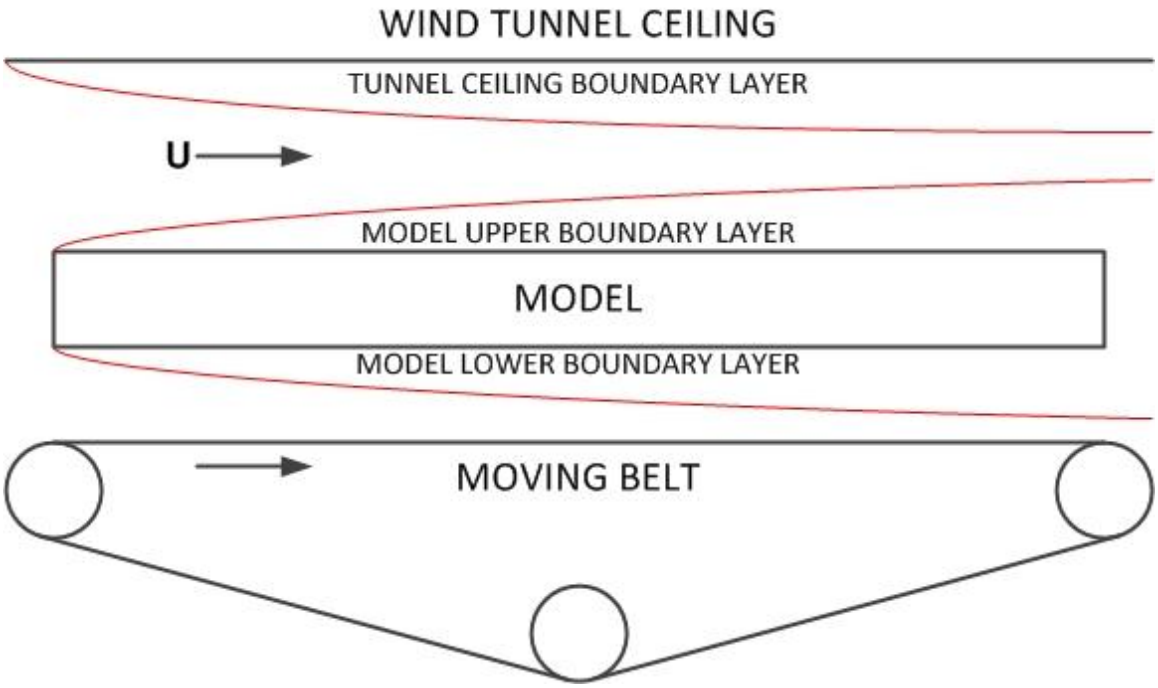

Figure 2: Boundary layers with a moving ground.

Literature Review of Scale Model Testing

The argument for using a scale model is cost. By using a scale model, modifications can be made at a fraction of a cost to a prototype. The justification that data collected from a scale model can be found by dimensional analysis. This can be accomplished by the Buckingham pi Theorem [White, 1999], as shown:

The drag coefficient is a function of the model height, model width, model length, the air viscosity, the air density, and the wind speed:

$$D = f(h, w, l, \mu, \rho, V)$$

Variable	D	h	w	l	μ	ρ	V
Dimension	MLT^{-2}	L	L	L	$ML^{-1}T^{-1}$	ML^{-3}	LT^{-1}

The following variables are shown for the first pi group:

$$\Pi_1 = Dl^a V^b \rho^c$$

$$(MLT^{-2})(L)^a (LT^{-1})^b (ML^{-3})^c = M^0 L^0 T^0$$

$$1 + c = 0$$

$$1 + a + b - 3c = 0$$

$$-2 - b = 0$$

$$\Pi_1 = \frac{D}{w^2 V^2 \rho}$$

The following variables are chosen for the second pi group:

$$\Pi_2 = hwl^a V^b \rho^c$$

$$(L^2)(L)^a (LT^{-1})^b (ML^{-3})^c = M^0 L^0 T^0$$

$$c = 0$$

$$2 + a + b - 3c = 0$$

$$b = 0$$

$$\Pi_2 = \frac{l^2}{hw}$$

The following variables are chosen for the third pi group:

$$\Pi_3 = \mu l^a V^b \rho^c$$

$$(ML^{-1}T^{-1})(L)^a (LT^{-1})^b (ML^{-3})^c = M^0 L^0 T^0$$

$$1 + c = 0$$

$$-1 + a + b - 3c = 0$$

$$-1 - b = 0$$

$$\Pi_3 = \frac{\mu}{lV\rho}$$

$$\Pi_1 = \frac{D}{w^2 V^2 \rho} = \frac{(F)}{(L)^2 (LT^{-1})^2 (FL^{-4}T^2)} = F^0 L^0 T^0$$

$$\Pi_2 = \frac{l^2}{hw} = \frac{(L^2)}{(L^2)} = F^0 L^0 T^0$$

$$\Pi_3 = \frac{\mu}{lV\rho} = \frac{(FL^{-2}T)}{(L)(LT^{-1})(FL^{-4}T^2)} = F^0 L^0 T^0$$

The pi groups are combined to show the relationship between the variables:

$$\frac{D}{w^2V^2\rho} = \phi\left(\frac{l^2}{hw}, \frac{\mu}{lV\rho}\right)$$

This relationship is rearranged to get more familiar terms:

$$\frac{D}{w^2\rho V^2} = \phi\left(\frac{wh}{l^2}, \frac{lV\rho}{\mu}\right)$$

This shows that drag is a function of the ratio of the model cross sectional area over the length of the model squared wh/l^2 and the Reynolds number, $lV\rho/\mu$. For the specific relationship between the Reynolds number and drag coefficient, Horner has shown the relationship to be minimal [Horerner, 1965]. See figure 3 for Horner's experimental results.

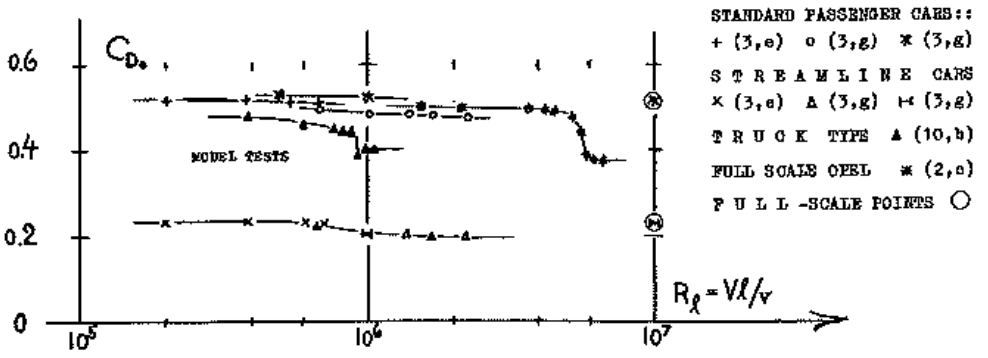

Drag of several automobile shapes (mostly tested in wind tunnels) as a function of Reynolds number.

Figure 3: The relationship between drag coefficient and Reynolds number [Horerner, 1965].

Literature Review of Ground Vehicle Drag

For a tractor trailer drag is the retarding force acting upon a body in relative to the direction of motion [Gunston, 2009]. Drag is composed of two parts, rolling resistance and aerodynamic drag. Rolling resistance is the force acting against the forward motion of the tractor trailer imparted by the tires interacting with the road. This force is beyond this study. Aerodynamic drag, the main area of interest of this study, is primarily made up of two components, skin friction drag and pressure drag [Stone, 2004].

Skin friction drag is defined as drag due to all forces tangential to surface, notably shearing of boundary layer [Gunston, 2009].

Pressure drag is defined as drag due to the sum of all forces normal to surface resolved along free-stream direction [Gunston, 2009].

One of the main areas of concern of ground vehicle aerodynamics is flow separation. Separation is defined as the breakdown of attached fluid flow around a body into gross turbulence, occurring at a particular place (separation point) [Gunston, 2009]. This separation prevents a further rise in pressure and thus an increase in pressure drag [Stone, 2004]. For a tractor trailer this flow separation at the rear of the trailer results in a wake behind the vehicle.

An effective method of dealing with flow separation is streamlining the vehicle. This can be achieved by two methods. The first is rounding corners. The second is extending surface areas. Hoerner has shown effects of streamline in the following figure (figure 4).

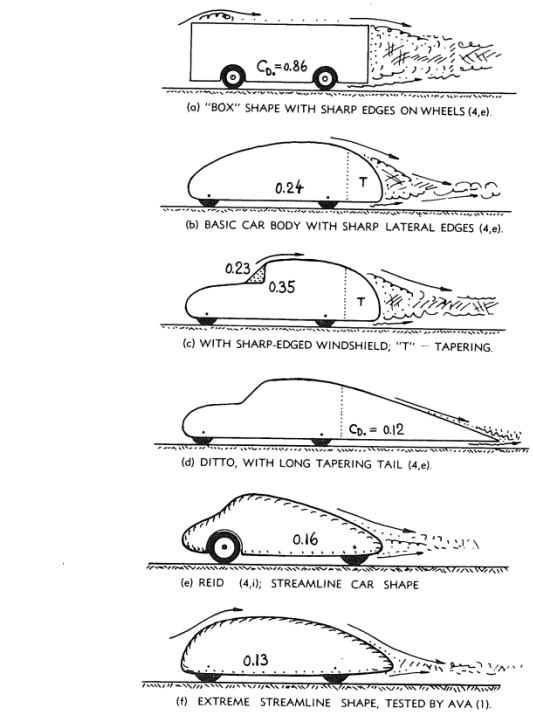

Drag coefficients of several smooth wind tunnel models (tested over fixed ground plate).

Figure 4: Hoerner's examples of streamlining [Horerner, 1965].

Figure 3 shows the dramatic effect on drag by adding a boat-tail to the vehicle. A boat tail is defined as a rear portion of aerodynamic body tapered to reduce drag. Taper angle must be gentle to avoid breakaway [Gunston, 2009]'

Understanding the wake zone behind an object can found by observing a rectangular column in a fluid flow. For a rectangular column in a steady flow, a wake will occur downstream of the column. This is caused by flow separation beginning at the end of the object. Behind the aft of the column is a low pressure zone. This low pressure zone imparts a force on the column in the direction of the fluid flow. This is one of the most significant causes of drag on an aerodynamic object [Horerner, 1965]. By streamlining the object drag can be significantly reduced, since both the region of low pressure and the pressure can be reduced and increased, respectively.

Eliminating the wake behind an object can significantly decrease the drag of an object. This can be achieved by adding a boat tail to the aft end of the device. How the boat tail reduces drag is twofold. First, the boat tail increases the distance before flow separation occurs. Second the boat tail eliminates the low pressure zone behind the object. This is done by physically occupying the space where this low pressure zone would be.

Literature Review of Previous Tractor Trailer Drag Reduction Device Studies

Side Skirts

The area underneath the trailer is an area of this investigation for the following reason, this area is of little value to a tractor trailer driver. For this reason, this area is an ideal place to install a drag reduction device because it will not affect the operation of the tractor trailer. The current method of reducing drag under the trailer is by the installation of side skirts. Previous studies have shown that side skirts can and do result in a reduction of drag [Ortega 2004, Storms 2004, Mokhtar 2012]. However, these studies have shown that the addition of these skirts has a relatively small effect on the drag of tractor trailer.

Behind Trailer

Some of the most significant reduction in drag of a tractor trailer can be achieved by the installation of a boat tail behind the tractor trailer [Salari, 2004 and Ortega 2004]. Computation fluid dynamic analysis have shown that an unmodified tractor trailer has a large wake behind it [Christoffersen, 2008, Ghuge, 2006, Doyle, 2008, Veluri, 2007], and this has been correlated with wind tunnel testing [Veluri, 2006].

The majority of drag reduction device that have been designed to address this issue are boat tails installed behind the trailer doors [Storms 2004, Ortega 2004]. These devices work by either filling in the wake region with a volume or modifying the vortex shedding behind the trailer. These devices become impractical to use in real world situations because they add length to the vehicle or hinder the operation of the trailer doors. Adding length to a vehicle that already is at the legal length limit cannot be done. Installing a device that would hinder the unloading or loading of a trailer is unlikely to adopted truck operators.

Another novel Idea that has been suggested is the use active flow control [Seifert, 2008]. In this study by Seifert, an active flow control device was added to the back of the trailer. This device consisted of a rotating cylinder controlled by pneumatic jets and was installed near the top of the trailer doors. This reduced drag in a model trailer in wind tunnel testing by reducing boundary layer separation. Other studies support this argument and have shown active flow control to have an effect on the aerodynamics of a ground vehicle [Englar, 2008]. Seifert's device presents some of the same issues by using a boat tail; specifically the device would need to be installed overtop the trailer doors.

Wheel Wells and Behind Wheels

The areas around the wheels of the tractor trailer present special concern. This is due to the complexity of the air flow around the wheel. Studies of wheel wells have shown that the flow around the wheels is complex [Fabijanic, 1996 and Damiani, 2004]. Fabijanic has shown that turbulent areas are generated behind the wheel wells and that reductions in drag can be achieved by modifications to areas around the wheel well. The complexity arises from the boundary layer interactions between the rotating tire and the boundary layer developed at the tractor trailer. In order to accurately study these effects, the wheels of the tractor trailer need to be turning, which can be achieved by the use of a moving belt.

Adding a device near the wheels to modify air flow may have a secondary benefit that it could result in reduction of truck splash and spray during raining or snowy conditions [Weir, 1980].

Another area of concern is the area directly behind the wheels [Hymans, 2011]. Hymans has shown that the addition of mud flaps installed directly behind the wheels increases the drag of a tractor trailer. In addition to this he has proposed several mud flap modifications that would reduce drag.

Literature Review Conclusions

The addition of drag reduction devices can reduce overall fuel consumption. The most dramatic decrease in drag is achieved by addressing the wake behind the trailer. The wake behind the tractor trailer can be modified by use of the redirected flow.

A proposal of this study is to study the effects of a diffuser installed at the back of the trailer. It is hypothesized that this diffuser will redirect flow into the wake region behind the trailer. This will have the benefit of reducing drag and reducing splash and spray at the wheels. This diffuser also meets the preliminary design constraints that it does not interfere with operation of the tractor trailer and does not lengthen the trailer and requires no work by the truck driver to operate.

CHAPTER III
MATERIALS AND METHODS

Selection of Facilities

The major considerations for the selection of the test facilities were: ability to accommodate the test article, ability to achieve wind speeds of 70 miles per hour and have a rolling bed able to achieve speeds of 70 miles per hour. For the first two requirements, wind speed and ability to handle a 21.5" long model, several options at UTSI were available. The two that were taken under serious consideration were a 24” open air fan and a 20” x 14” open loop wind tunnel. However, neither of these two facilities had a moving bed. This equipment would ultimately have to be designed and fabricated for this experiment.

Proposals were drafted on how to use each of these two facilities. Both of these proposals included preliminary designs on how to incorporate a moving bed to accurately simulate travel over a road.

For the open air fan, the initial design was to couple the fan with an ordinary treadmill. The advantages of this set up were assumed to be ease of access to the model, limited modification to an existing treadmill, and a preconfigured control system for the setting the speed of the belt.

The disadvantage of this set up was the lack of control of turbulent flow around the model and the inability of the treadmill to achieve maximum speeds for the testing required for this testing. Both of these issues could have been addressed by: placing the model close to the fan exhaust and modifying the pulley arrangement for the treadmill/belt/motor arrangement. A mockup of this setup is shown in figure 5.

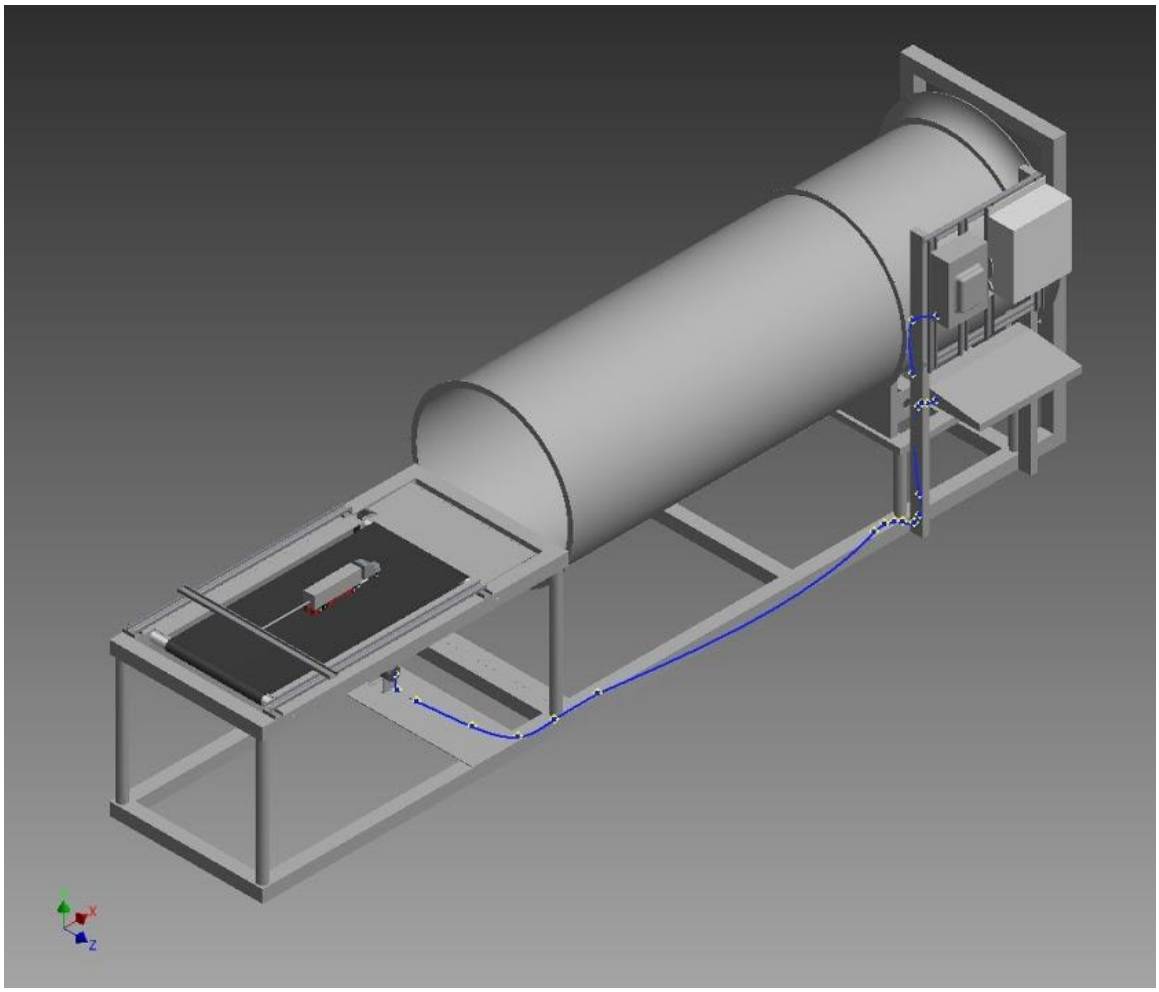

Figure 5. Open fan assembly using a treadmill as a moving bed.

For the 20” x 14” open loop wind tunnel, the proposal for use included a modification to the wind tunnel floor to include a moving bed. Because of the size and configuration of the test section of the wind tunnel, installing a prefabricated rolling belt (i.e. belt sander, tread mill, conveyer belt…) was not feasible. This resulted in a requirement to design a moving bed designed specifically for the wind tunnel.

The disadvantage to this approach would be the increased cost and time required to fabricate the rolling bed. The advantages of this approach were much more accurate control over the speed of the moving belt and a less turbulent flow around the model.

Ultimately the decision was made to modify the 20” x 14” open loop wind tunnel to include a moving bed. The belt was designed to make the most of the area under the floor of the tunnel. This resulted in the area of the floor where the belt was to be interfaced with the tunnel to be 28” x 9.5”, which would be adequate to accommodate the model. Figure 6 shows a simplified schematic of the moving belt design.

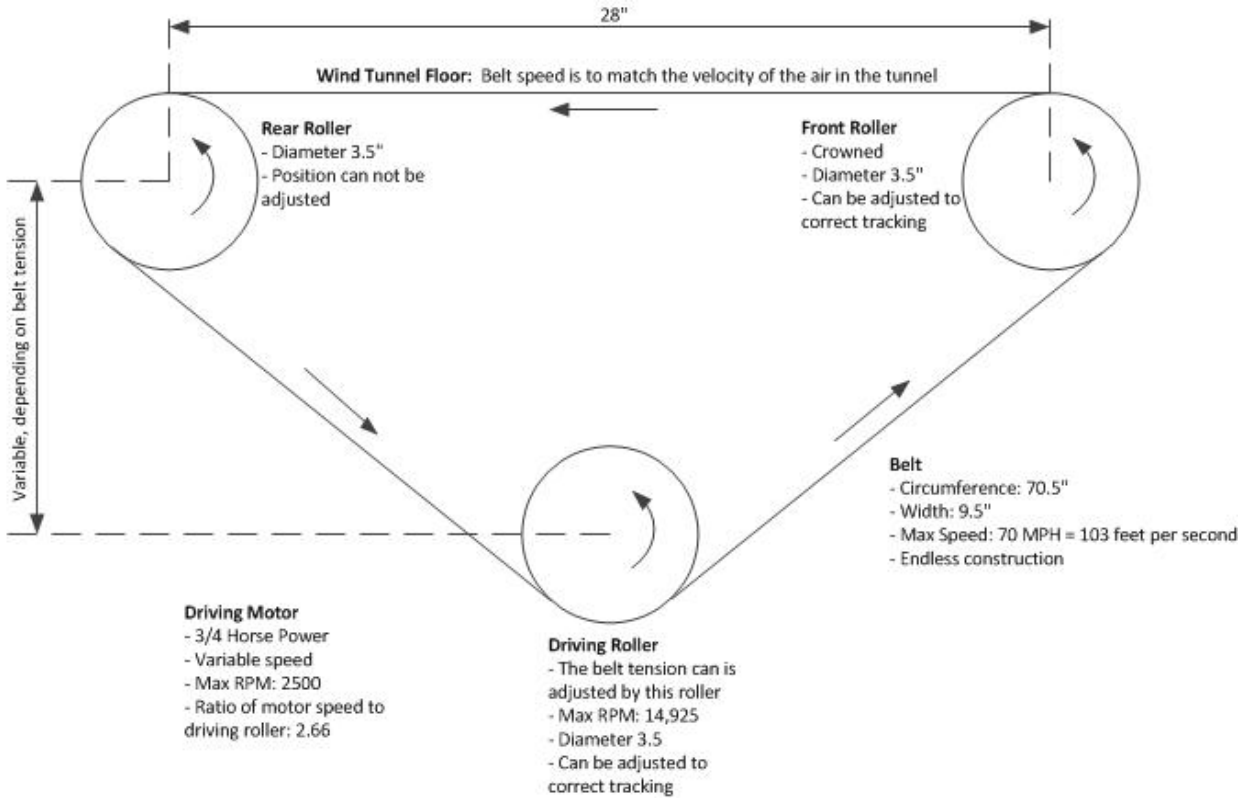

Figure 6: Schematic of the rolling bed configuration.

Addressing these design requirements, the moving bed was designed using Autodesk Inventor. Figure 7 shows a screenshot of the moving bed as designed in Inventor. Inventor was also used to produce design drawings that would ultimately be used by the UTSI machine shop to manufacture the moving bed. See appendix section 1: rolling bed drawings.

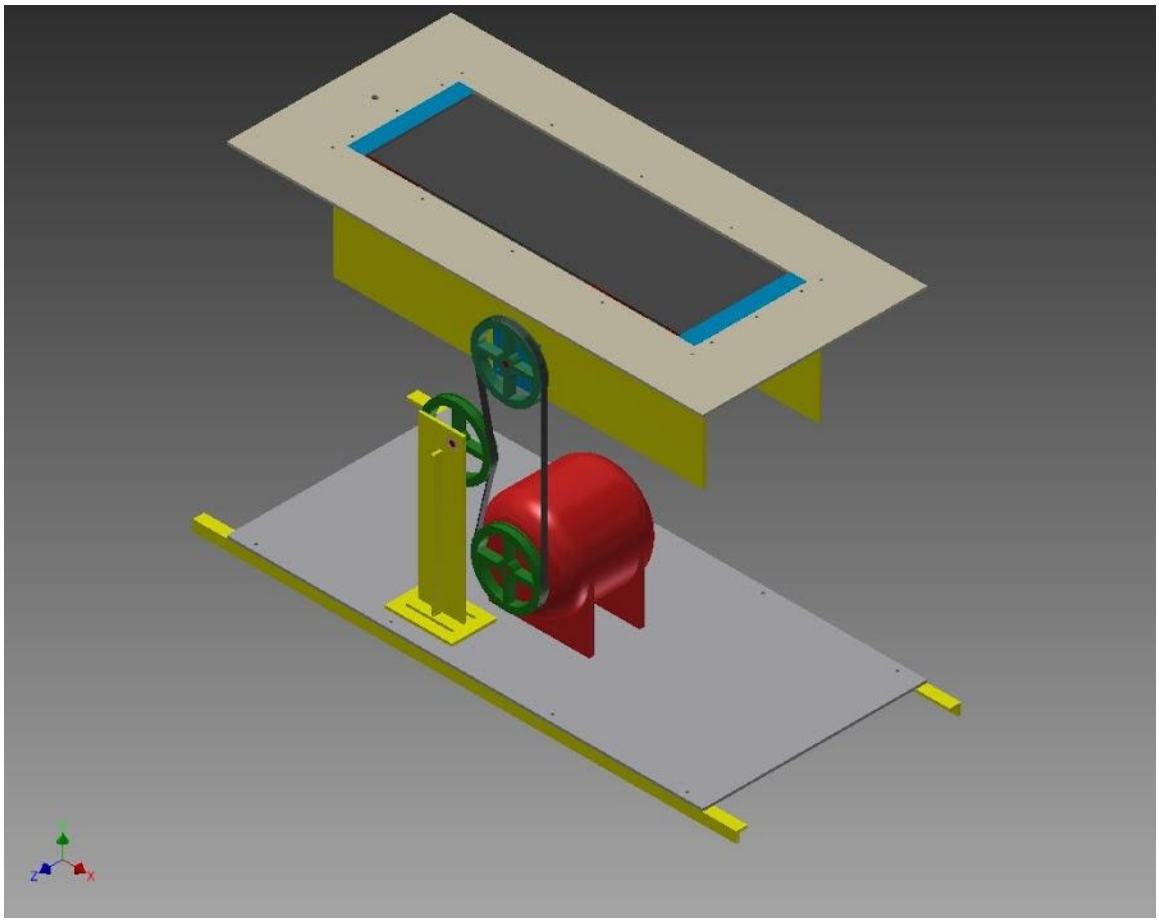
Figure 7. Moving bed assembly as drawn in Autodesk Inventor.

After the design of the moving bed was agreed upon, a wood mockup of the moving belt was fabricated. This model was made to the dimensions specified to the original design. This resulted in a model that could be used to verify that the dimensions of the moving bed were correct and that the final assembly would fit in the tunnel. Figure 8 shows a wood mockup of the rolling bed. Figure 9 shows the final moving bed.

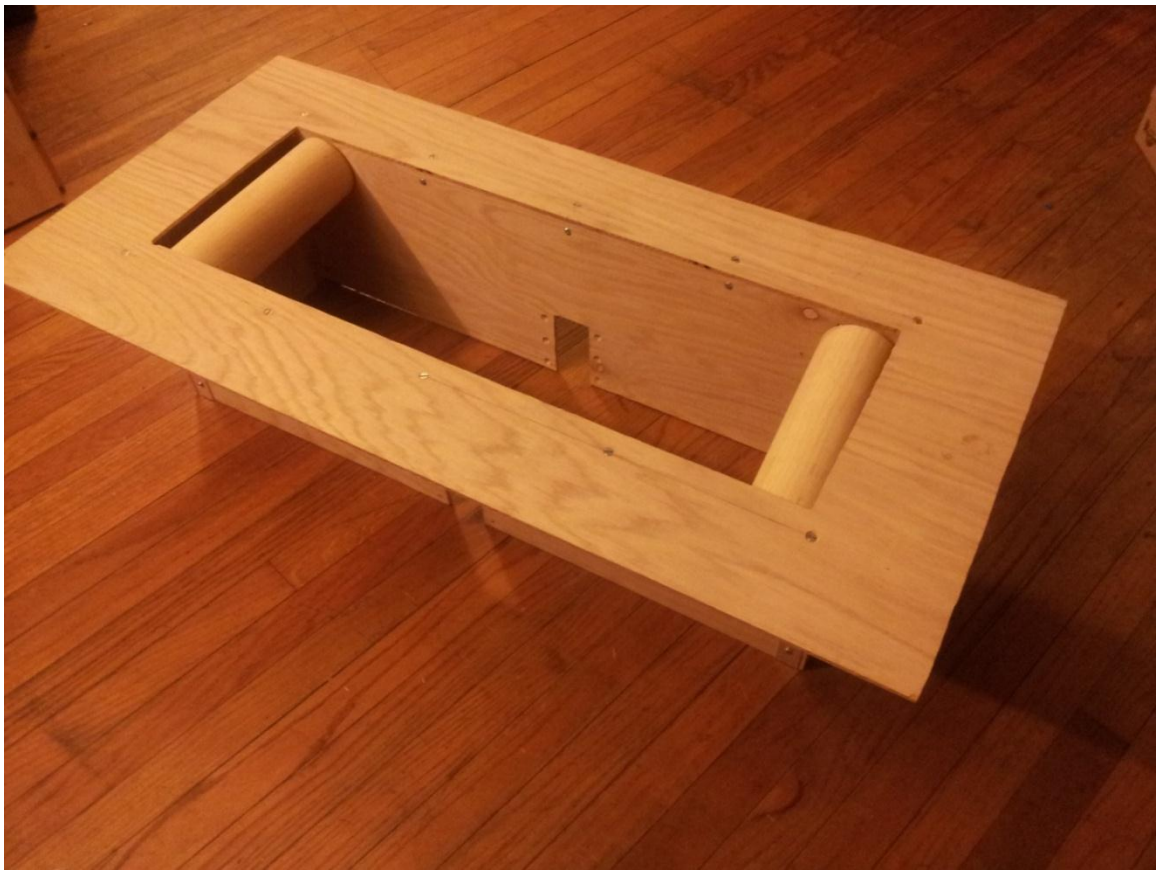

Figure 8: Wood mockup of the moving bed.

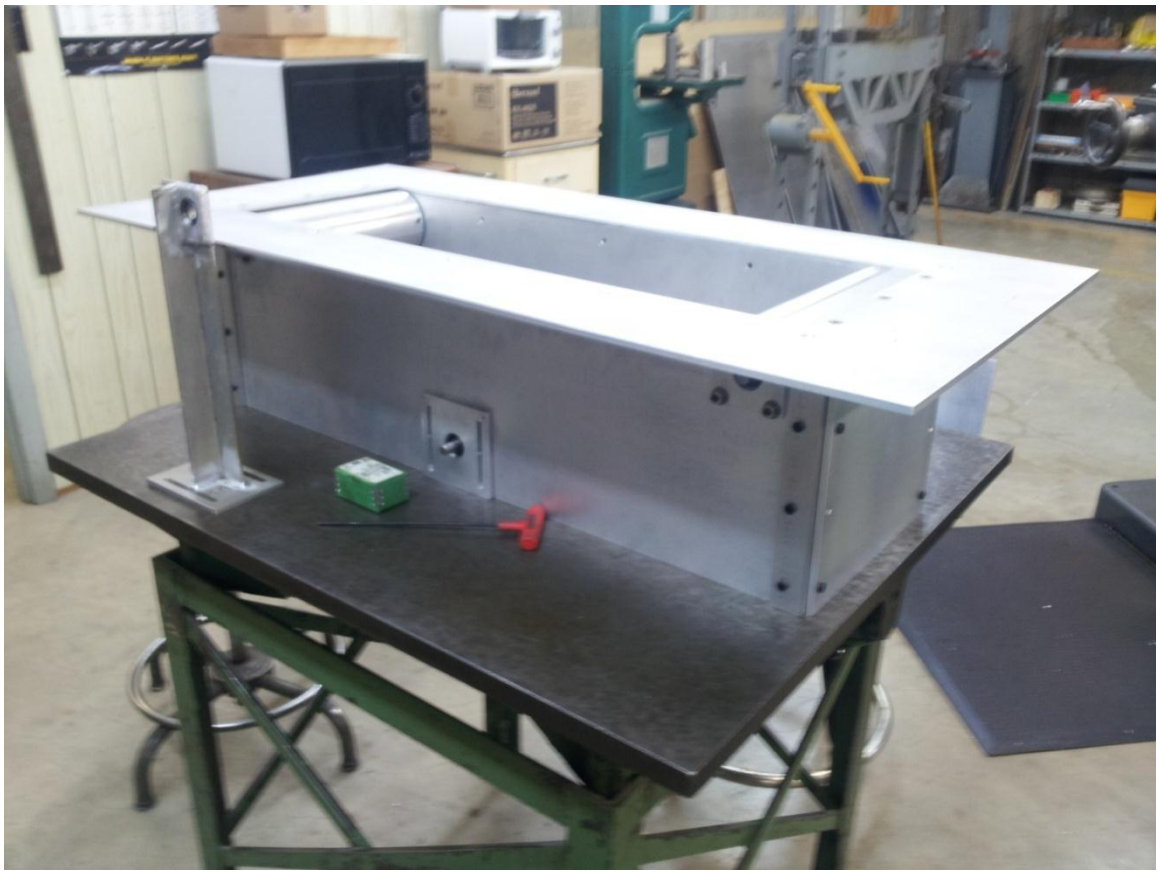
Figure 9: Completed moving bed assembly.

After the manufacturing of the moving bed by the machine shop, it became evident that belt tracking was an issue with the current design. Belt tracking is the act of keeping the belt centered on the rollers and not moving from side to side. The belt in its current configuration was running into the walls of the moving bed. Two methods were used to address the tracking issue. The first was to modify one of the rollers to be crowned. This results in a roller with a lager diameter at its center and narrow diameters on either of its ends. The optimal crown for the roller is 1/8” per foot of face [Basaraba, 1988], and this feature was added to the driving roller. See appendix section 2: crowned roller step table. The second approach was to install an adjuster arm on one of the rollers. This adjuster arm was designed to change the roller centerline, thereby changing the angle of contact between the roller and the belt. This would allow fine adjustment of the roller system, while the belt was running. Figure 10 shows the adjuster arm as designed in Autodesk Inventor. See appendix section 3 adjuster arm drawings. Both of these modifications were made to the moving bed, correcting the belt tracking issue.

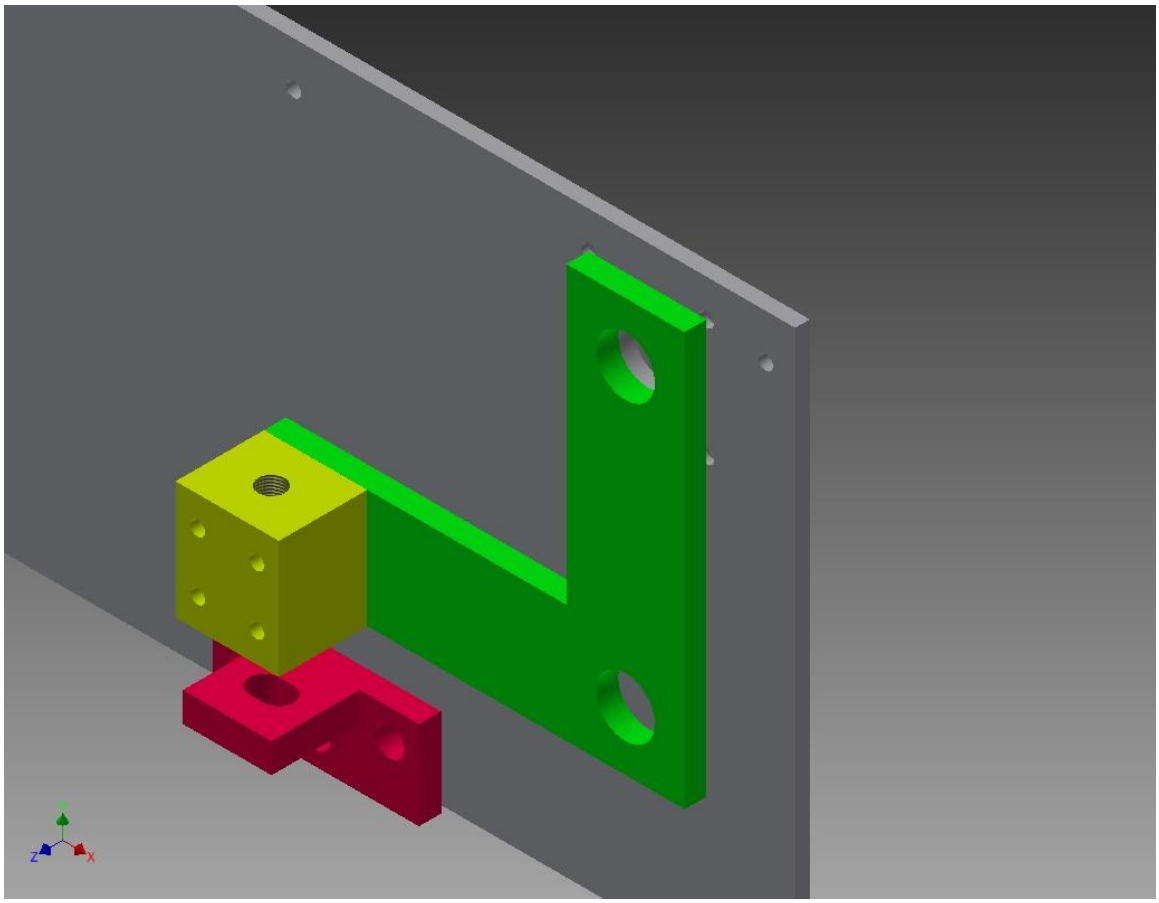
Figure 10: Adjuster arm.

The final test cell modification was the installation of a sting to hold the model in place inside the test cell. The sting has a simple design of two steel rods bolted together at a right angle to each other. A bracket was designed to hold the rod configuration to the tunnel ceiling. A second bracket with jack screws was installed on top of the first bracket so that the entire sting/model assembly could be raised from outside of the test cell. Figure 11 shows the sting assembly as drawing in Inventor. See appendix section 4: sting drawings.

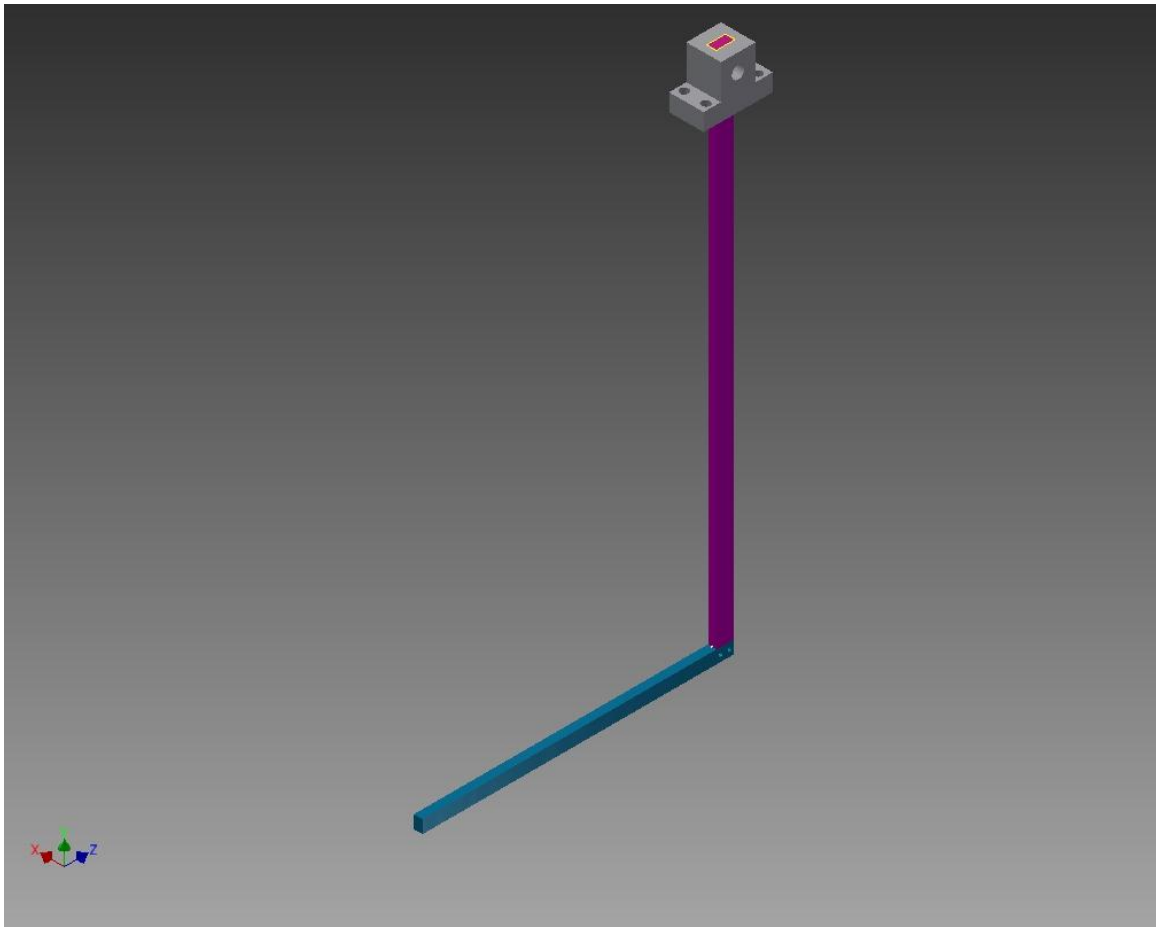
Figure 11: Sting assembly.

Selection of Model

Model Selection and Modification

The major consideration when selecting a model was that it is an accurate representation of a tractor trailer. This was found in a commercial model (desktop model) of a tractor trailer. The model used for this experiment has amazing amount of detail and very closely resembles a typical tractor trailer. The scale of the model is1/32. Figure 12 shows the model of the tractor trailer.


Figure 12: Tractor trailer model.

In order to be installed in the wind tunnel, the model had to be modified so that it could be connected to the sting. This was accomplished by installing a support structure inside the tractor trailer model. This internal support structure was designed to be assembled on top of the existing features of the tractor trailer model and was fabricated using a Makerbot Replicator 3D printer. A detailed explanation of this 3D printer is given in the next section (Drag Reduction Device Fabrication). The only modification to the model required by this approach was the drilling of two 3/8” holes between the trailer and cab of the model. This was required to anchor the cab to the tractor trailer by use of two bolts and custom printed spacer. The doors also had to be removed to accommodate the installation of sting to the trailer. The trailer doors were then replaced by printed plate. Figure 13 shows the internal structure (in red) that was printed and installed inside the trailer of the model. This approach resulted in very little alteration to the exterior of the model.


Figure 13: Internal 3D printed model modification.

Drag Reduction Device Fabrication

For the production of the drag reduction devices the following methods were originally considered: shaping the devices out of polystyrene foam using a hot wire cutter, setting up a molding technique using clay and rubber molds, and having the devices manufactured by a machine shop. To have a machinist fabricate the drag reduction devices would have been extremely cost prohibited for this investigation. Upwards of 24 separate drag reduction devices were made to support this testing. Several of these drag reduction devices had extremely complex geometries and would have required days of machinist support to make. The molding technique mentioned earlier would have consisted of making an original pattern of the drag reduction device out of clay, pouring a rubber mold around the pattern, removing the pattern, and casting the final piece in plastic in the rubber mold. This method is analogous to plaster mold metal casting. This method would have resulted in an ability to make a high volume of identical parts that would then need to be individually modified to the shape of the final unique drag reduction devices. The drawback of this method of production was that the accuracy of the original pattern would depend the ability of person making the original pattern. This resulted in little confidence in this repeatability of this method. The last method considered for the manufacturing of the devices was to shape the

devices out of polystyrene using a hot wire cutter. This method was thought to be the easiest way to manufacture the devices, as it used material that was readily available, polystyrene, and the shaping tool could be easily be made from a inexpensive power supply and ni-chrome wire. The foam wire cutter was made and attempts were made to make some of the devices with this setup. The results were undesirable and unrepeatable. One of the main difficulties with using the hot wire cutter was obtaining smooth curves and flat surfaces. Steadily feeding the foam through the hot wire to get desired results was not achievable with this method.

At this time the idea of using a 3D printer was discussed, as one was available on the UTSI campus. Compared to the other methods of manufacture proposed, the 3D printer was vastly superior. Compared to the foam cutting technique, the 3D printer was a much better choice because of the repeatability and accuracy of the prints. Compared to molding technique the 3D printer was better choice because the devices could be printed once and would not need to be modified thereafter. As for machine shop, the price and time to print the devices are not comparable. The cost of a kilogram of the plastic used by the printer is $49 and it took 30 minutes to set up the machine to print 3 to 5 different parts. The printer would then run by itself for about six hours to make the parts. It was expected for a machine shop to make the same set of pieces that it would take at least a day. For all of these reasons the other methods of manufacture were abandoned and the use of the 3D printer was pursued.

The 3D printer used for the work was the Makerbot Replicator. This 3D desktop printer has a build envelope of 8.9 x 5.7 x 5.9 inches and uses accrylonitrile butadiene styrene (ABS) plastic to make parts. The Makerbot Replicator uses the process of fused deposition modeling (FDM), an additive process, to make parts. This method of manufacturing extrudes thermoplastic through a heated nozzle. The nozzle is used to create a layer of the part by moving along a certain path (tool path) in the horizontal plane. After a layer is made, the part is lowered one layer height and another layer is deposited on top the previous one. The parts used in this investigation were made with following print settings: 10% infill, 2 shells, layer height of .2 mm, extruder temperature 230 degrees Celsius, build plate temperature 110 degrees Celsius, and an extruder travel speed of 40 mm/s.

The drag reduction devices were designed using 3D modeling software Autodesk Inventor. 3D modeled parts were exported to a stereolithography file format (.stl file extension). From there the .stl file was uploaded into the Makerbot Makerware software. This Makerware software was used to generate the G-Code (.x3g file extension) that would dictate the 3d printer's tool path when it fabricated the parts. The .x3g file was then transferred to a SD memory card and then uploaded to Makerbot Replicator.

In order to get high quality printed parts, the following steps were performed when running the Replicator. First, print speeds were set to 40 mm/sec. Print speeds faster than this would result in defects being imparted into the part, especially for taller parts. Second, the build plate was coated in Kapton tape. This step is recommended

by the printer manufacture and is essential to the adhesion between the extruded ABS plastic and the build plate. Third the Kapton tape was coated in ABS plastic dissolved in acetone. The dissolved ABS was applied to the Kapton plate using a brush after the build plate had been heated to 110 degrees Celsius. The heated plate would evaporate the acetone in the mixture resulting in a textured build plate. This textured surface improved the adhesion of the extruded ABS plastic to the build plate. Proper adhesion of the first layer of the printed part was required to prevent curling of the part as the build process continued. Fourth, the build plate was leveled using Makerbot's leveling procedure. This amounted to adjusting the distance between the print head the build head at five different locations on the build. The adjustments were made by adjusting four set screws underneath the build plate.

A set (between 3 and 5) of drag reduction devices could be printed in about six hours. Because of this quick production time, model modification could be made in one evening. This 24 hour turn around consisted of a set of drag reduction devices being tested, data reviewed, modifications made to the drag reduction device design, and new devices printed that night ready to be tested the next day. This economy of using a desktop 3D printer for this type of testing allowed for a greater number of devices to be tested in a shorter amount of time and a far cheaper overall cost compared to the alternatives.

Drag Reduction Device Design

The drag reduction devices were designed using Autodesk Inventor and printed on the Makerbot Replicator 3D printer. Five categories of devices were designed and printed, including side skirts, front wheel devices, rear wheel keels, rear wheel diffusers, and rear wheel mudflaps. Figure 14 and 15 show the different configurations of the drag reduction devices. Table 1 Drag Reduction Device Schematics lists the drag reduction device schematics as shown in appendix section 5. The devices were designed using the streamlining ideas described in the literature review section of this paper.

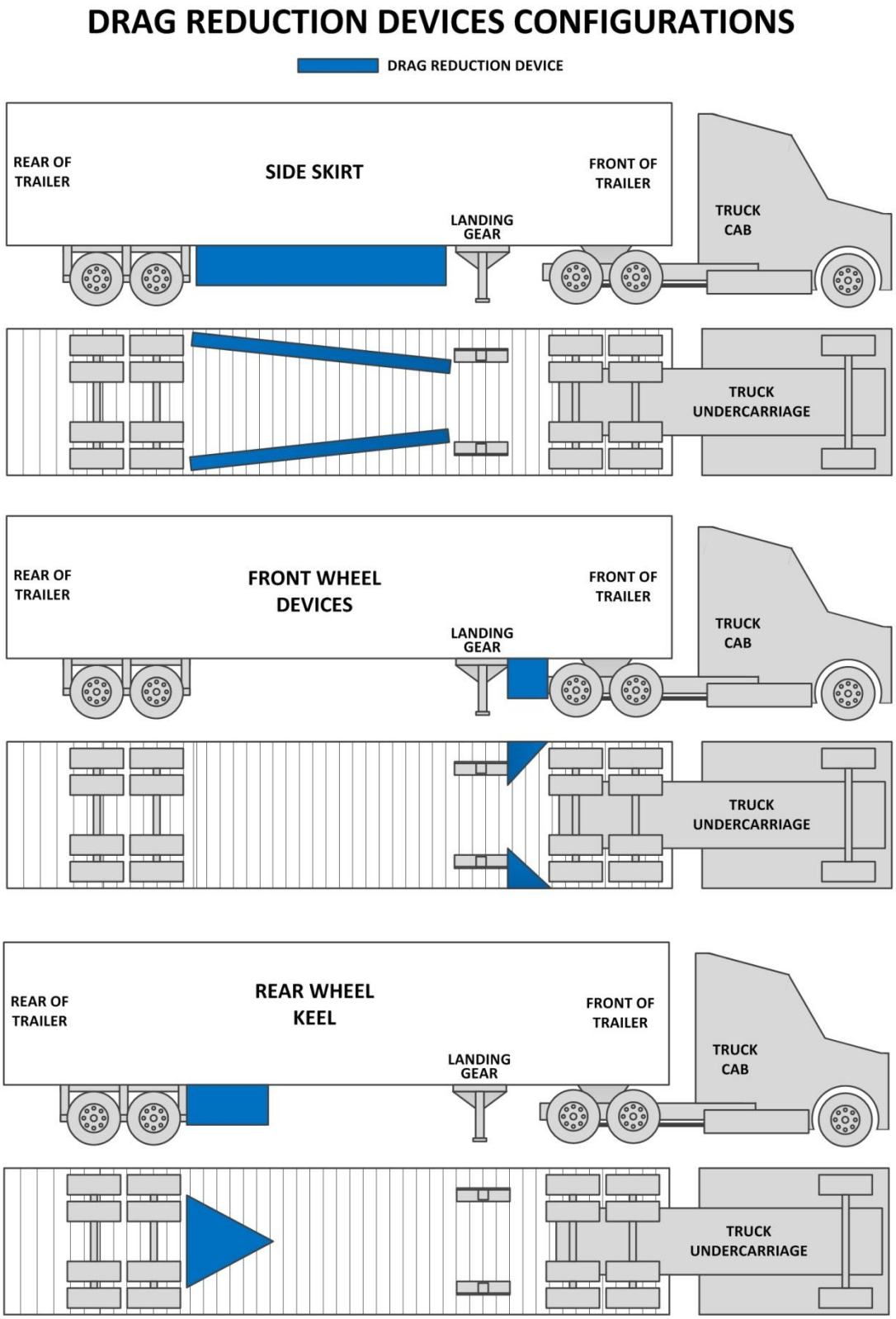

Figure 14: Drag reduction devices configurations

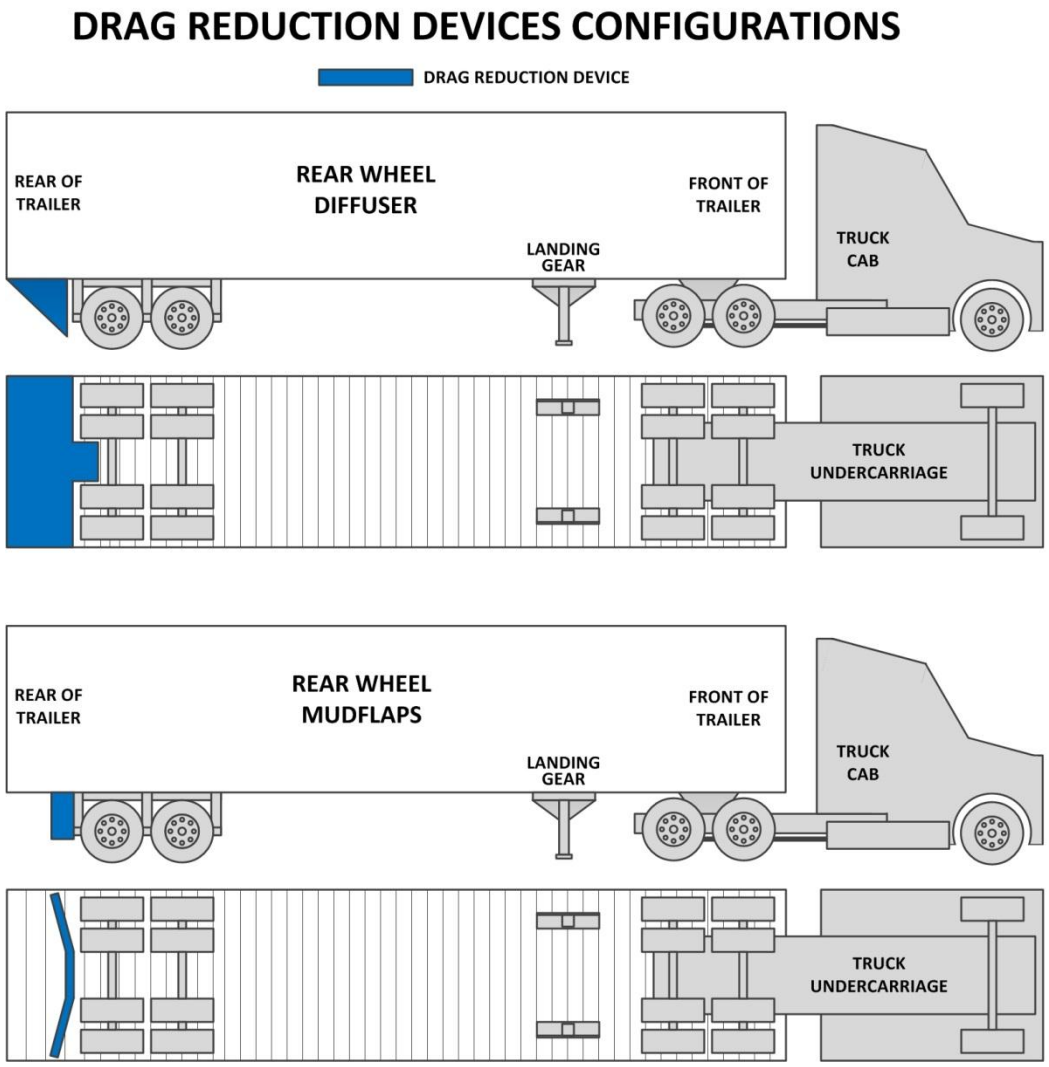

Figure 15: Drag reduction devices configurations, continued

Table 1. Drag Reduction Device Schematics, Appendix Section 5

Test Article	***Page #***
Side skirt, flat plate	73
Side skirt, flat plate, mid angle	74
Side skirt, flat plate, full angle	75
Side skirt, curved plate	76
Side skirt, half trough	77
Side skirt, trough	78
Side skirt, lofted trough	79
Side skirt, lofted horizontal to vertical plate	80
Side skirt, lofted arch with flat side	81
Side skirt, lofted arch	82
Front wheel diffuser	83
Front wheel nozzle	84
Horizontal wedge	85
Rear wheel keel, horizontal wedge	86
Rear wheel keel, vertical wedge	87
Rear wheel keel, combination horizontal and vertical wedge	88
Rear wheel keel, bow wedge	89
Rear wheel keel, round wedge	90
Rear diffuser with no axle faring	91
Rear diffuser with half axle faring	92
Rear diffuser with full axle faring	93
Wheel well	94
Mudflap, mid angle	95
Mudflap, full angle	96

Selection of Instrumentation

Flow visualization was performed using tufts installed on the surface of the model. The tufting used was red sewing thread for the light colored areas and white sewing thread for dark areas. Tufts are defined as short pieces of wool, thread or other very light flexible and easily visible material which give a qualitative picture of local airflow direction and (from steadiness or oscillatory motion or turbulence) vorticity or turbulence [Gunston, 2009]. The tufts are 1.25” long and installed on the model using pressure sensitive tape. They were placed in rows 1” apart and the distance between each tuft in the row is .5”. Each row of tufts was offset .25” from previous row. This resulted in the pattern shown if figure 16.

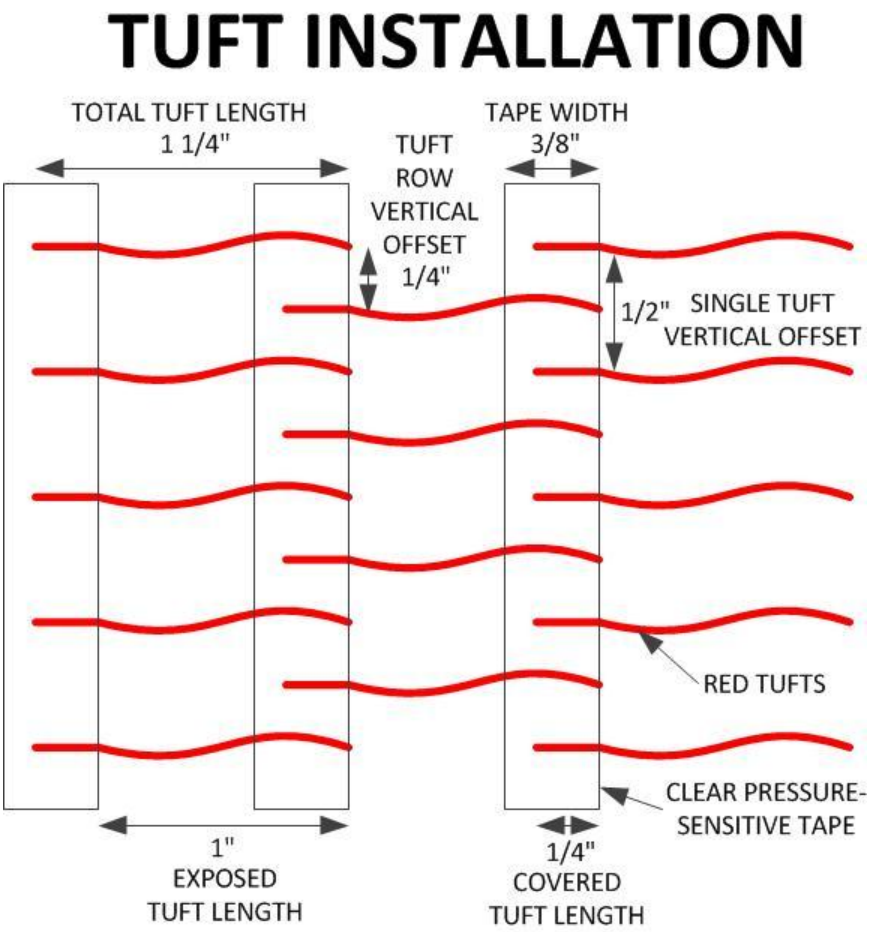

Figure 16: Tuft installation.

For setting the moving bed speed a stroboscope was used.

As a part of the wind tunnel, air velocity was set using a pitot tube and National Instruments LABView software.

Measurement Approach for Testing and Comparative Data Acquisition

Photographs of the model with and without the drag reduction devices were compared to each other. From these photographs the effects of the drag reduction devices on model were determined through comparison and observation of the changes obtained and or observed.

Anticipation of Data Accuracy

The photographs and video taken for this testing were done using a 10-14 megapixel camera and video recorder. This will give an adequate level of accurate representation of the orientation of tufting. Areas of turbulent flow were determined from the interaction of the tufting. However, these are for the purposes of concept evaluation and trends determination. In the future, detail quantitative studies would be needed using full scale tests and or scaled force balance measurements for actual implementation of the best devices and their cost justifications.

CHAPTER IV
RESULTS AND DISCUSSION

Results

Results of the tufting experiments are as follows:

Table 2. Wind Tunnel Pictures, Appendix Section 6

Test Article	*Wind Tunnel Speed*	*Moving Bed at Speed*	*Page #*
No devices	55 MPH	no	98
No devices	65 MPH	no	99
No devices	70 MPH	no	100
Side skirt, flat plate	55 MPH	no	101
Side skirt, flat plate	65 MPH	no	102
Side skirt, flat plate	70 MPH	no	103
Side skirt, flat plate, mid angle	55 MPH	no	104
Side skirt, flat plate, mid angle	65 MPH	no	105
Side skirt, flat plate, mid angle	70 MPH	no	106
Side skirt, flat plate, full angle	55 MPH	no	107
Side skirt, flat plate, full angle	65 MPH	no	108
Side skirt, flat plate, full angle	70 MPH	no	109
Side skirt, curved plate	55 MPH	no	110
Side skirt, curved plate	65 MPH	no	111
Side skirt, curved plate	70 MPH	no	112
Side skirt, half trough	55 MPH	no	113
Side skirt, half trough	65 MPH	no	114
Side skirt, half trough	70 MPH	no	115
Side skirt, trough	55 MPH	no	116
Side skirt, trough	65 MPH	no	117
Side skirt, trough	70 MPH	no	118
Side skirt, lofted trough	55 MPH	no	119
Side skirt, lofted trough	65 MPH	no	120
Side skirt, lofted trough	70 MPH	no	121
Side skirt, lofted horizontal to vertical plate	55 MPH	no	122

Table 2. Continued

Test Article	*Wind Tunnel Speed*	*Moving Bed at Speed*	*Page #*
Side skirt, lofted horizontal to vertical plate	65 MPH	no	123
Side skirt, lofted horizontal to vertical plate	70 MPH	no	124
Side skirt, lofted arch with flat side, installed with arch facing rear wheels	55 MPH	no	125
Side skirt, lofted arch with flat side, installed with arch facing rear wheels	65 MPH	no	126
Side skirt, lofted arch with flat side, installed with arch facing rear wheels	70 MPH	no	127
Side skirt, lofted arch with flat side, installed with arch facing front wheels	55 MPH	no	128
Side skirt, lofted arch with flat side, installed with arch facing front wheels	65 MPH	no	129
Side skirt, lofted arch with flat side, installed with arch facing front wheels	70 MPH	no	130
Side skirt, lofted arch installed with arch facing rear wheels	55 MPH	no	131
Side skirt, lofted arch installed with arch facing rear wheels	65 MPH	no	132
Side skirt, lofted arch installed with arch facing rear wheels	70 MPH	no	133
Side skirt, Lofted arch, installed with arch facing front wheels	55 MPH	no	134
Side skirt, Lofted arch, installed with arch facing front wheels	65 MPH	no	135
Side skirt, Lofted arch, installed with arch facing front wheels	70 MPH	no	136

Table 2. Continued

Test Article	*Wind Tunnel Speed*	*Moving Bed at Speed*	*Page #*
Front wheel diffuser	55 MPH	no	137
Front wheel diffuser	65 MPH	no	138
Front wheel diffuser	70 MPH	no	139
Front wheel nozzle	55 MPH	no	140
Front wheel nozzle	65 MPH	no	141
Front wheel nozzle	70 MPH	no	142
Rear wheel keel, horizontal wedge	55 MPH	no	143
Rear wheel keel, horizontal wedge	65 MPH	no	144
Rear wheel keel, horizontal wedge	70 MPH	no	145
Rear wheel keel, vertical wedge	55 MPH	no	146
Rear wheel keel, vertical wedge	65 MPH	no	147
Rear wheel keel, vertical wedge	70 MPH	no	148
Rear wheel keel, combination horizontal and vertical wedge	55 MPH	no	149
Rear wheel keel, combination horizontal and vertical wedge	65 MPH	no	150
Rear wheel keel, combination horizontal and vertical wedge	70 MPH	no	151
Rear wheel keel, bow wedge	55 MPH	no	152
Rear wheel keel, bow wedge	65 MPH	no	153
Rear wheel keel, bow wedge	70 MPH	no	154
Rear wheel keel, round wedge	55 MPH	no	155
Rear wheel keel, round wedge	65 MPH	no	156
Rear wheel keel, round wedge	70 MPH	no	157
Rear diffuser with no axle faring	55 MPH	no	158
Rear diffuser with no axle faring	65 MPH	no	159
Rear diffuser with no axle faring	70 MPH	no	160

Table 2. Continued

Test Article	*Wind Tunnel Speed*	*Moving Bed at Speed*	*Page #*
Rear diffuser with half axle faring	55 MPH	yes	161
Rear diffuser with half axle faring, rear view	55 MPH	no	162
Rear diffuser with half axle faring	55 MPH	no	163
Rear diffuser with half axle faring, rear view	65 MPH	yes	164
Rear diffuser with half axle faring, rear view	65 MPH	no	165
Rear diffuser with half axle faring, rear view	70 MPH	yes	166
Rear diffuser with half axle faring, rear view	70 MPH	no	167
Rear diffuser with full axle faring, rear view	55 MPH	no	168
Rear diffuser with full axle faring, rear view	65 MPH	no	169
Rear diffuser with full axle faring, rear view	70 MPH	yes	170
Rear diffuser with full axle faring, rear view	70 MPH	no	171
Wheel well	55 MPH	no	172
Wheel well	65 MPH	no	173
Wheel well	70 MPH	no	174
Diffusers behind and in front of rear wheels, rear view	55 MPH	no	175
Diffusers behind and in front of rear wheels, rear view	55 MPH	yes	176
Diffusers behind and in front of rear wheels, front view	55 MPH	yes	177
Diffusers behind and in front of rear wheels, front view	55 MPH	no	178

Table 2. Continued

Test Article	*Wind Tunnel Speed*	*Moving Bed at Speed*	*Page #*
Diffusers behind and in front of rear wheels, rear view	65 MPH	no	179
Diffusers behind and in front of rear wheels, rear view	65 MPH	yes	180
Diffusers behind and in front of rear wheels, front view	65 MPH	yes	181
Diffusers behind and in front of rear wheels, front view #1	65 MPH	no	182
Diffusers behind and in front of rear wheels, front view #2	65 MPH	no	183
Diffusers behind and in front of rear wheels, rear view	70 MPH	no	184
Diffusers behind and in front of rear wheels, rear view	70 MPH	yes	185
Diffusers behind and in front of rear wheels, front view	70 MPH	yes	186
Diffusers behind and in front of rear wheels, rear view	70 MPH	no	187
Diffusers behind and in front of rear wheels, and lofted arch side skirt, rear view	55 MPH	no	188
Diffusers behind and in front of rear wheels, and lofted arch side skirt, rear view	65 MPH	no	189
Diffusers behind and in front of rear wheels, and lofted arch side skirt, rear view	70 MPH	no	190
Diffusers behind and in front of rear wheels, and lofted arch side skirt, front view	70 MPH	no	191
Diffusers behind and in front of rear wheels, and lofted arch side skirt, rear view	70 MPH	yes	192

Table 2. Continued

Test Article	*Wind Tunnel Speed*	*Moving Bed at Speed*	*Page #*
Diffusers behind and in front of rear wheels, and lofted arch side skirt, front view	70 MPH	yes	193
Mudflap, mid angle	55 MPH	no	194
Mudflap, mid angle	65 MPH	no	195
Mudflap, mid angle	70 MPH	no	196
Mudflap, full angle	55 MPH	no	197
Mudflap, full angle	65 MPH	no	198
Mudflap, full angle	70 MPH	no	199

Discussion

The first set of pictures, titled no devices (appendix section 6, pages 98-100) show the model with no drag devices installed and are the base line by which to compare the remainder of the figures. This first set shows the turbulent area under the trailer. The remainder of figures (appendix section 6, pages 101-199) show the model with the drag reduction devices installed. Distinct flow patterns can be seen around each drag reduction device.

For the flat side skirts (appendix section 6, pages 101-112), those installed closest to the edge of the trailer side skirt, flat pate (appendix section 6, pages 101-103) streamlined the flow the best of the this subset. The remainder of these flat side skirts (appendix section 6 pages 104-112) show flow towards the ground.

For the trough side skirts (appendix section 6, pages 113-118), flow separation can be seen at the front of the half trough devices, while the trough devices show less flow separation.

The remainder of the side skirts (appendix section 6, pages 119-136) are lofted designs. The best results of this subset were the devices that had a low profile at the front of the trailer and then gradually shifted to vertical orientation at the rear tires. This included the lofted arch side skirt installed with arch facing front wheels (appendix section 6 pages 134-136). The worst of this subset were the devices that were the opposite of this, that is to say a side skirt with a vertical orientation facing the front of the trailer that lofted to the low profile at the rear tires. This configuration showed continuous flow separation along the length of the side skirt as seen in side skirt, lofted

arch with flat side, installed with arch facing rear wheels (appendix section 6, pages 125-127),

The set of devices installed behind the front wheels, showed a negligible to negative effect on the flow management behind the front tires. The front wheel diffuser device (appendix section 6, pages 134-136) showed flow being pushed towards the floor of the tunnel, while the front wheel nozzle device (appendix section 6, pages 140-142) showed some streamlining.

For the rear wheel keel devices (appendix section 6, pages 143-17), those with lowest horizontal profile, rear wheel keel, horizontal wedge (appendix section 6, pages 140-142) and rear wheel keel, combination horizontal and vertical wedge (appendix section 6, pages 146-148), showed the least amount of flow separation. The remainders of these devices have a much larger vertical profile and show significantly more flow separation, and redirection of the flow downward towards the tunnel floor.

For each the rear wheel diffuser devices (appendix section 6, pages 158-171), flow behind the rear wheels was redirected into the wake zone behind the trailer. This can especially be seen on the picture titled rear diffuser with full axle faring, rear view 55 MPH. In this picture the tufts installed on the diffuser are pointing at an upward angle. This shows that flow is being redirected into the wake region of the trailer.

For the wheel well devices (appendix section 6, pages 172-174) and angled mud flaps (appendix section 6, pages 194-199), no noticeable streamline effect could be seen with the installed tufts. Different tuft installation and different camera orientations could provide more information on the effects of these devices.

The remainder of the configurations (appendix section 6, pages 175-193), are of multiple devices installed. This combination of devices show varying degrees of effectiveness. The rear diffuser effect of redirecting flow into the wake region is preserved with the addition of multiple devices. The addition of side skirts with diffuser appears to negate the effectiveness of the side skirts. This can be seen in appendix section 6 pages 189 and 190 where more flow separation off the side skirt is shown.

Several tests were performed with the moving belt in operation. The most noticeable effect of the belt moving is the flow around the tires. This can be seen on appendix section 6 pages 175, 176, and 177. On page 175 the belt is not moving and a tuft installed over the rear wheel is pointed slight downward angle. On page 176 and 177 the belt has been turned and this same tuft has more pronounced downward angle, showing that when the tires are rotating air flow around the tires has changed.

CHAPTER V
CONCLUSIONS AND RECOMMENDATIONS

Conclusions

A 1/32 scale detail model of a truck with its trailer was used for testing in a 20"x14" low speed wind tunnel at the University of Tennessee Space Institute. Major modifications were made to the wind tunnel so that it would include a moving bed (floor) section for ground effect simulation and is a permanent capability added to the tunnel for future studies which would require the ground effect. The drag reduction devices were fabricated using a desktop 3D printer. Flow visualization was performed using sewing (twisted) string as tufts to validate if there were any flow improvement effectiveness as a result of the flow management devices. Test results from this investigations showed the addition of drag reduction devices changed flow paths under the tractor trailer and appear to lead to smoother flow under the trailer.

Test results from this investigation showed the addition of drag reduction devices did change flow paths under the tractor trailer and did provide methods for managing flow under and around the wheel of the trailer.

For the side skirts, devices that were lofted from a low profile at the front of the trailer to a vertical profile at the rear wheel showed the best management of flow (appendix section 6, pages 134-137).

For the devices installed in front of the rear wheels or rear wheel keels, the devices that showed the least separation of flow where those that had a low vertical profile (appendix section 6, pages 143-145 and pages 149-152).

A possibly novel method for addressing the wake zone behind the tractor trailer, by addition of drag reduction devices installed under the trailer, was also investigated. The rear wheel diffusers showed a possible novel method for addressing the wake zone behind the tractor trailer (appendix section 6, pages 158-171).

Quantitative measurements are needed to determine the overall and individual contributions, and to select the best configuration of a number of configurations for a maximum level of drag reduction

Recommendations

The methodology described here makes an excellent first step in investigating the aerodynamics of ground vehicles. Numerous model modifications can be made quickly and cheaply. This results in a very cost effective way to examine a wide range of ideas. Devices that are not promising can be eliminated quickly, while those that may produce the desired results can be narrowed down for further study.

The ground effect of the road on a vehicle traveling at speed has been shown in this investigation. Further testing should investigate how the drag reduction devices effect spray from wet roads.

For the devices tested during this investigation, those installed behind the rear wheels showed the most promise. A drag reduction device that modifies the wake behind the trailer, that is installed under the trailer, which would not interfere with the operation of the tractor trailer would be more appealing to a truck driver than a device installed in a way that interfered with his operation of the vehicle.

With fuel economy being of utmost importance in shipping, further investigation into the ability of drag reduction devices should be continued. Quantified measurements of drag could be found by installing load cells into the model mounting device. All of this testing should build to eventual full scale testing on a modified tractor trailer to define device effectiveness.

LIST OF REFERENCES

Table 1- Commercial Freight Activity in the United States by Mode of Transportation: 2002. *Freight in America.* Bureau of Transportation Statistics. http://www.rita.dot.gov/bts/sites/rita.dot.gov.bts/files/publications/freight_in_america/index.html

United States Department of Energy Transportation Energy Data Book: Edition 32, 2006. http://cta.ornl.gov/data/download32.shtml

RITA – State Transportation Facts, 2011. U.S. Department of Transportation, Research and Innovative Technology Administration, Bureau of Transportation Statistics, 2012 http://gis.rita.dot.gov/StateFacts/

Horerner, S. F. (1965) Fluid-Dynamic Drag, *Self-Published*

Stone, Richard Ball, Jeffrey K. (2004). Automotive Engineering Fundamentals. Society of Automotive Engineers, Inc.

Buckley Jr., F. T., W. H. Walston Jr., and C. H. Marks (1978), Fuel Savings form Truck Aerodynamic Drag Reducers and Correlation with Wind-Tunnel Data, *Journal of Energy,* Volume 2, Number 6, Page 321

Gunston, Bill (2009). Cambridge Aerospace Dictionary (2nd Edition). Cambridge University Press.

White, Frank (1999). Fluid Mechanics, *WCB McGraw-Hill*

Ortega, J. M., and K. Salari (2004), An Experimental Study of Drag Reduction Devices for a Trailer Underbody and Base, *American Institute of Aeronautics and Astronautics,* AIAA 2004-2252

Storms, B. L., D. R. Satran, J. T. Heineck, and S. M. Walker (2004), A Study of Reynolds Number Effects and Drag-Reduction Concepts on a Generic Tractor-Trailer, *American Institute of Aeronautics and Astronautics,* AIAA 2004-2251

Mokhtar, W. A., and N. Pervez (2012), Underbody drag for Pickup Trucks, *American Institute of Aeronautics and Astronautics,* AIAA 2012-3210

Christoffersen, L., C. Landstrom, L. Lofdahl, R. Quartey-Papafio, and A. Jonson (2008), Influence of Moving Ground Conditions on the Cooling Flows of Road Vehicles, *American Institute of Aeronautics and Astronautics,* AIAA 2008-6737

Ghuge, H. A., and C. J. Roy (2006), Preliminary Detached Eddy Simulations of a Generic Tractor/Trailer, *American Institute of Aeronautics and Astronautics,* AIAA 2006-3858

Doyle, J. B., R. J. Hartfield, and C. Roy (2008), Aerodynamic Optimization for Freight Trucks Using a Genetic Algorithm and CFD, *American Institute of Aeronautics and Astronautics,* AIAA 2008-323

Veluri, S. P., C. J. Roy, A. Ahmed, R. Rifki, J. C. Worley, and B. Recktenwald (2007), Joint Computational/Experimental Aerodynamic Study of a Simplified Tractor/Trailer Geometry, *American Institute of Aeronautics and Astronautics,* AIAA 2007-4430

Veluri, S. P., C. J. Roy, A. Ahmed, and R. Rifki (2006), Preliminary RANS Simulations and Experimental Study of a Simplified Tractor/Trailer Geometry, *American Institute of Aeronautics and Astronautics,* AIAA 2006-3857

Seifert, A., O. Stalnov, D. Sperber, G. Arwatz, V. Palei, S. David, I. Dayan, and I. Fono (2008), Large Trucks Drag Reduction Using Active Flow Control, *American Institute of Aeronautics and Astronautics,* AIAA 2008-743

Englar, R. J. (2008), Application of Advanced Aerodynamic Technology of Ground and Sport Vehicles, *American Institute of Aeronautics and Astronautics,* AIAA 2008-6731

Fabijanic, J., and A. R. George (1996), An Experimental Investigation of the Aerodynamics of Automobile Wheel Wells, *American Institute of Aeronautics and Astronautics,* AIAA-96-2475-CP

Weir, D. H. (1980), Truck Splash and Spray - Full Scale Tests and Alleviation Devices

Hymans, D. G., K. Sreenivas, R. Pankajakshan, D. S. Nichols, W. R. Briley, and D. L. Whitfield (2011), Computational Simulation of Model and Full Scale Class 8 Trucks with Drag Reduction Devices, *Computers and Fluids,* Volume 41, Page 27

Basaraba, Bruce (1988). IPT's Industrial Trades Handbook Power Transmission Systems, *IPT Publishing and Training LTD.*

APPENDIX

Appendix Section 1
Rolling Bed Drawings

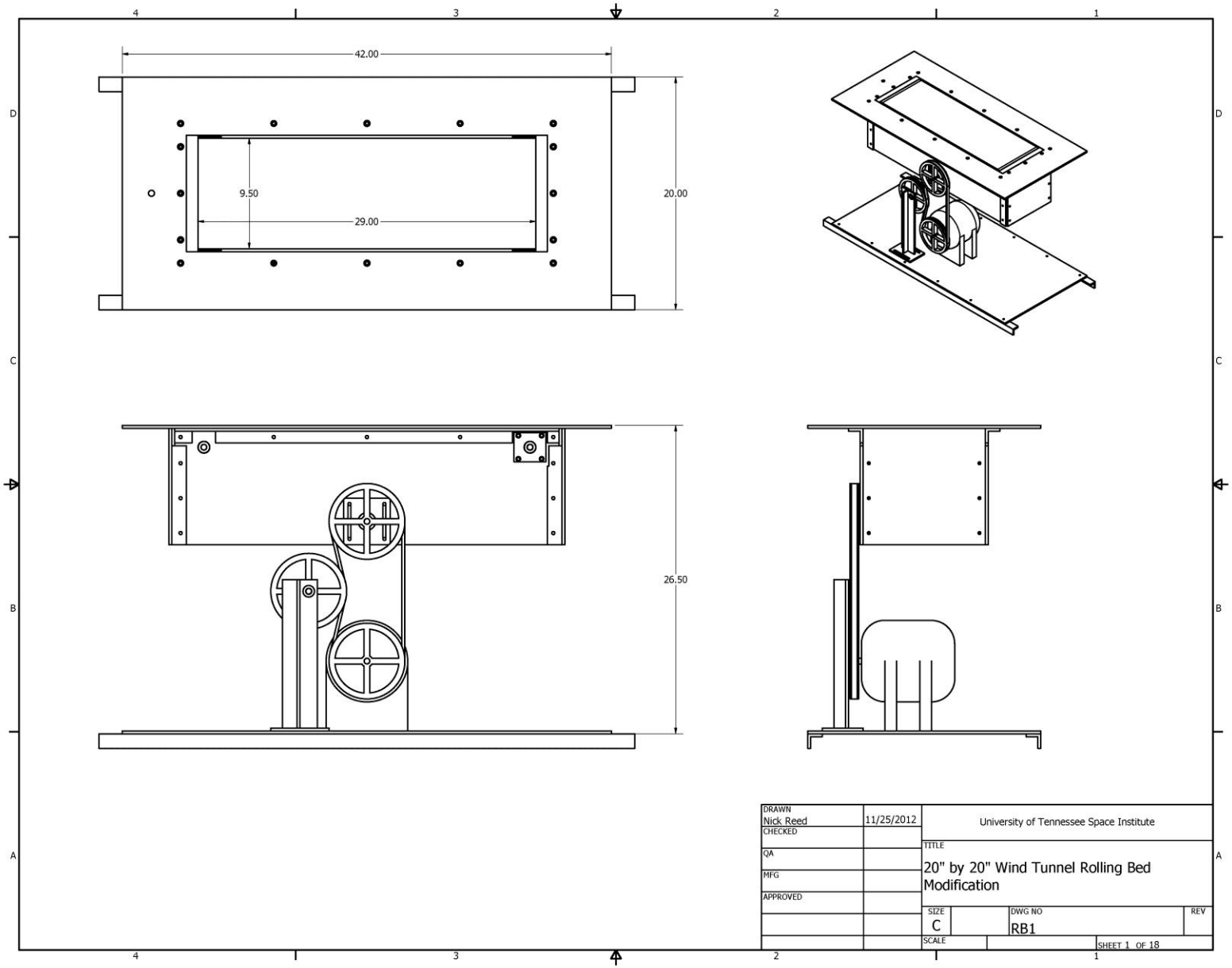
42.00
9.50
29.00
20.00
26.50
DRAWN
Nick Reed
11/25/2012
CHECKED
QA
MFG
APPROVED
University of Tennessee Space Institute
TITLE
20" by 20" Wind Tunnel Rolling Bed Modification
SIZE
C
DWG NO
RB1
REV
SCALE
SHEET 1 OF 18

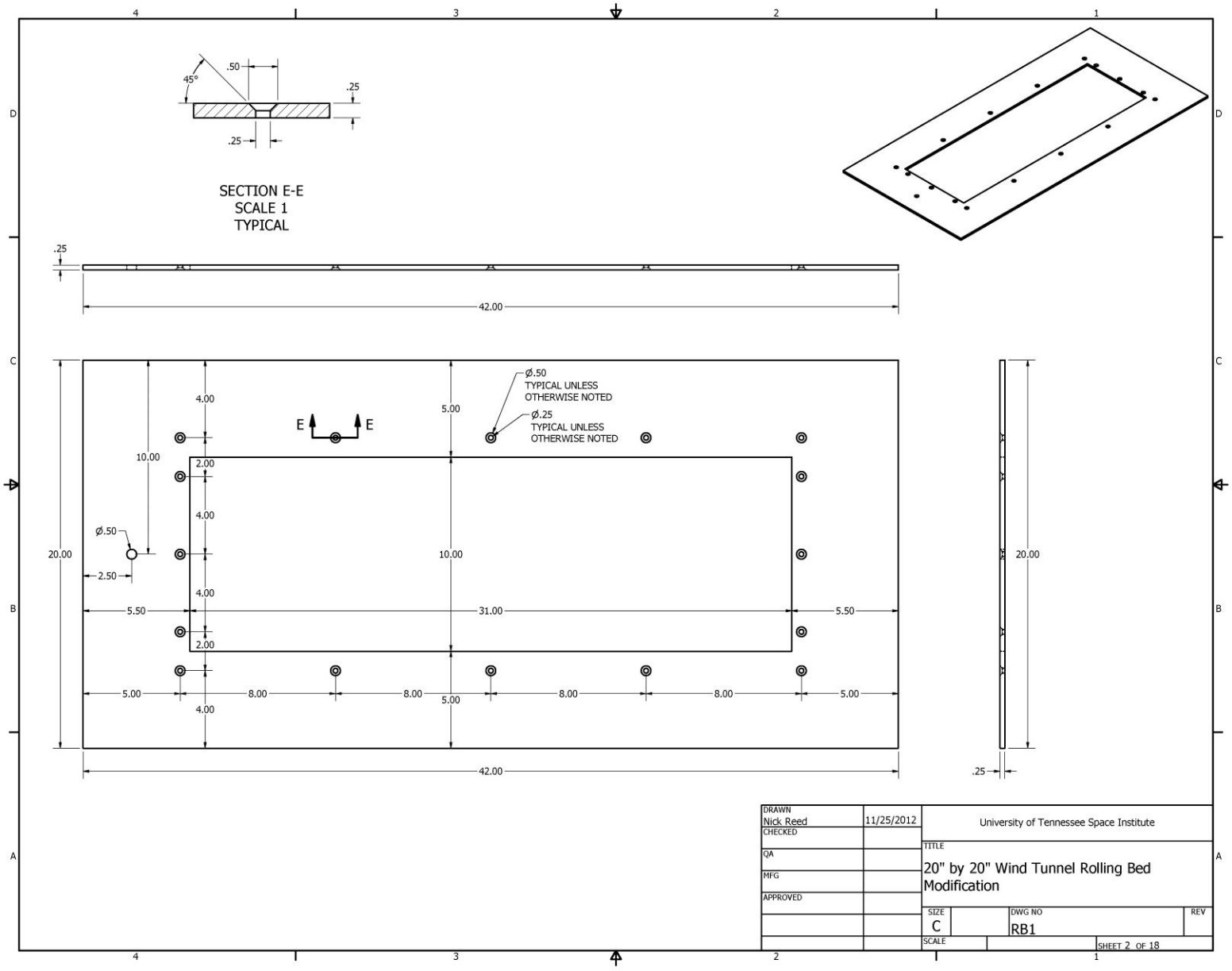
45°
.50
.25
.25
SECTION E-E
SCALE 1
TYPICAL
.25
42.00
Ø.50
TYPICAL UNLESS
OTHERWISE NOTED
Ø.25
TYPICAL UNLESS
OTHERWISE NOTED
E
E
4.00
10.00
2.00
4.00
4.00
2.00
20.00
Ø.50
2.50
5.00
10.00
5.50
31.00
5.50
5.00
8.00
8.00
5.00
8.00
8.00
5.00
4.00
42.00
20.00
.25
DRAWN
Nick Reed
11/25/2012
CHECKED
QA
MFG
APPROVED
University of Tennessee Space Institute
TITLE
20" by 20" Wind Tunnel Rolling Bed Modification
SIZE
C
DWG NO
RB1
REV
SCALE
SHEET 2 OF 18

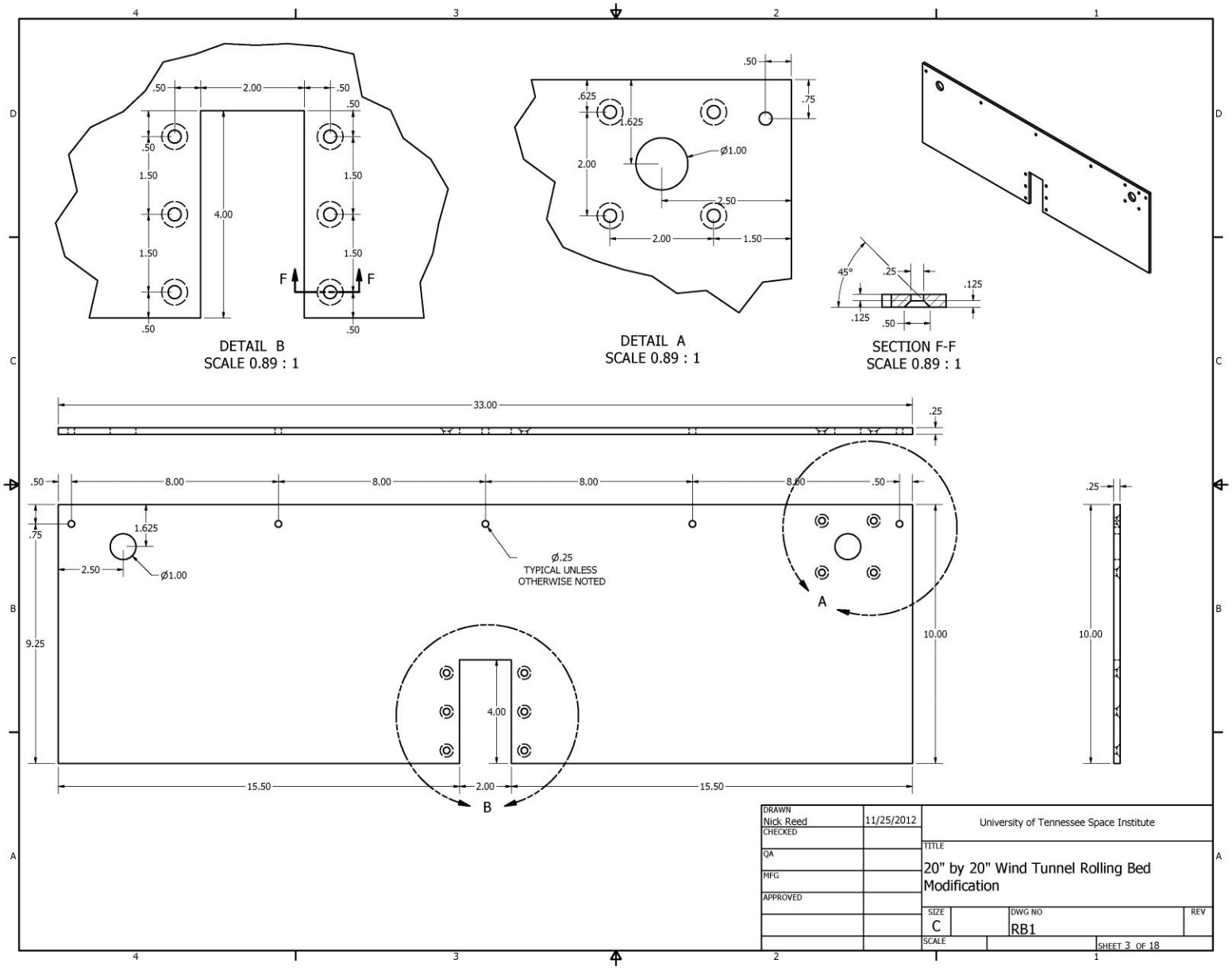
DETAIL B
SCALE 0.89 : 1
DETAIL A
SCALE 0.89 : 1
SECTION F-F
SCALE 0.89 : 1
Ø.25
TYPICAL UNLESS
OTHERWISE NOTED
DRAWN
Nick Reed
11/25/2012
CHECKED
QA
MFG
APPROVED
University of Tennessee Space Institute
TITLE
20" by 20" Wind Tunnel Rolling Bed
Modification
SIZE
C
DWG NO
RB1
REV
SCALE
SHEET 3 OF 18

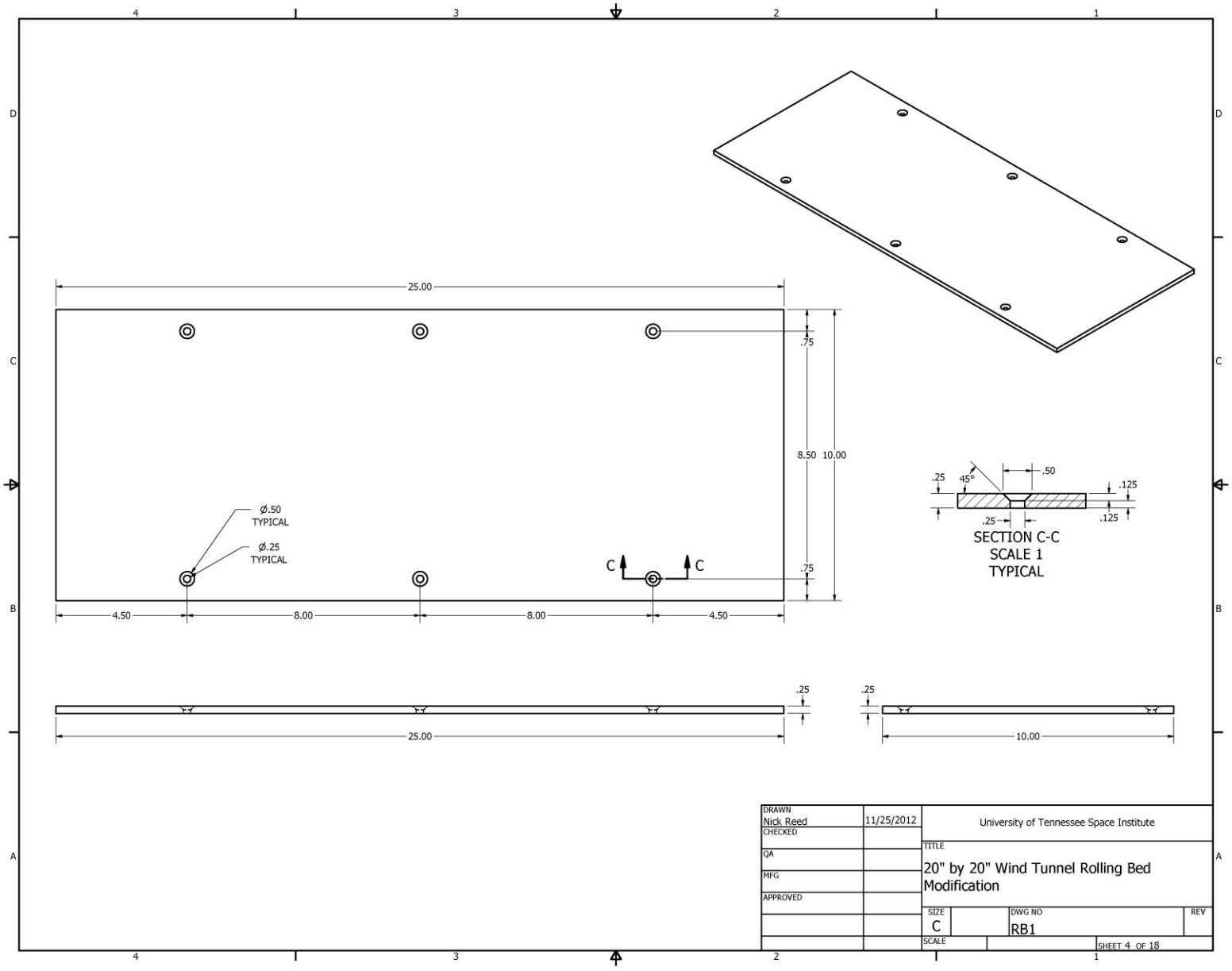
25.00
.75
8.50
10.00
.75
Ø.50
TYPICAL
Ø.25
TYPICAL
C
C
4.50
8.00
8.00
4.50
.25
45°
.50
.125
.25
.125
SECTION C-C
SCALE 1
TYPICAL
.25
25.00
.25
10.00
DRAWN
Nick Reed
11/25/2012
CHECKED
QA
MFG
APPROVED
University of Tennessee Space Institute
TITLE
20" by 20" Wind Tunnel Rolling Bed Modification
SIZE
C
DWG NO
RB1
REV
SCALE
SHEET 4 OF 18

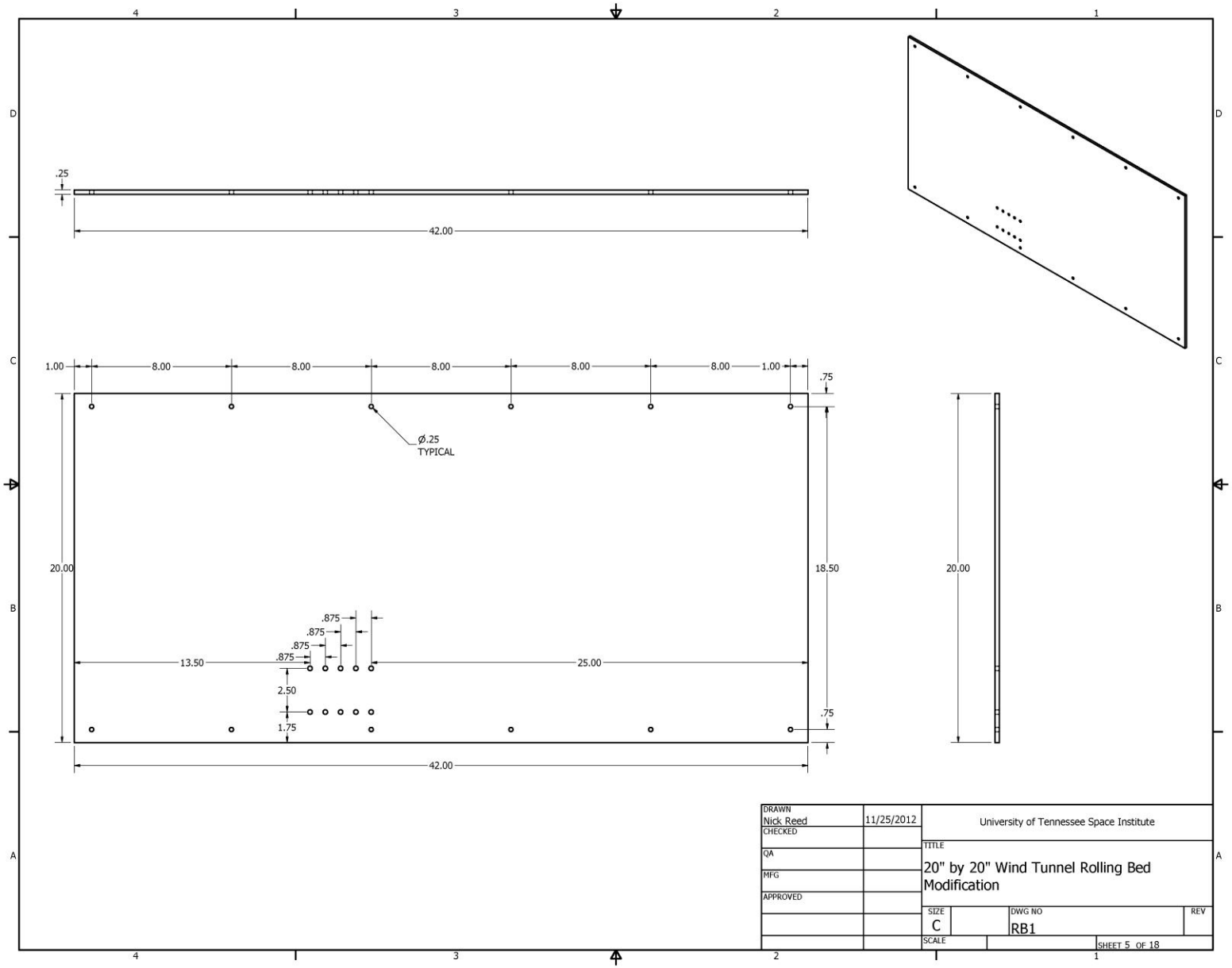
.25
42.00
1.00
8.00
8.00
8.00
8.00
8.00
1.00
.75
Ø.25
TYPICAL
20.00
18.50
20.00
.875
.875
.875
.875
13.50
25.00
2.50
1.75
.75
42.00
DRAWN
Nick Reed
11/25/2012
CHECKED
QA
MFG
APPROVED
University of Tennessee Space Institute
TITLE
20" by 20" Wind Tunnel Rolling Bed Modification
SIZE
C
DWG NO
RB1
REV
SCALE
SHEET 5 OF 18

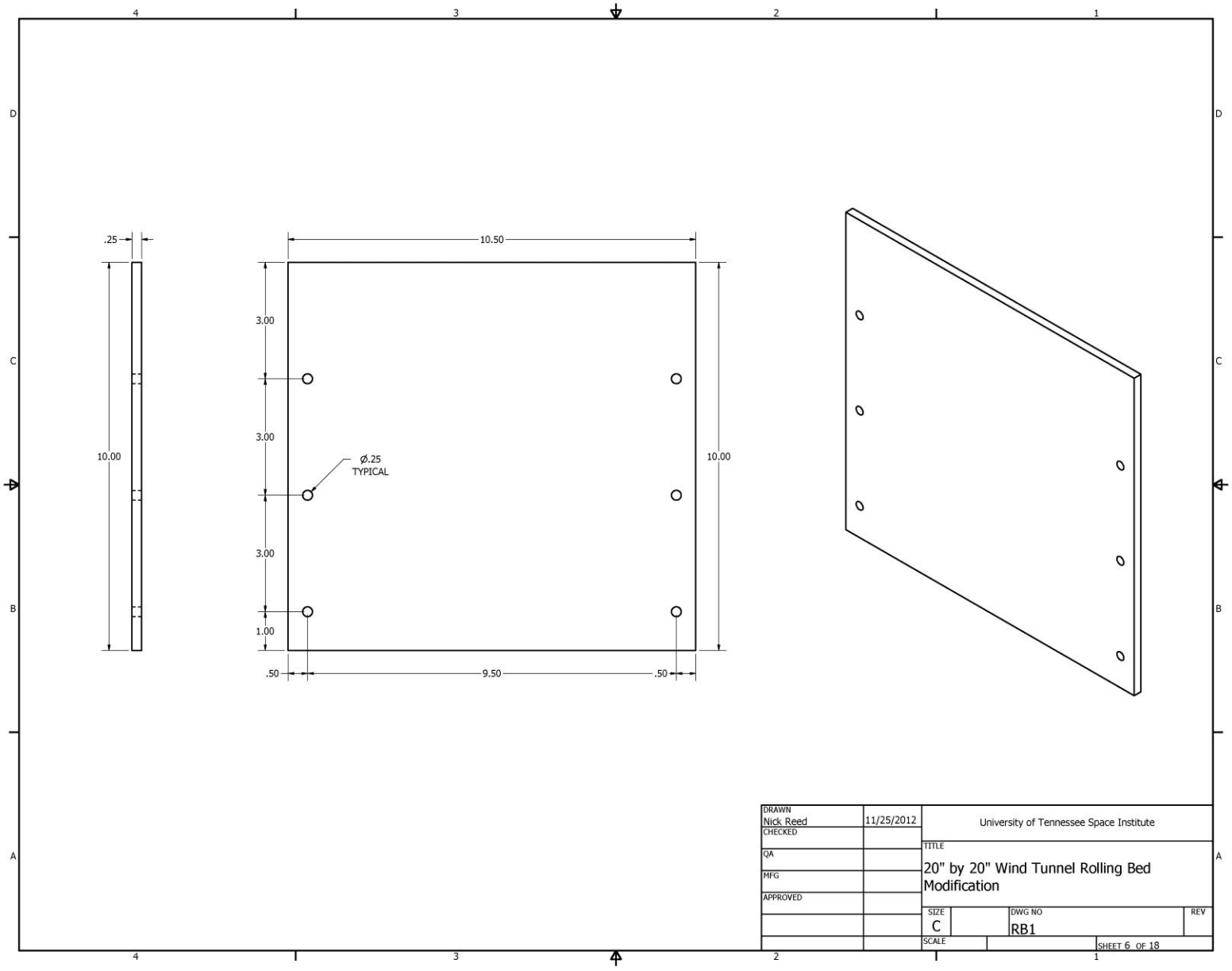
.25
10.00
10.50
3.00
3.00
3.00
1.00
Ø.25
TYPICAL
10.00
.50
9.50
.50
DRAWN
Nick Reed
11/25/2012
CHECKED
QA
MFG
APPROVED
University of Tennessee Space Institute
TITLE
20" by 20" Wind Tunnel Rolling Bed Modification
SIZE
C
DWG NO
RB1
REV
SCALE
SHEET 6 OF 18

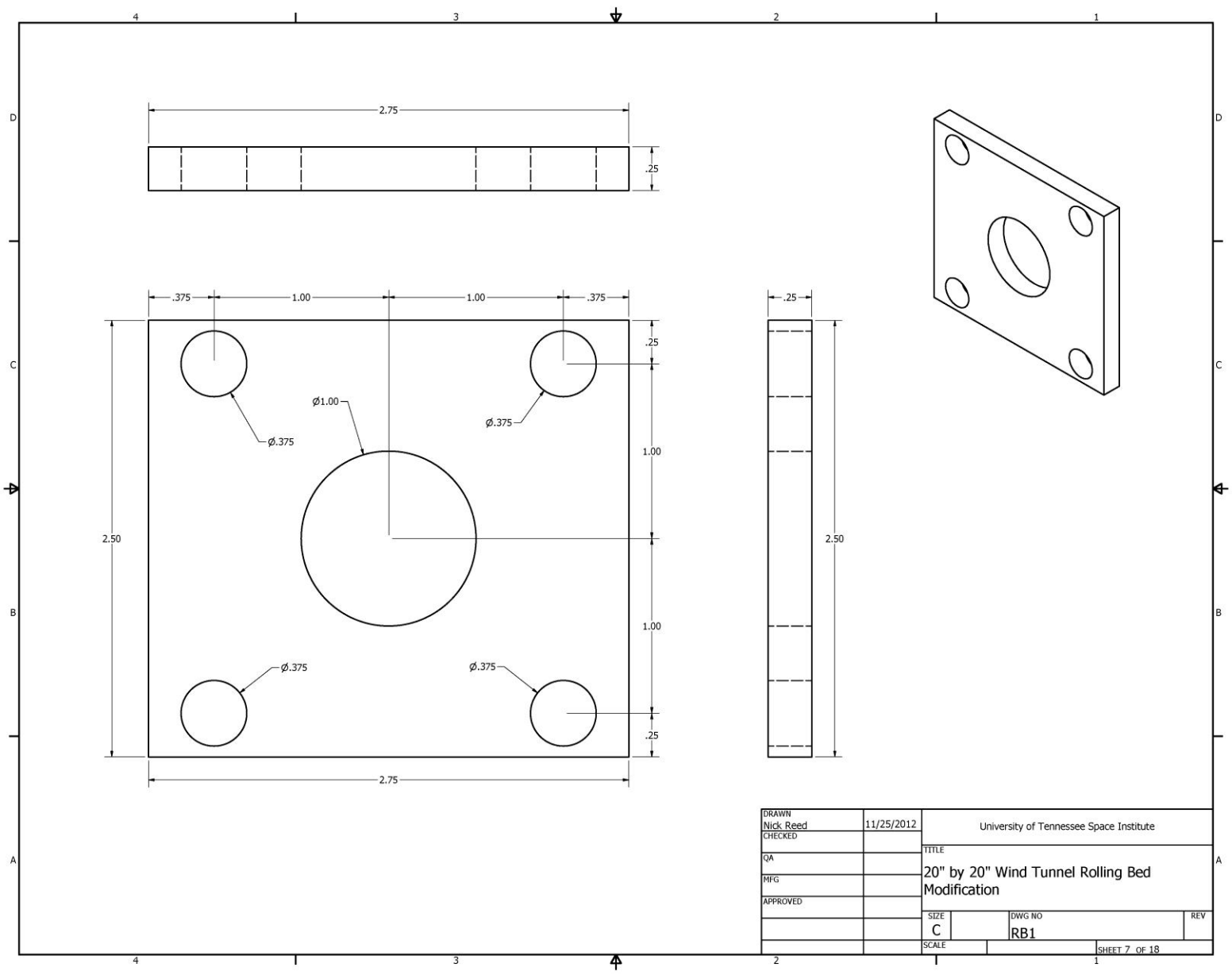
2.75
.25
.375
1.00
1.00
.375
.25
Ø1.00
Ø.375
Ø.375
1.00
2.50
1.00
Ø.375
Ø.375
.25
2.75
.25
2.50
DRAWN
Nick Reed
11/25/2012
CHECKED
QA
MFG
APPROVED
University of Tennessee Space Institute
TITLE
20" by 20" Wind Tunnel Rolling Bed Modification
SIZE
C
DWG NO
RB1
REV
SCALE
SHEET 7 OF 18

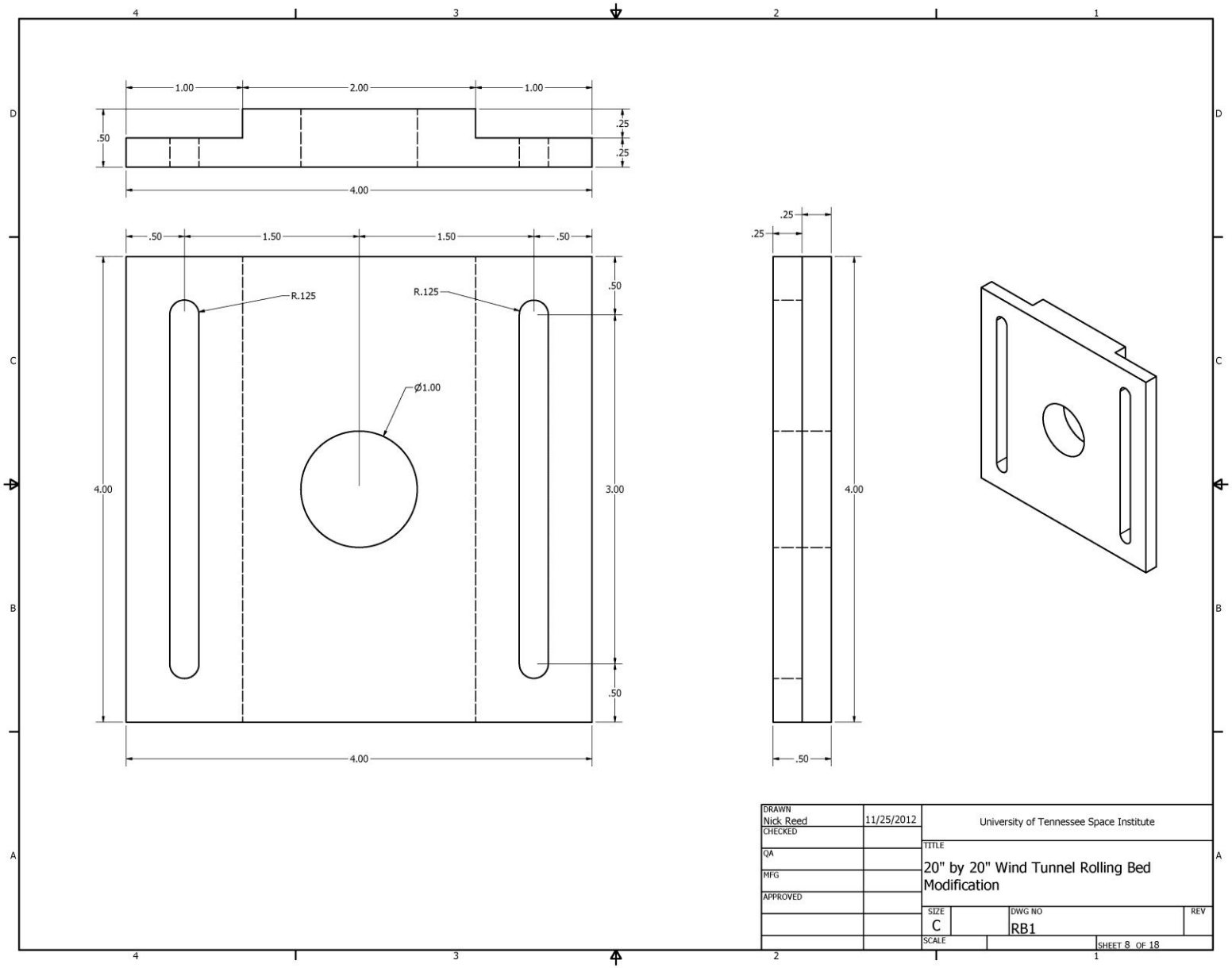
1.00
2.00
1.00
.50
.25
.25
4.00
.50
1.50
1.50
.50
R.125
R.125
Ø1.00
4.00
3.00
.50
.50
.25
.25
4.00
.50
DRAWN
Nick Reed
11/25/2012
CHECKED
QA
MFG
APPROVED
University of Tennessee Space Institute
TITLE
20" by 20" Wind Tunnel Rolling Bed Modification
SIZE
C
DWG NO
RB1
REV
SCALE
SHEET 8 OF 18

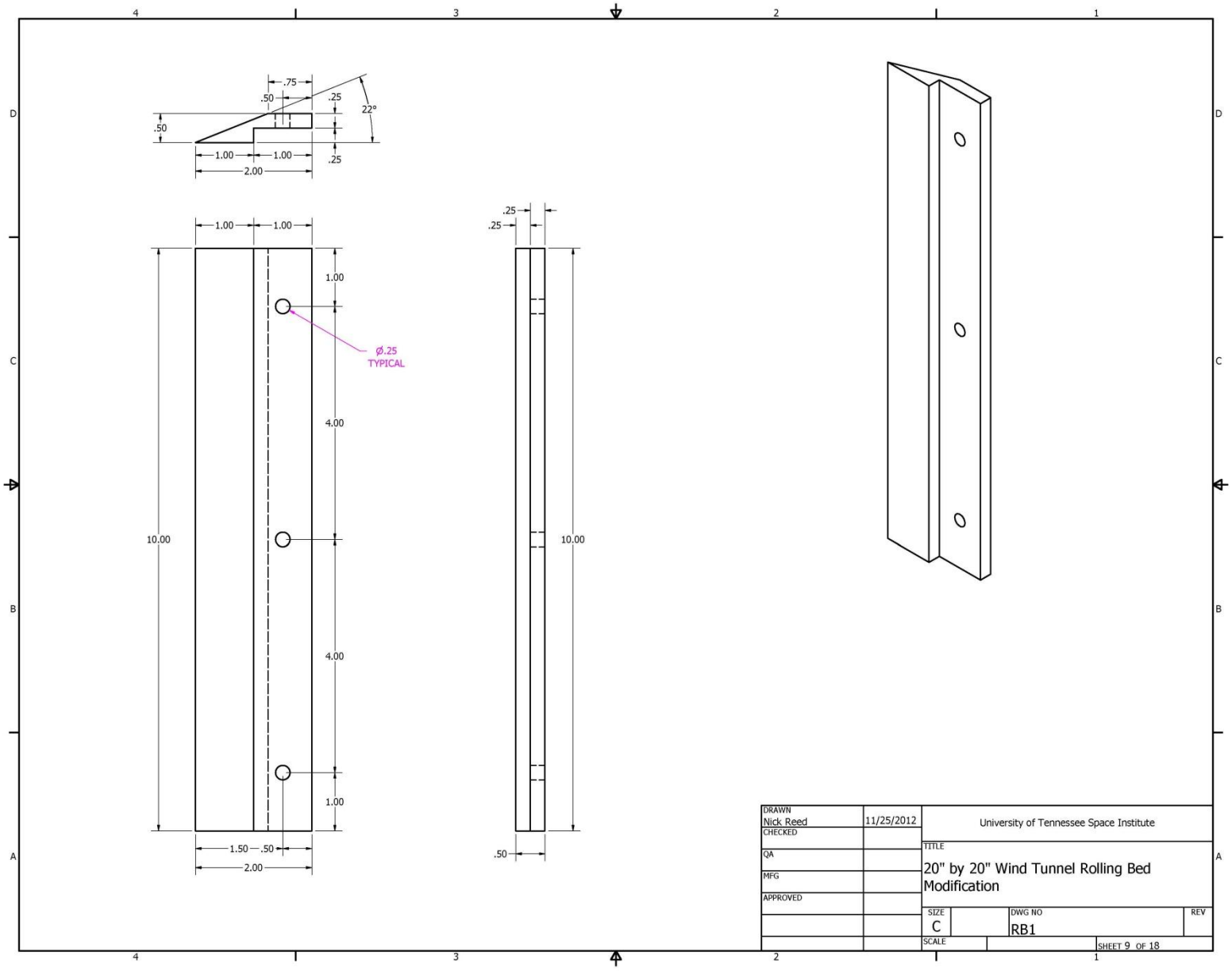
.75
.50
.25
22°
.50
1.00
1.00
.25
2.00
1.00
1.00
1.00
Ø.25
TYPICAL
4.00
10.00
4.00
1.00
1.50
.50
2.00
.25
.25
10.00
.50
DRAWN
Nick Reed
11/25/2012
CHECKED
QA
MFG
APPROVED
University of Tennessee Space Institute
TITLE
20" by 20" Wind Tunnel Rolling Bed Modification
SIZE
C
DWG NO
RB1
REV
SCALE
SHEET 9 OF 18

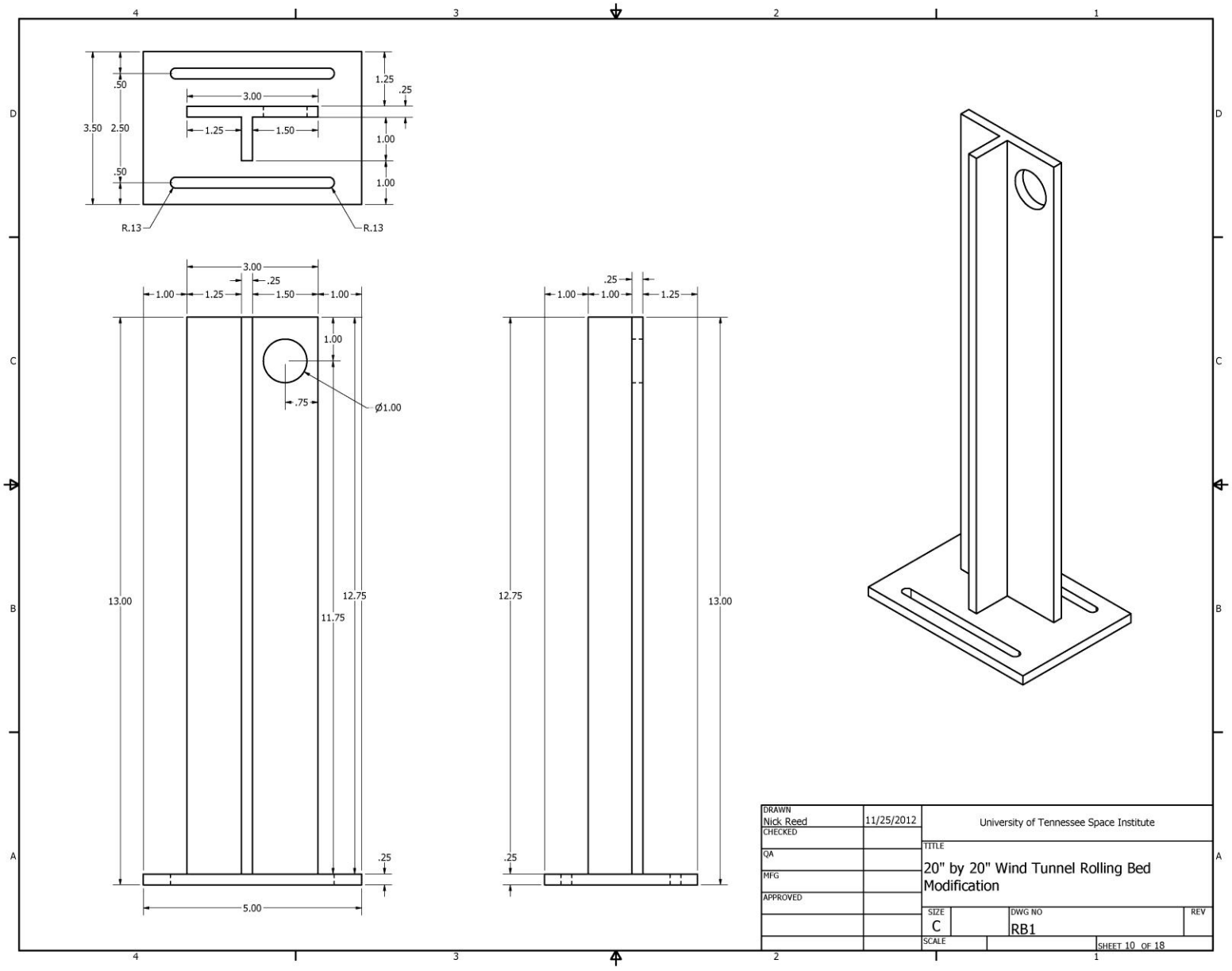
3.50
2.50
.50
.50
3.00
1.25
1.50
1.25
.25
1.00
1.00
R.13
R.13
3.00
.25
1.00
1.25
1.50
1.00
1.00
.75
Ø1.00
13.00
12.75
11.75
.25
5.00
.25
1.00
1.00
1.25
12.75
13.00
.25
DRAWN
Nick Reed
11/25/2012
CHECKED
QA
MFG
APPROVED
University of Tennessee Space Institute
TITLE
20" by 20" Wind Tunnel Rolling Bed Modification
SIZE
C
DWG NO
RB1
REV
SCALE
SHEET 10 OF 18

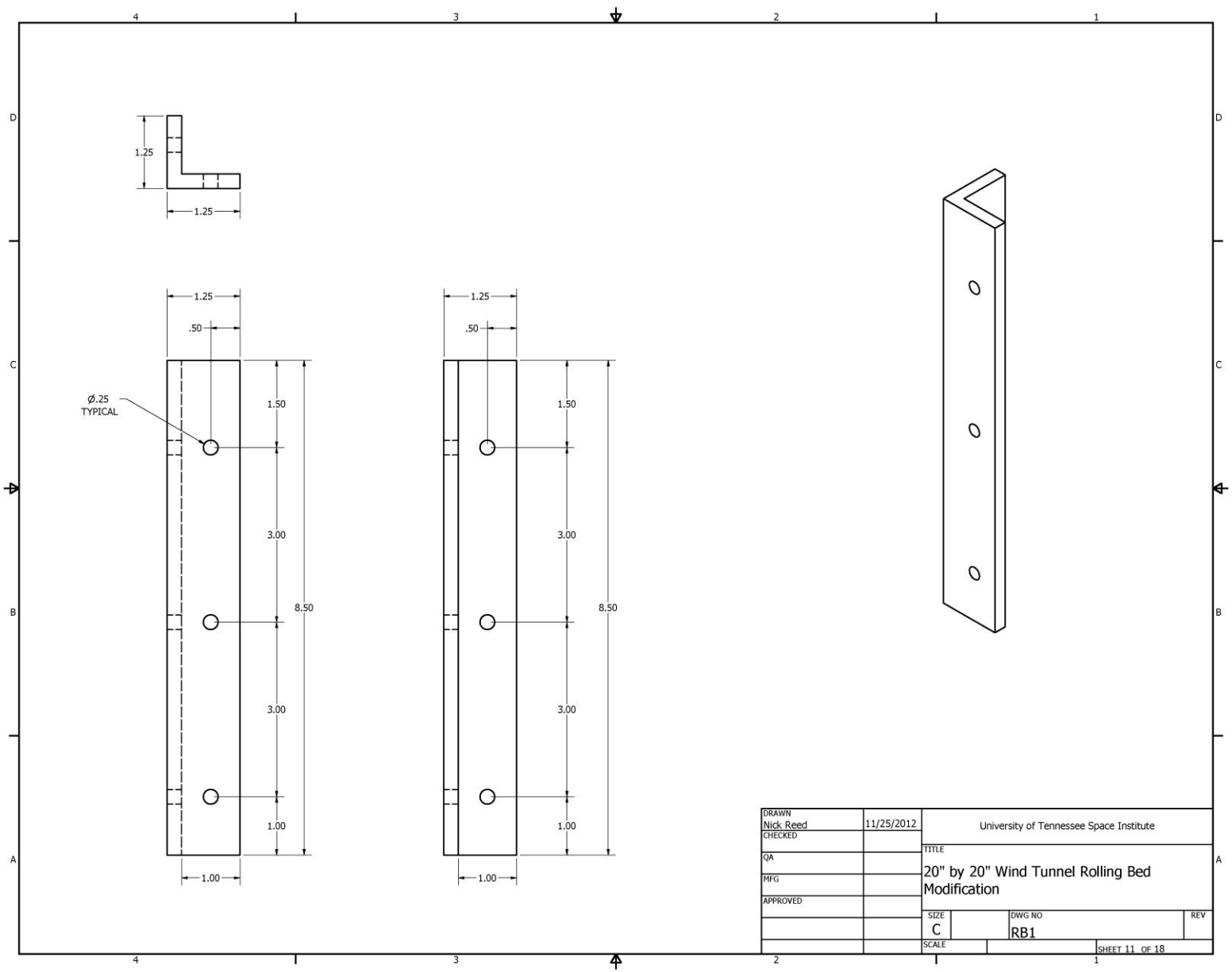
1.25
1.25
1.25
.50
Ø.25
TYPICAL
1.50
3.00
3.00
1.00
8.50
1.00
1.25
.50
1.50
3.00
3.00
1.00
8.50
1.00
DRAWN
Nick Reed
11/25/2012
CHECKED
QA
MFG
APPROVED
University of Tennessee Space Institute
TITLE
20" by 20" Wind Tunnel Rolling Bed Modification
SIZE
C
DWG NO
RB1
REV
SCALE
SHEET 11 OF 18

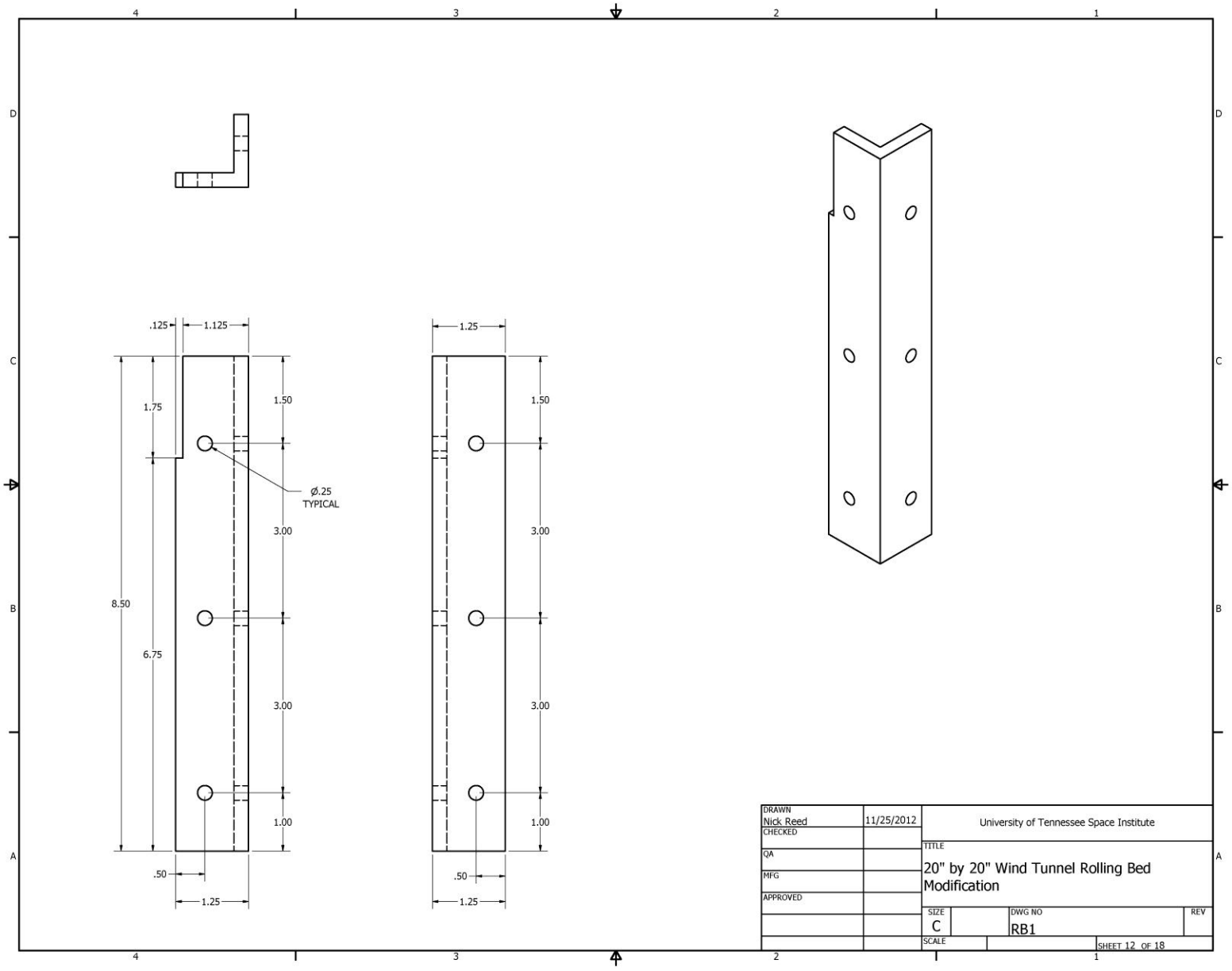
.125
1.125
1.75
1.50
Ø.25
TYPICAL
3.00
8.50
6.75
3.00
1.00
.50
1.25
1.25
1.50
3.00
3.00
1.00
.50
1.25
DRAWN
Nick Reed
11/25/2012
CHECKED
QA
MFG
APPROVED
University of Tennessee Space Institute
TITLE
20" by 20" Wind Tunnel Rolling Bed Modification
SIZE
C
DWG NO
RB1
REV
SCALE
SHEET 12 OF 18

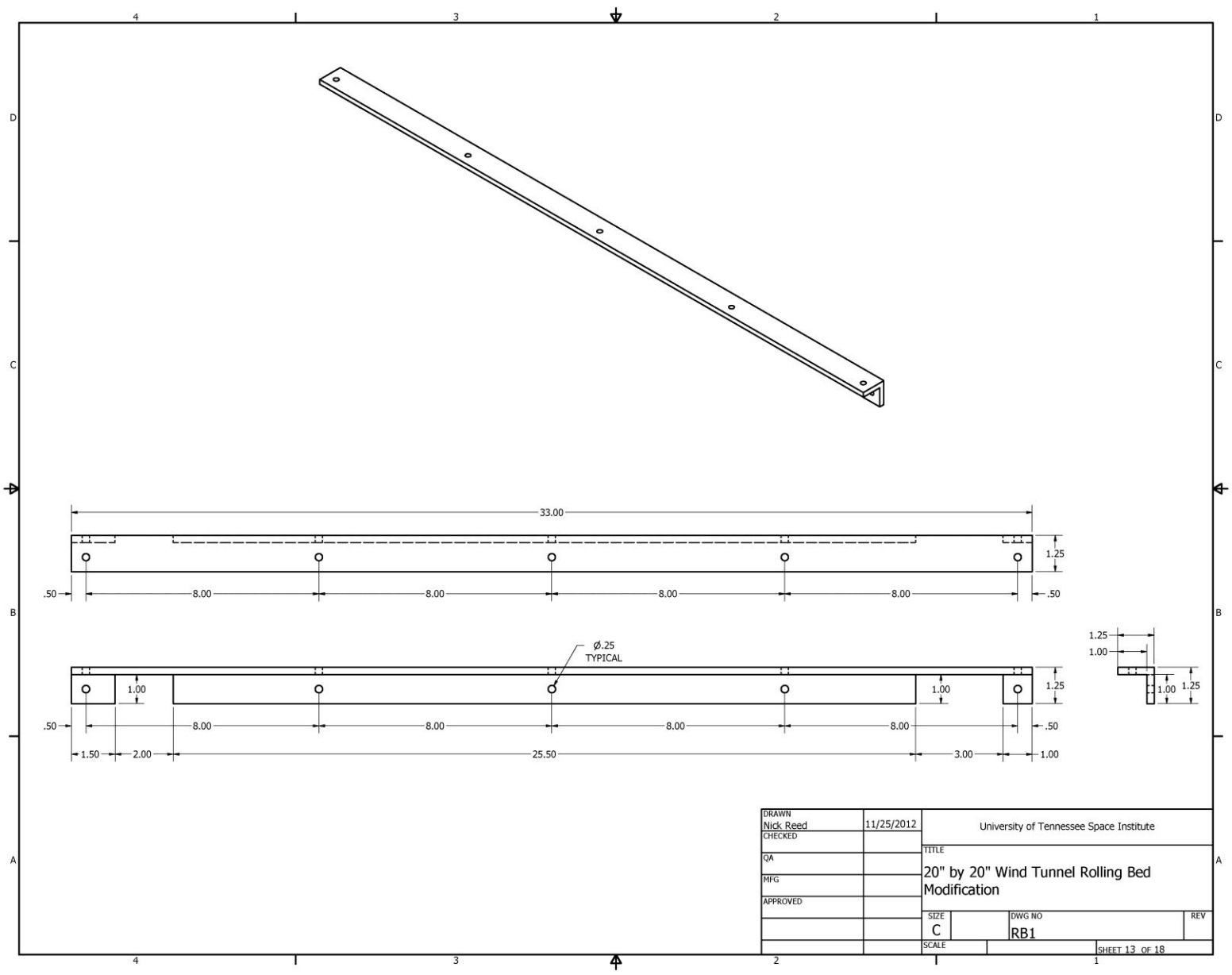
33.00
1.25
.50
8.00
8.00
8.00
8.00
.50
Ø.25
TYPICAL
1.00
1.00
1.25
1.50
2.00
25.50
3.00
1.00
1.25
1.00
1.00
1.25
DRAWN
Nick Reed
11/25/2012
CHECKED
QA
MFG
APPROVED
University of Tennessee Space Institute
TITLE
20" by 20" Wind Tunnel Rolling Bed Modification
SIZE
C
DWG NO
RB1
REV
SCALE
SHEET 13 OF 18

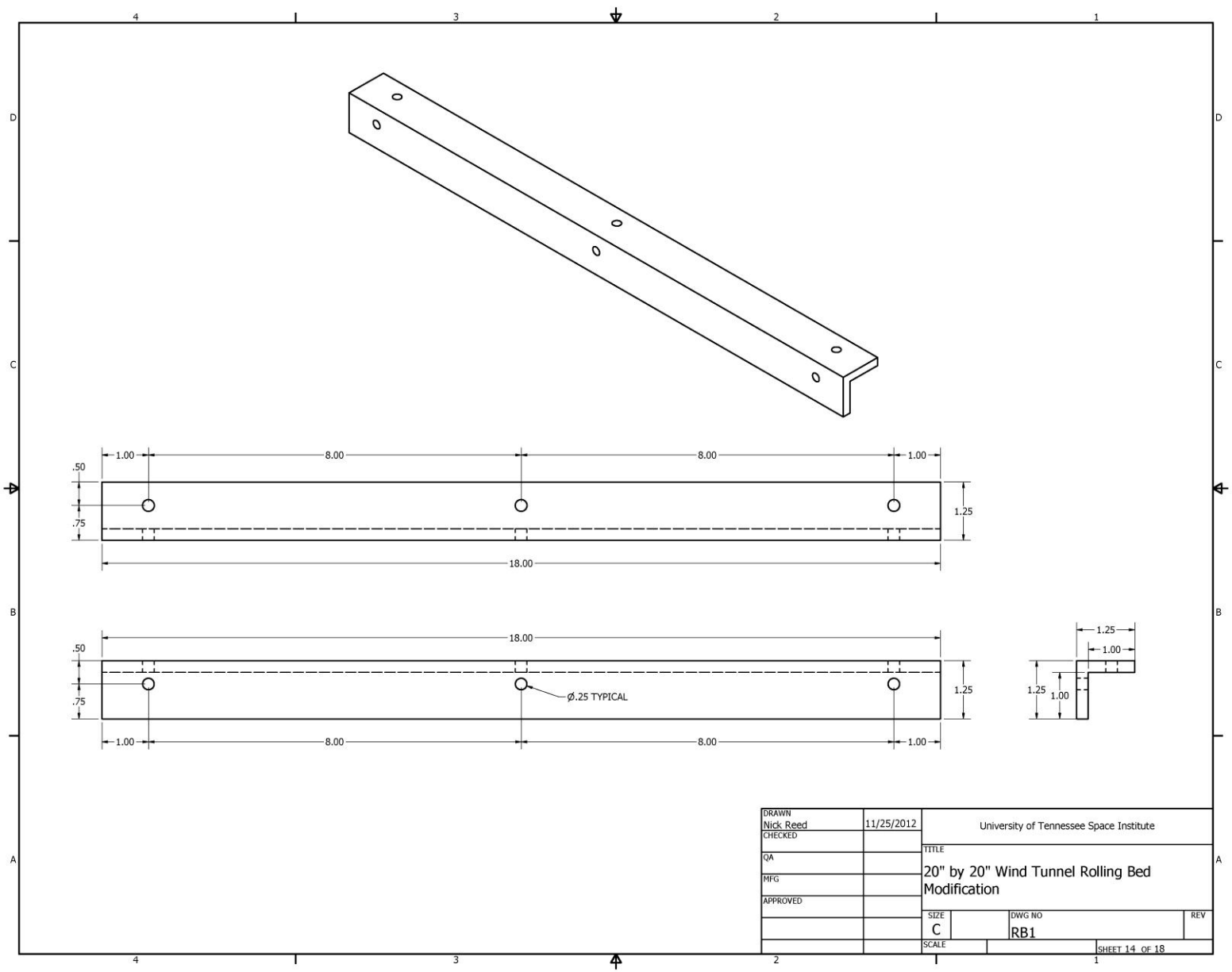
1.00
8.00
8.00
1.00
.50
.75
1.25
18.00
18.00
.50
.75
Ø.25 TYPICAL
1.25
1.00
1.25
1.00
1.00
8.00
8.00
1.00
DRAWN
Nick Reed
11/25/2012
CHECKED
QA
MFG
APPROVED
University of Tennessee Space Institute
TITLE
20" by 20" Wind Tunnel Rolling Bed Modification
SIZE
C
DWG NO
RB1
REV
SCALE
SHEET 14 OF 18

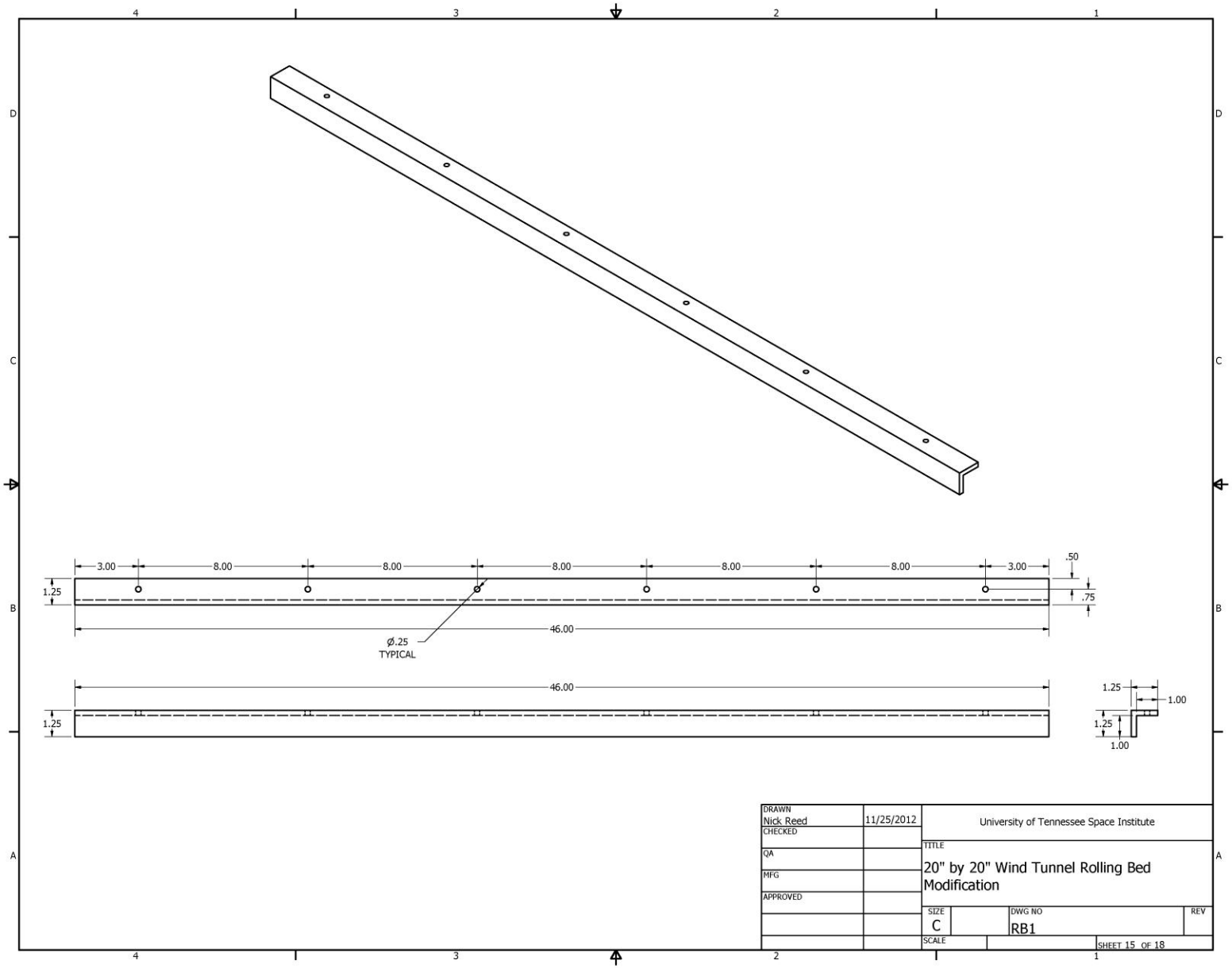
3.00
8.00
8.00
8.00
8.00
8.00
3.00
.50
.75
1.25
46.00
Ø.25
TYPICAL
46.00
1.25
1.25
1.25
1.00
1.00
DRAWN
Nick Reed
11/25/2012
CHECKED
QA
MFG
APPROVED
University of Tennessee Space Institute
TITLE
20" by 20" Wind Tunnel Rolling Bed Modification
SIZE
C
DWG NO
RB1
REV
SCALE
SHEET 15 OF 18

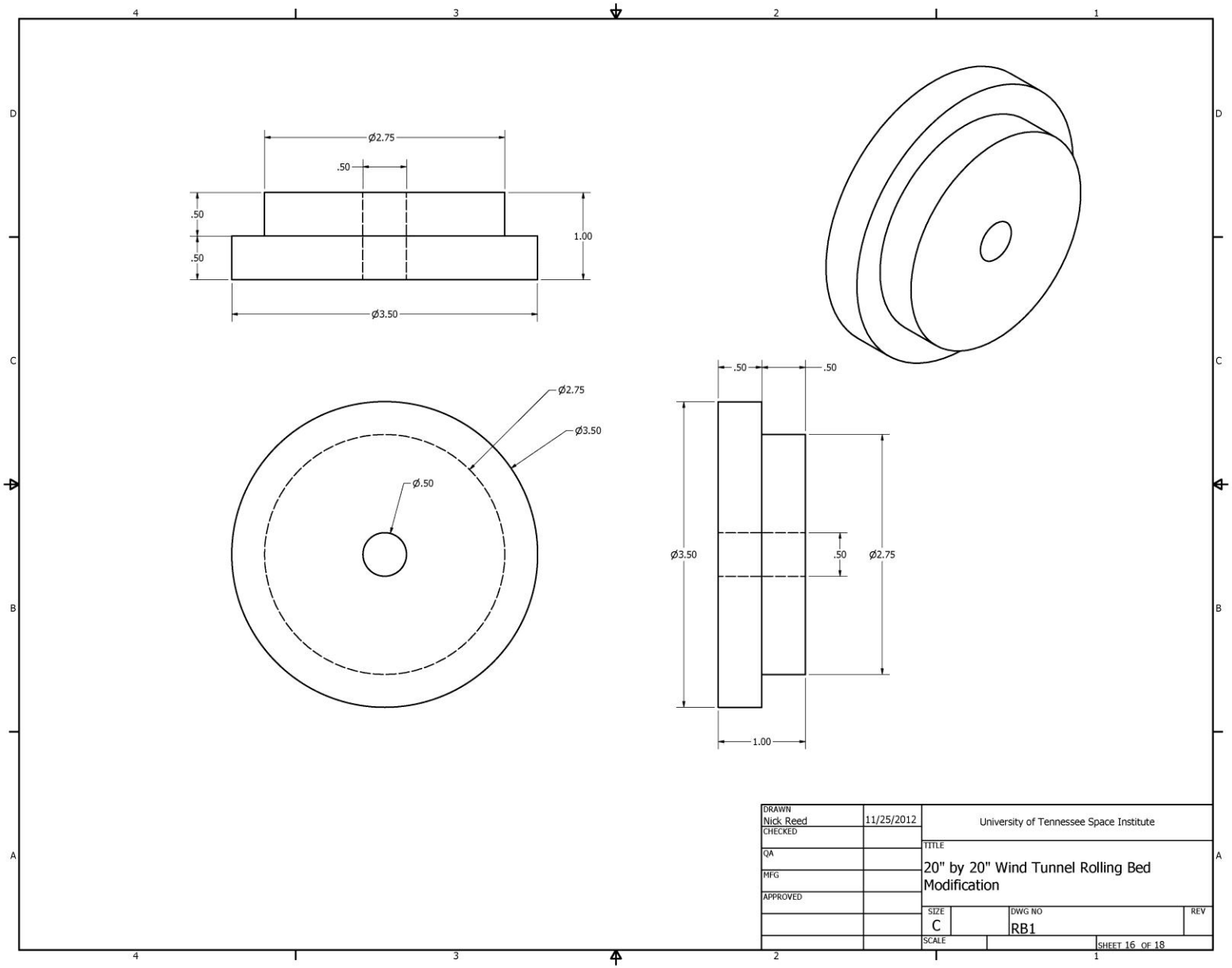
Ø2.75
.50
.50
.50
1.00
Ø3.50
Ø2.75
Ø3.50
Ø.50
.50
.50
Ø3.50
.50
Ø2.75
1.00
DRAWN
Nick Reed
11/25/2012
CHECKED
QA
MFG
APPROVED
University of Tennessee Space Institute
TITLE
20" by 20" Wind Tunnel Rolling Bed Modification
SIZE
C
DWG NO
RB1
REV
SCALE
SHEET 16 OF 18

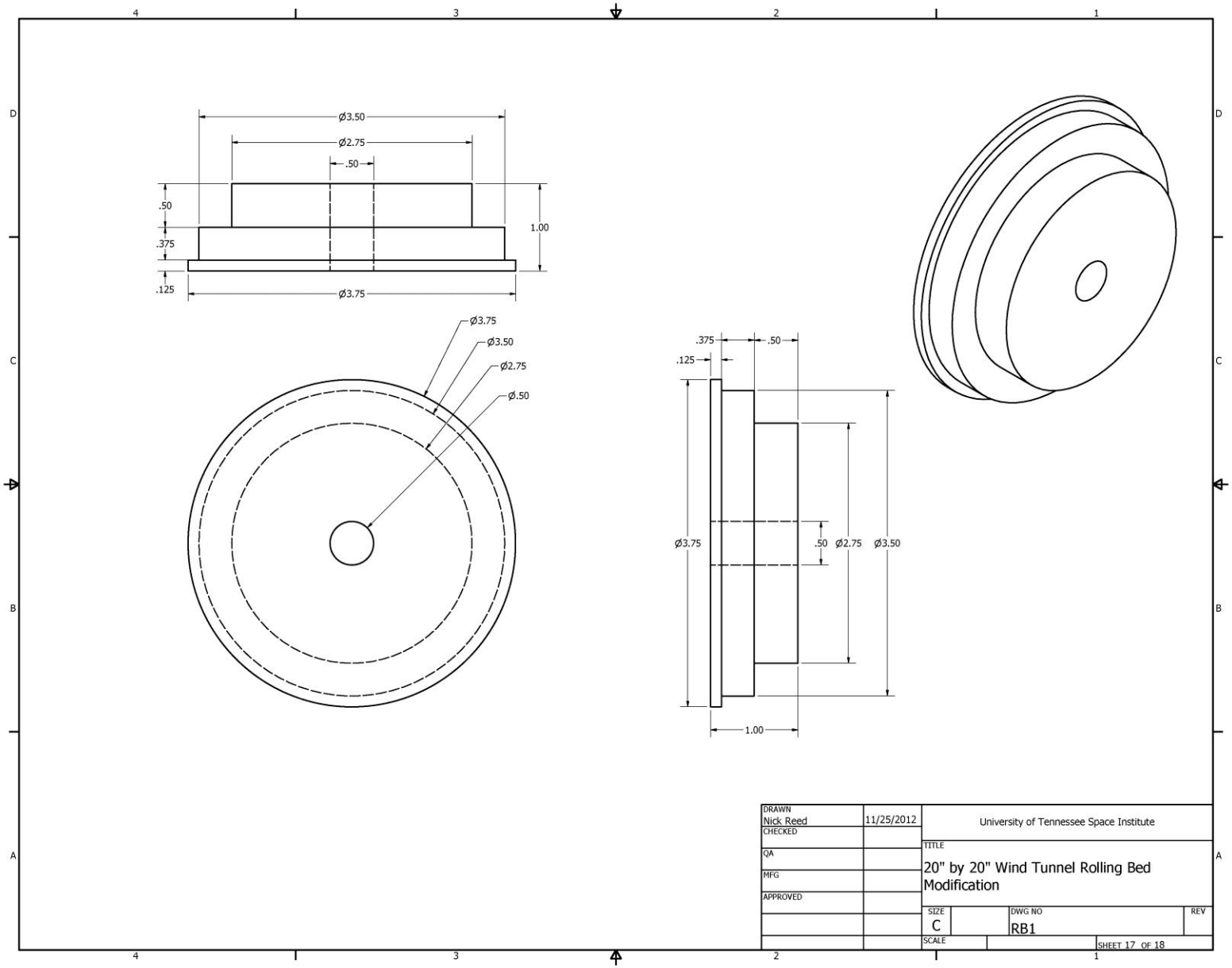
Ø3.50
Ø2.75
.50
.50
.375
.125
1.00
Ø3.75
Ø3.75
Ø3.50
Ø2.75
Ø.50
.375
.125
.50
Ø3.75
.50
Ø2.75
Ø3.50
1.00
DRAWN
Nick Reed
11/25/2012
CHECKED
QA
MFG
APPROVED
University of Tennessee Space Institute
TITLE
20" by 20" Wind Tunnel Rolling Bed Modification
SIZE
C
DWG NO
RB1
REV
SCALE
SHEET 17 OF 18

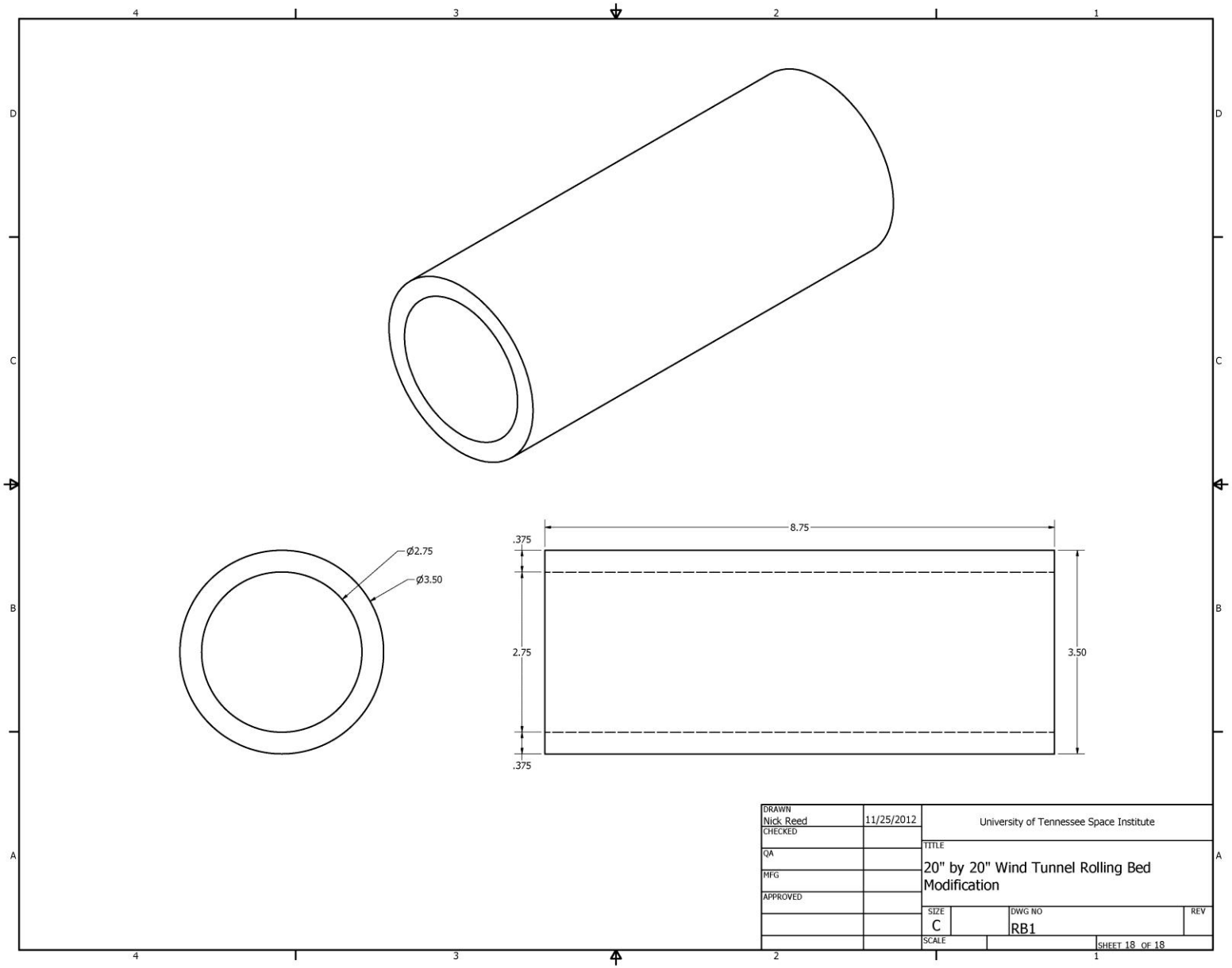
Ø2.75
Ø3.50
8.75
.375
2.75
3.50
.375
DRAWN
Nick Reed
11/25/2012
CHECKED
QA
MFG
APPROVED
University of Tennessee Space Institute
TITLE
20" by 20" Wind Tunnel Rolling Bed Modification
SIZE
C
DWG NO
RB1
REV
SCALE
SHEET 18 OF 18

Appendix Section 2
Crowned Roller Step Table

Distance From Edge of Roller	Step Diameter		Distance From Edge of Roller	Step Diameter		Distance From Edge of Roller	Step Diameter
0	3.31250		2	3.43480		4	3.49396
0.05	3.31633		2.05	3.43705		4.05	3.49463
0.1	3.32012		2.1	3.43926		4.1	3.49526
0.15	3.32387		2.15	3.44143		4.15	3.49585
0.2	3.32758		2.2	3.44356		4.2	3.49641
0.25	3.33125		2.25	3.44565		4.25	3.49692
0.3	3.33488		2.3	3.44770		4.3	3.49739
0.35	3.33847		2.35	3.44971		4.35	3.49783
0.4	3.34202		2.4	3.45169		4.4	3.49822
0.45	3.34553		2.45	3.45362		4.45	3.49858
0.5	3.34900		2.5	3.45551		4.5	3.49889
0.55	3.35243		2.55	3.45736		4.55	3.49917
0.6	3.35583		2.6	3.45918		4.6	3.49940
0.65	3.35918		2.65	3.46095		4.65	3.49960
0.7	3.36250		2.7	3.46269		4.7	3.49976
0.75	3.36577		2.75	3.46438		4.75	3.49988
0.8	3.36901		2.8	3.46604		4.8	3.49996
0.85	3.37220		2.85	3.46766		4.85	3.50000
0.9	3.37536		2.9	3.46924		4.875	3.50000
0.95	3.37847		2.95	3.47077			
1	3.38155		3	3.47227			
1.05	3.38459		3.05	3.47373			
1.1	3.38759		3.1	3.47515			
1.15	3.39055		3.15	3.47653			
1.2	3.39347		3.2	3.47787			
1.25	3.39635		3.25	3.47917			
1.3	3.39919		3.3	3.48044			
1.35	3.40199		3.35	3.48166			
1.4	3.40475		3.4	3.48284			
1.45	3.40747		3.45	3.48398			
1.5	3.41015		3.5	3.48509			
1.55	3.41279		3.55	3.48615			
1.6	3.41540		3.6	3.48718			
1.65	3.41796		3.65	3.48817			
1.7	3.42049		3.7	3.48911			
1.75	3.42297		3.75	3.49002			
1.8	3.42542		3.8	3.49089			
1.85	3.42782		3.85	3.49171			
1.9	3.43019		3.9	3.49250			
1.95	3.43252		3.95	3.49325			

Appendix Section 3
Adjuster Arm Drawings

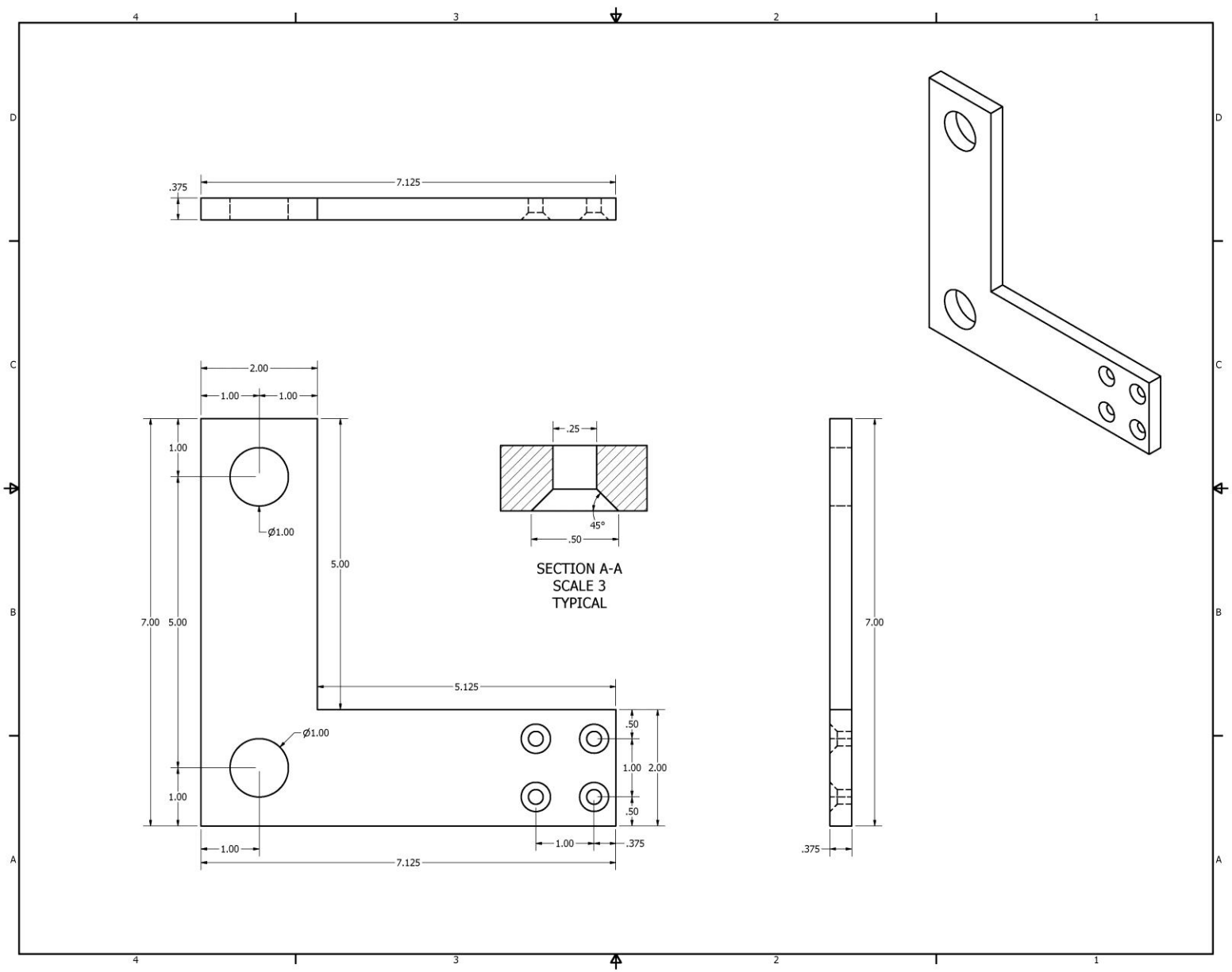
.375
7.125
2.00
1.00
1.00
1.00
Ø1.00
5.00
7.00
5.00
Ø1.00
1.00
5.125
.50
1.00
2.00
.50
1.00
.375
7.125
.25
45°
.50
SECTION A-A
SCALE 3
TYPICAL
7.00
.375

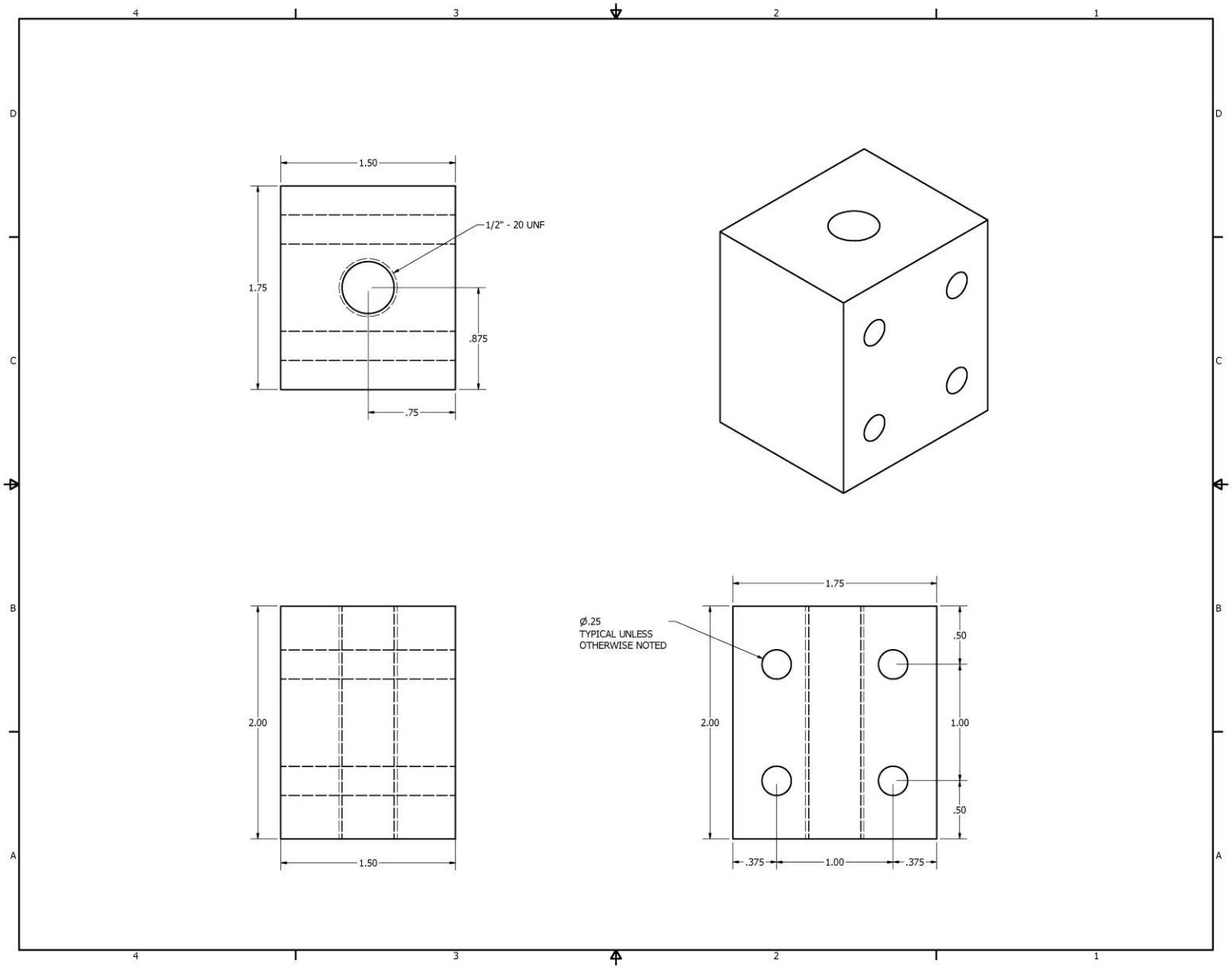
1.50
1/2" - 20 UNF
1.75
.875
.75
2.00
1.50
1.75
Ø.25
TYPICAL UNLESS
OTHERWISE NOTED
.50
2.00
1.00
.50
.375
1.00
.375

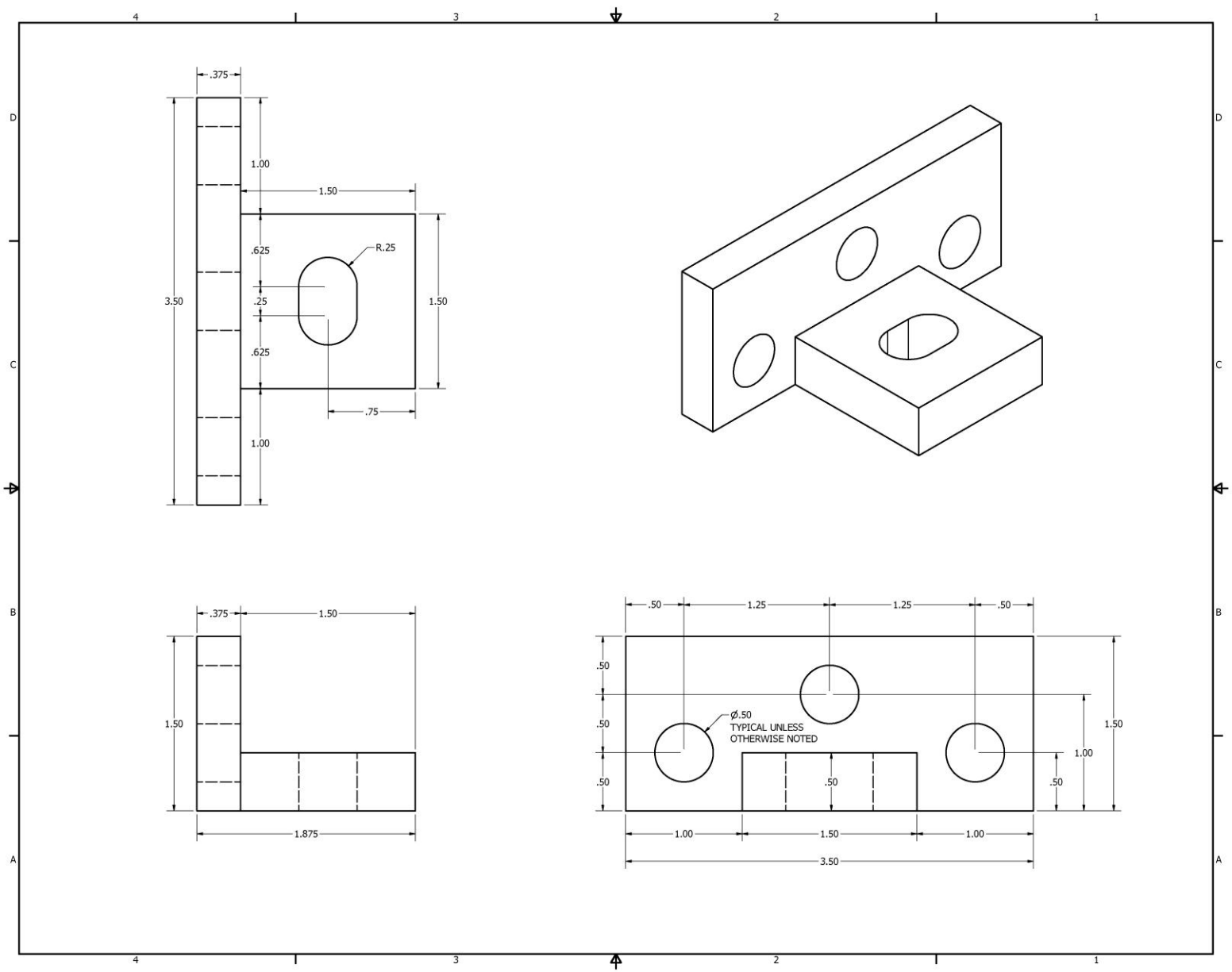
.375
1.00
1.50
.625
R.25
3.50
.25
1.50
.625
.75
1.00
.375
1.50
1.50
1.875
.50
1.25
1.25
.50
.50
.50
.50
Ø.50
TYPICAL UNLESS
OTHERWISE NOTED
1.50
1.00
.50
.50
1.00
1.50
1.00
3.50

Appendix Section 4
Sting Drawings

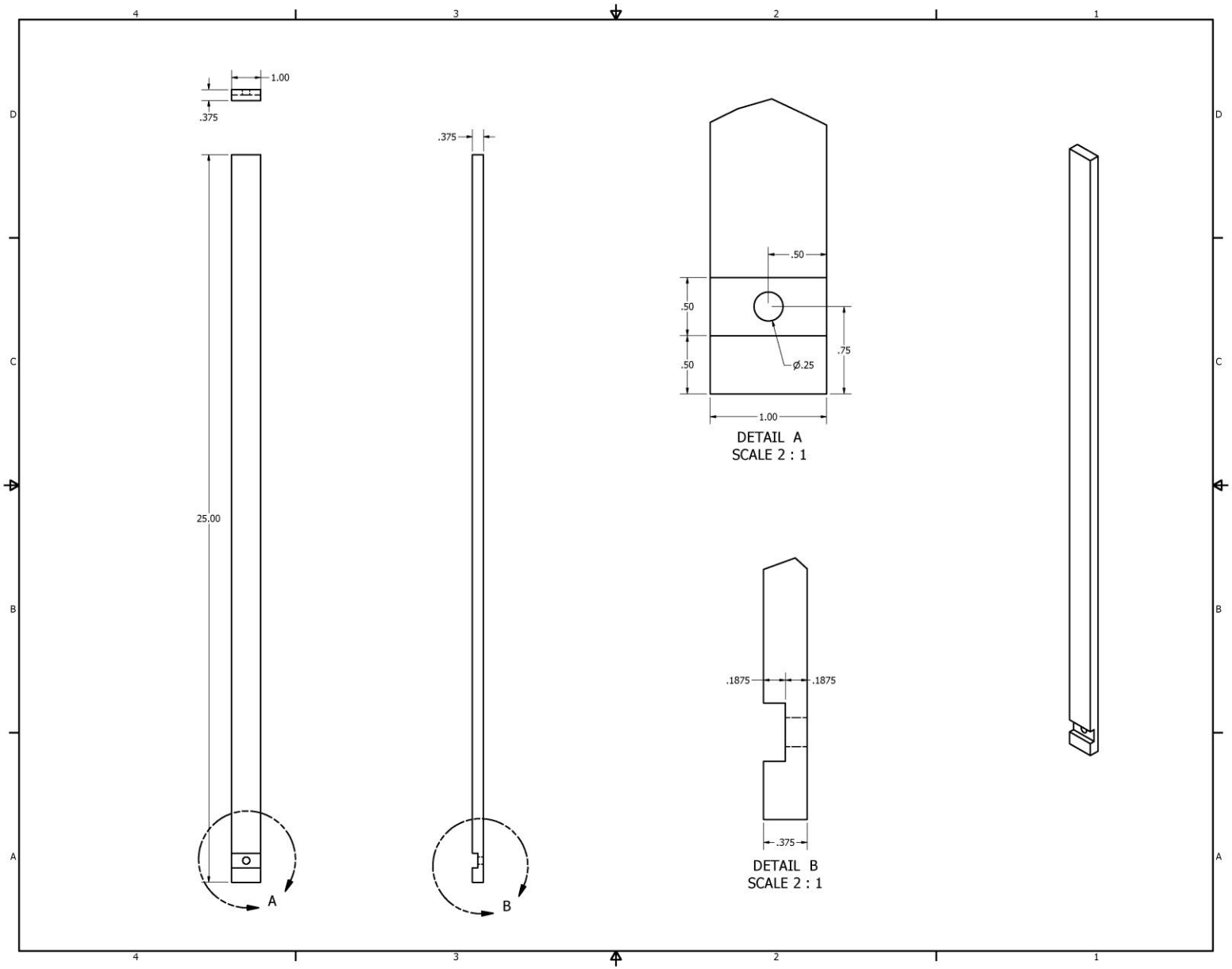
1.00
.375
25.00
A
.375
B
.50
.50
.50
Ø.25
.75
1.00
DETAIL A
SCALE 2 : 1
.1875
.1875
.375
DETAIL B
SCALE 2 : 1

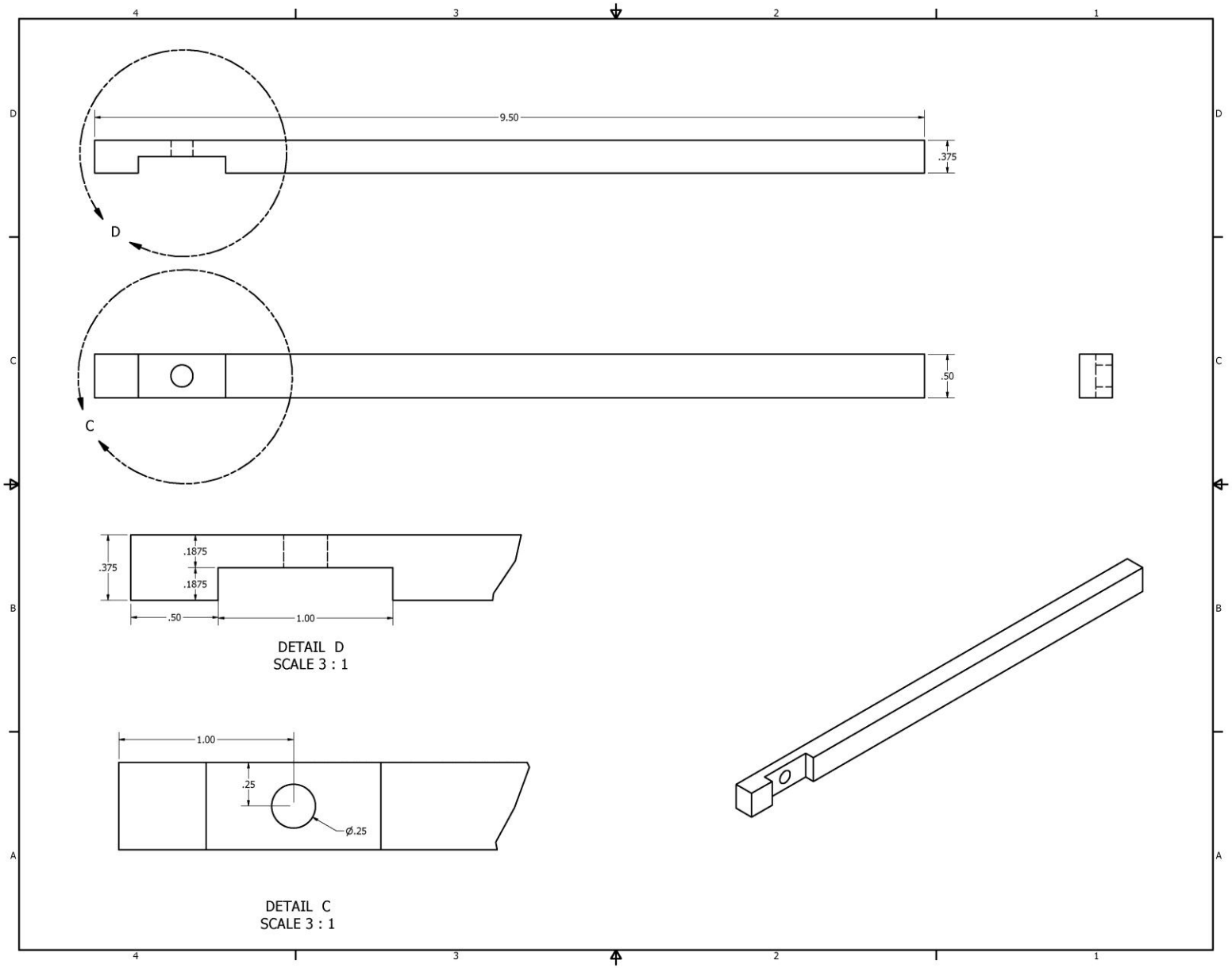
9.50
.375
D
.50
C
.375
.1875
.1875
.50
1.00
DETAIL D
SCALE 3 : 1
1.00
.25
Ø.25
DETAIL C
SCALE 3 : 1

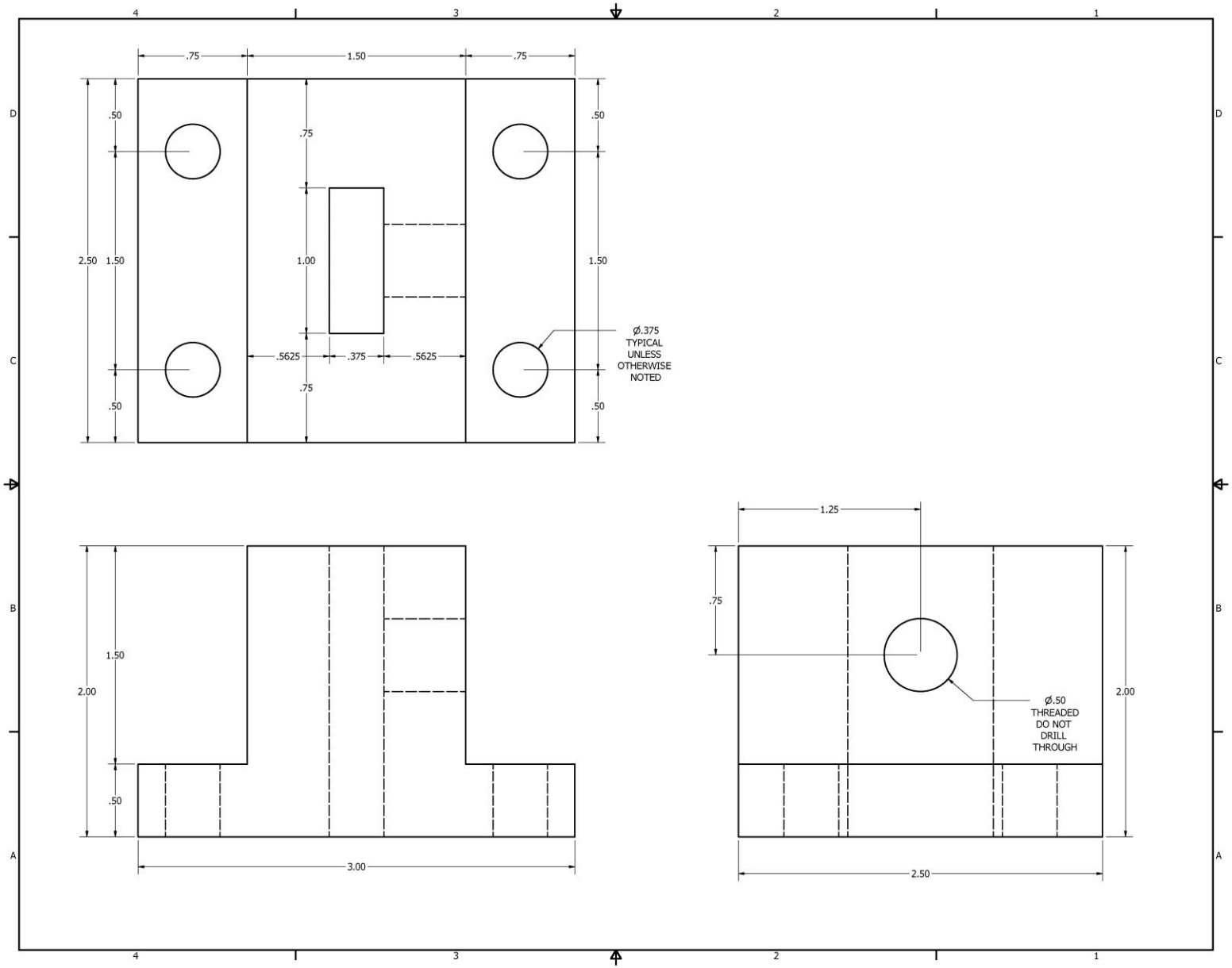
.75
1.50
.75
.50
.75
.50
2.50
1.50
1.00
1.50
Ø.375
TYPICAL
UNLESS
OTHERWISE
NOTED
.5625
.375
.5625
.75
.50
.50
1.25
.75
1.50
2.00
Ø.50
THREADED
DO NOT
DRILL
THROUGH
2.00
.50
3.00
2.50

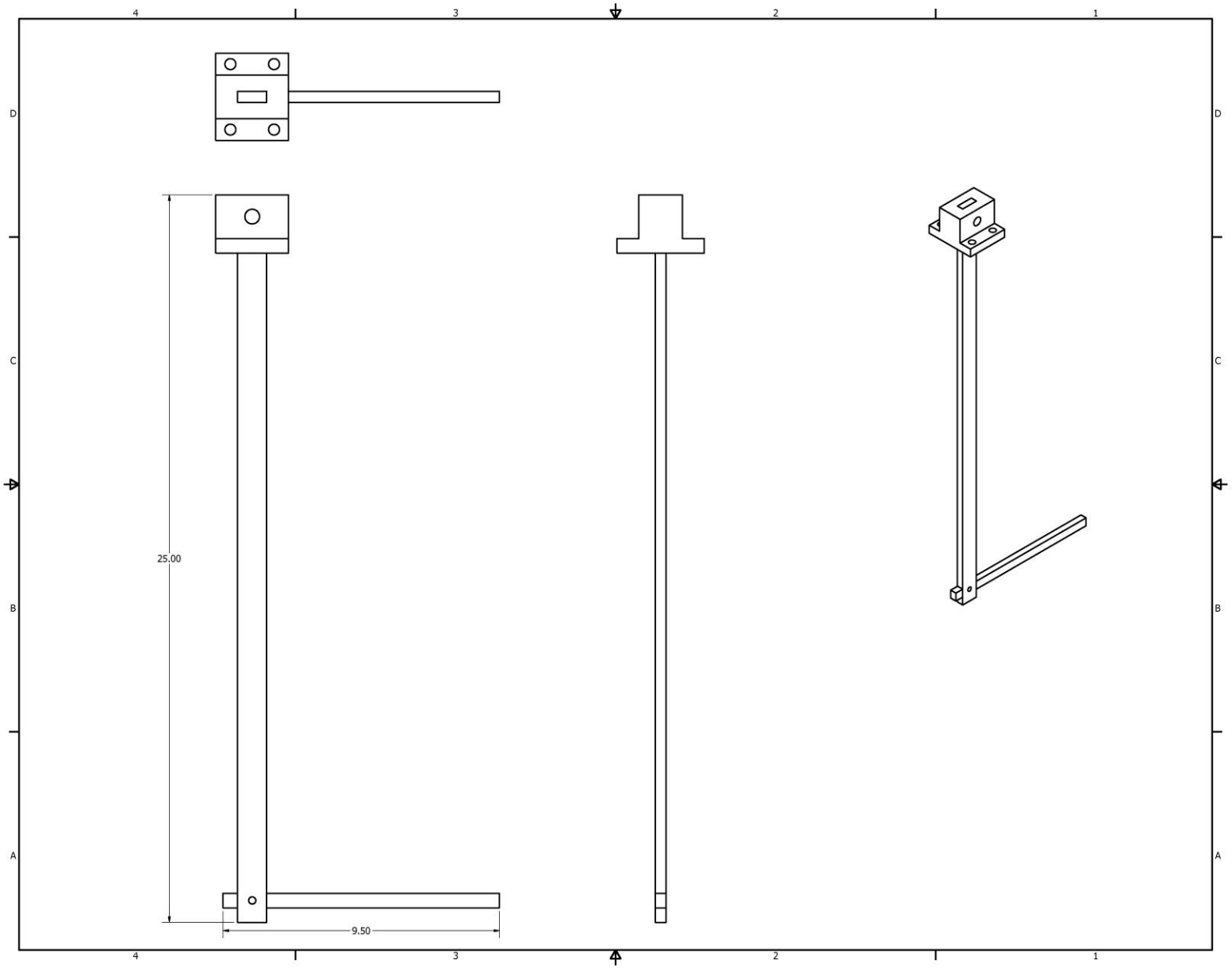
4
3
2
1
D
C
B
A
25.00
9.50

Appendix Section 5
Drag Reduction Device Drawings

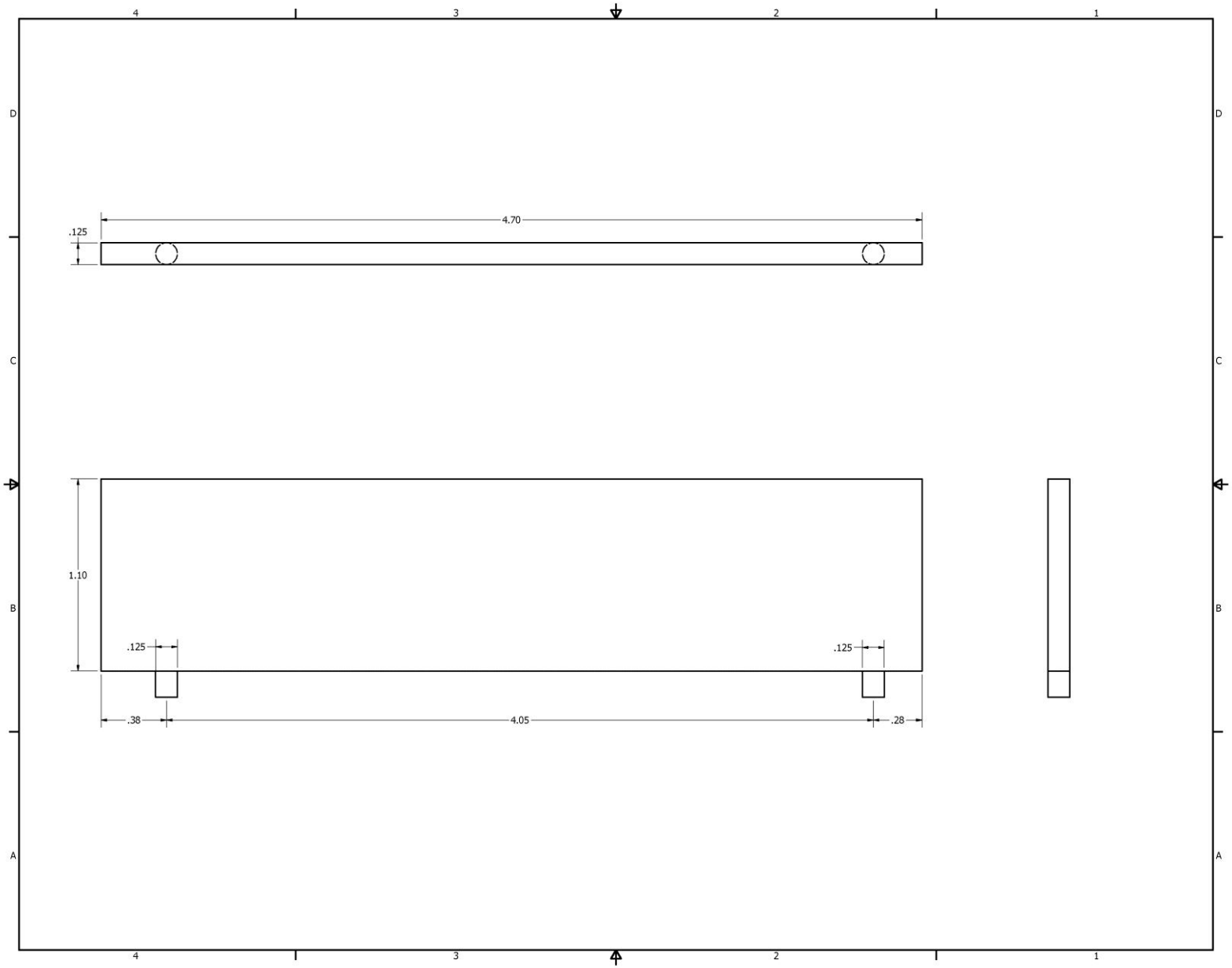
4
3
2
1
D
C
B
A
.125
4.70
1.10
.125
.125
.38
4.05
.28

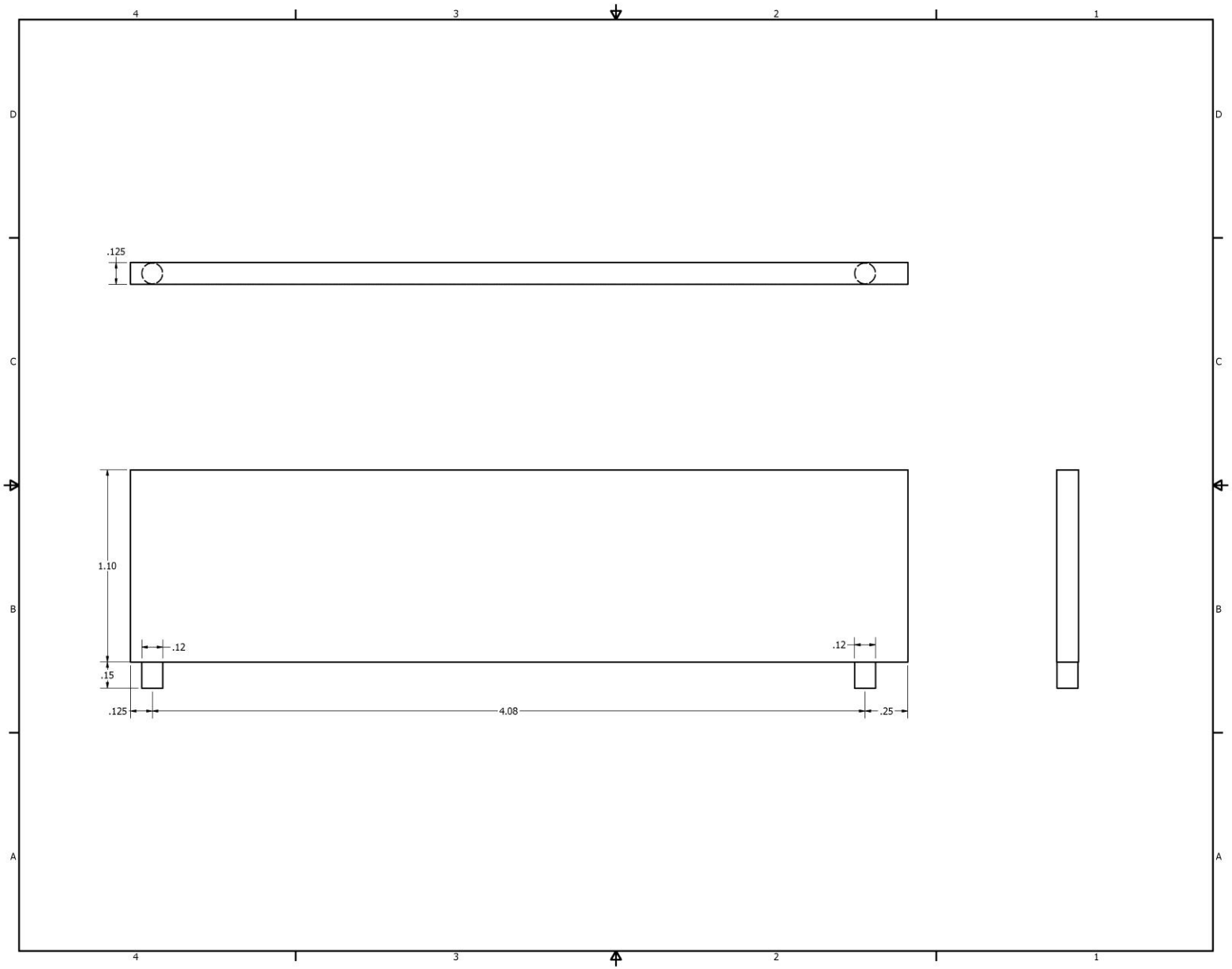
4
3
2
1
D
C
B
A
.125
1.10
.12
.12
.15
.125
4.08
.25

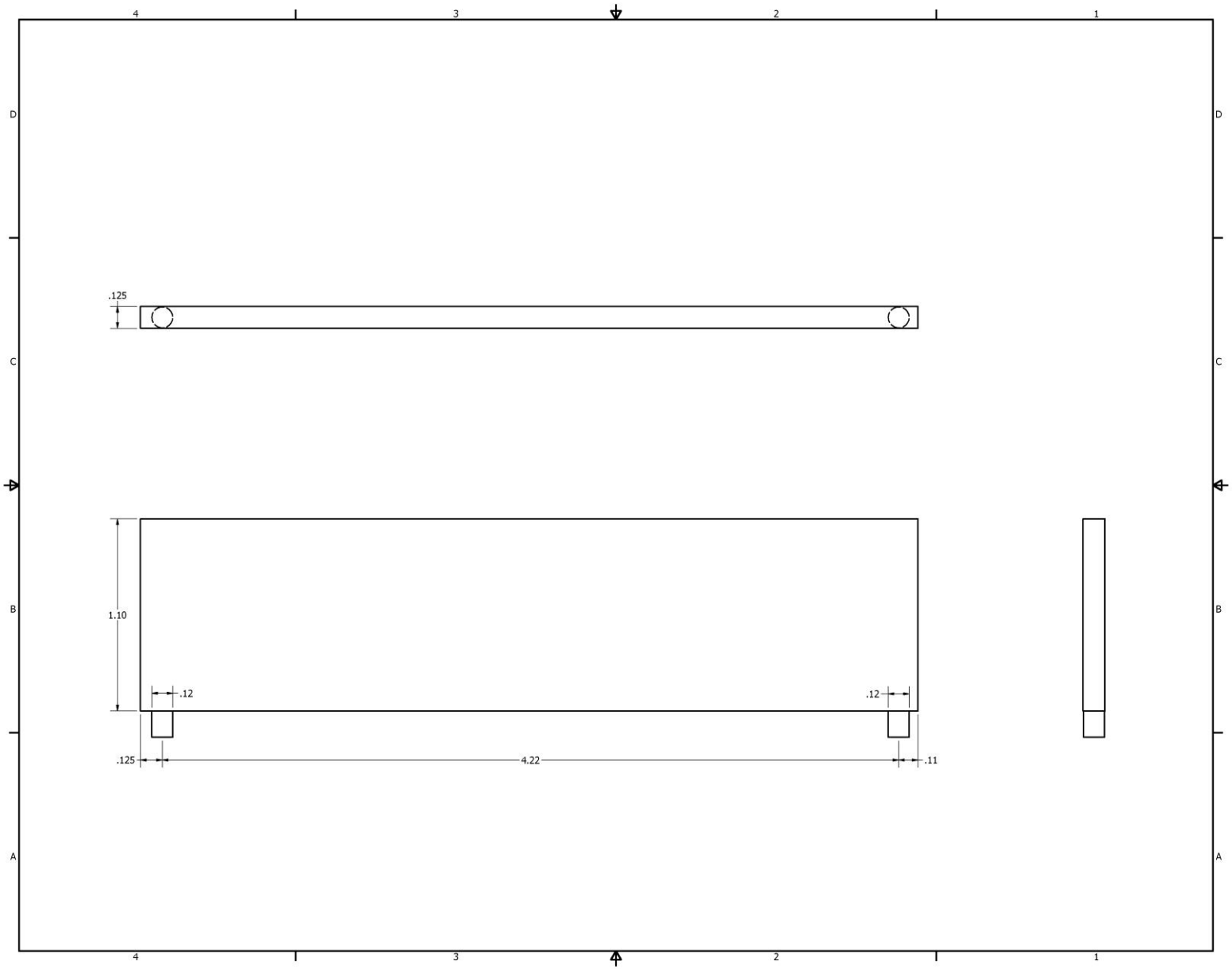
4
3
2
1
D
C
B
A
.125
1.10
.12
.12
.125
4.22
.11

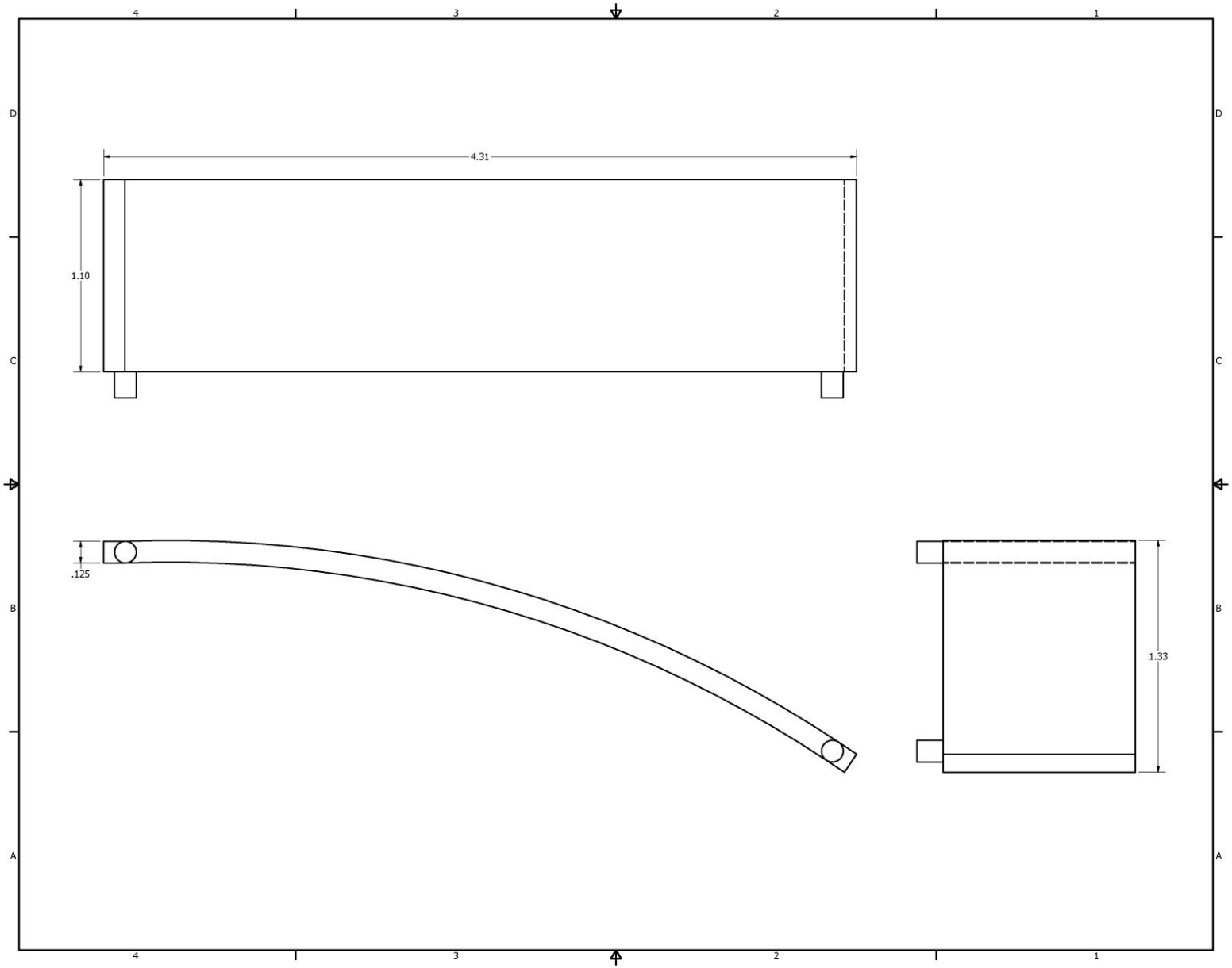
4.31
1.10
.125
1.33

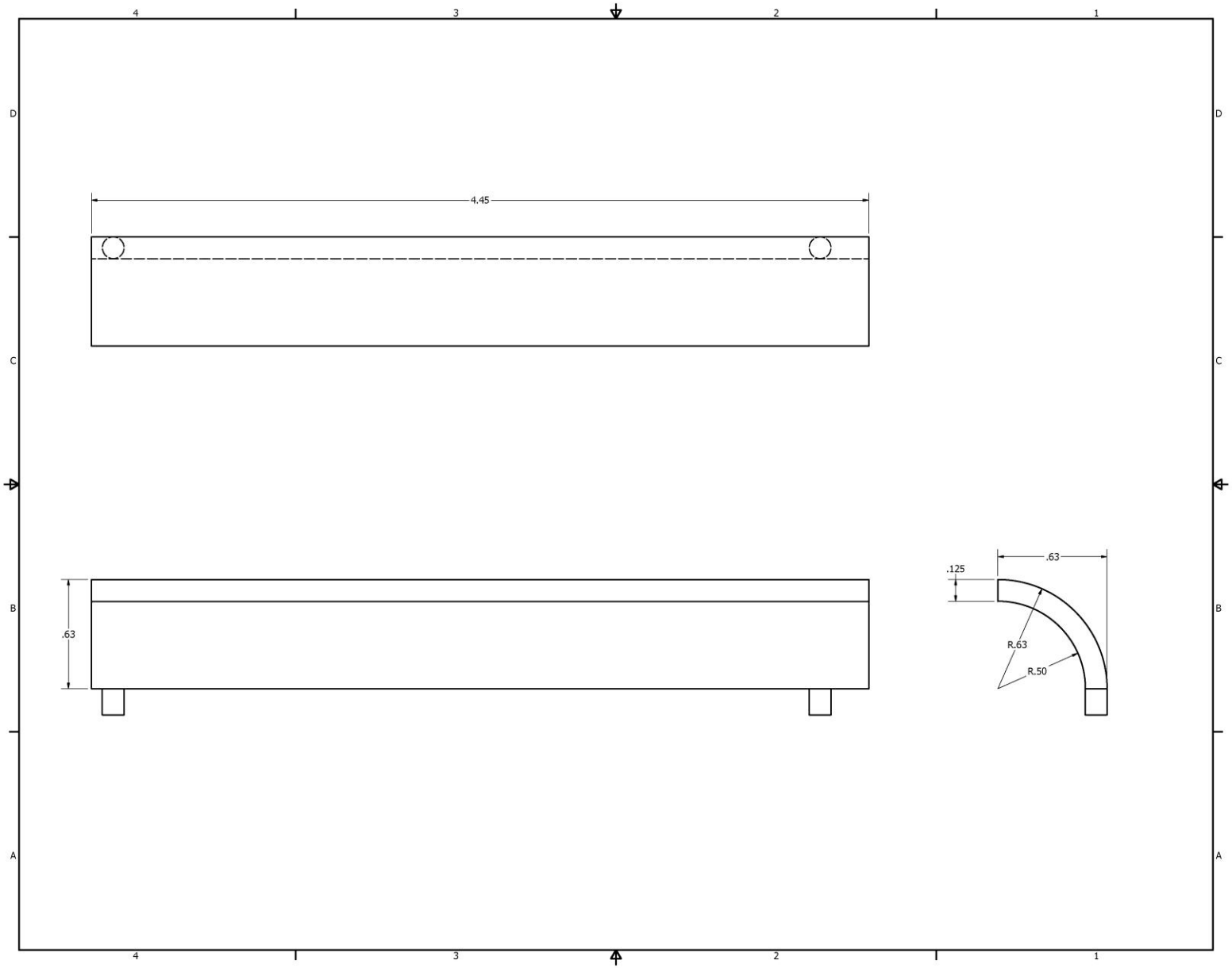
4
3
2
1
D
C
B
A
4.45
.63
.125
.63
R.63
R.50

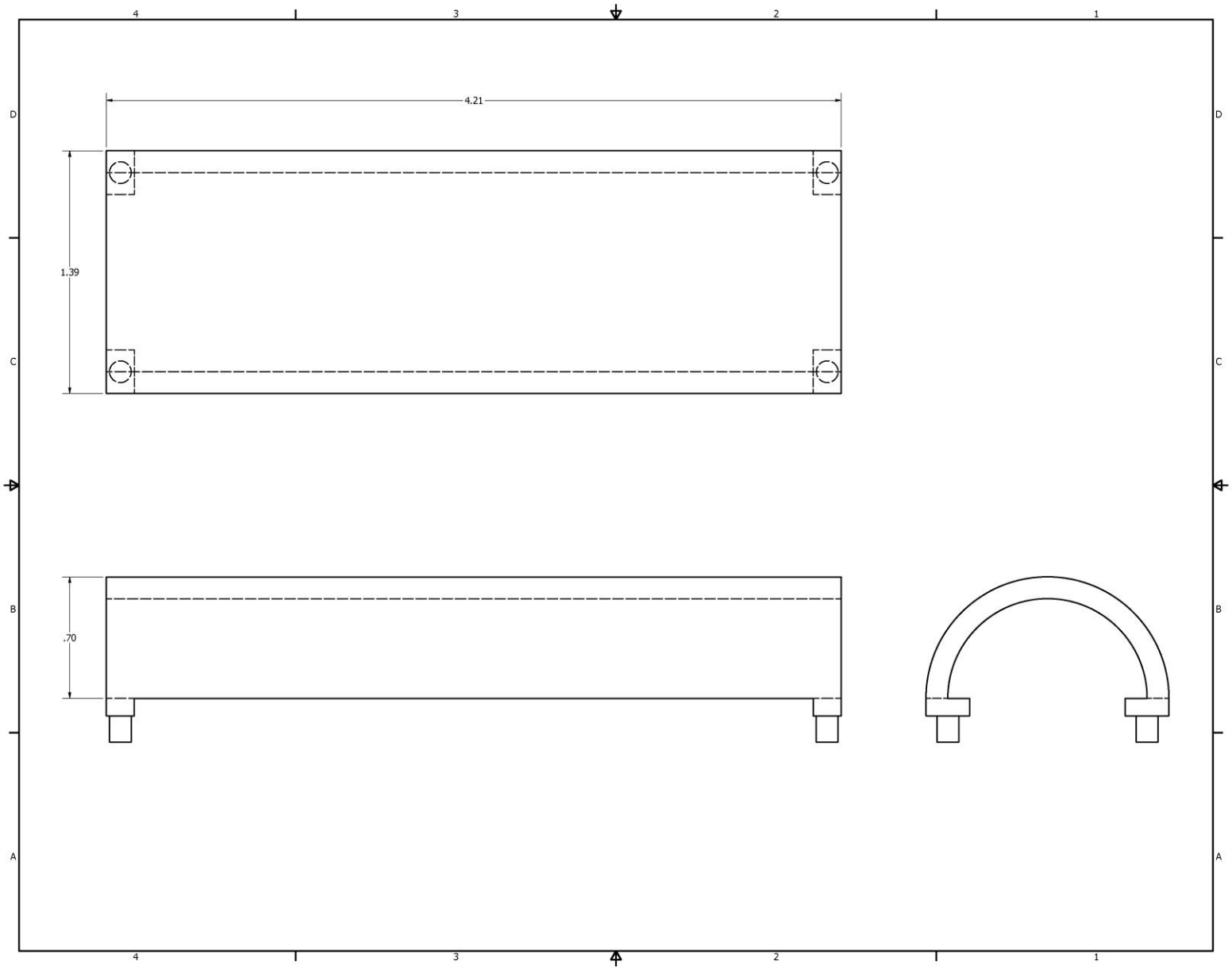
4.21
1.39
.70

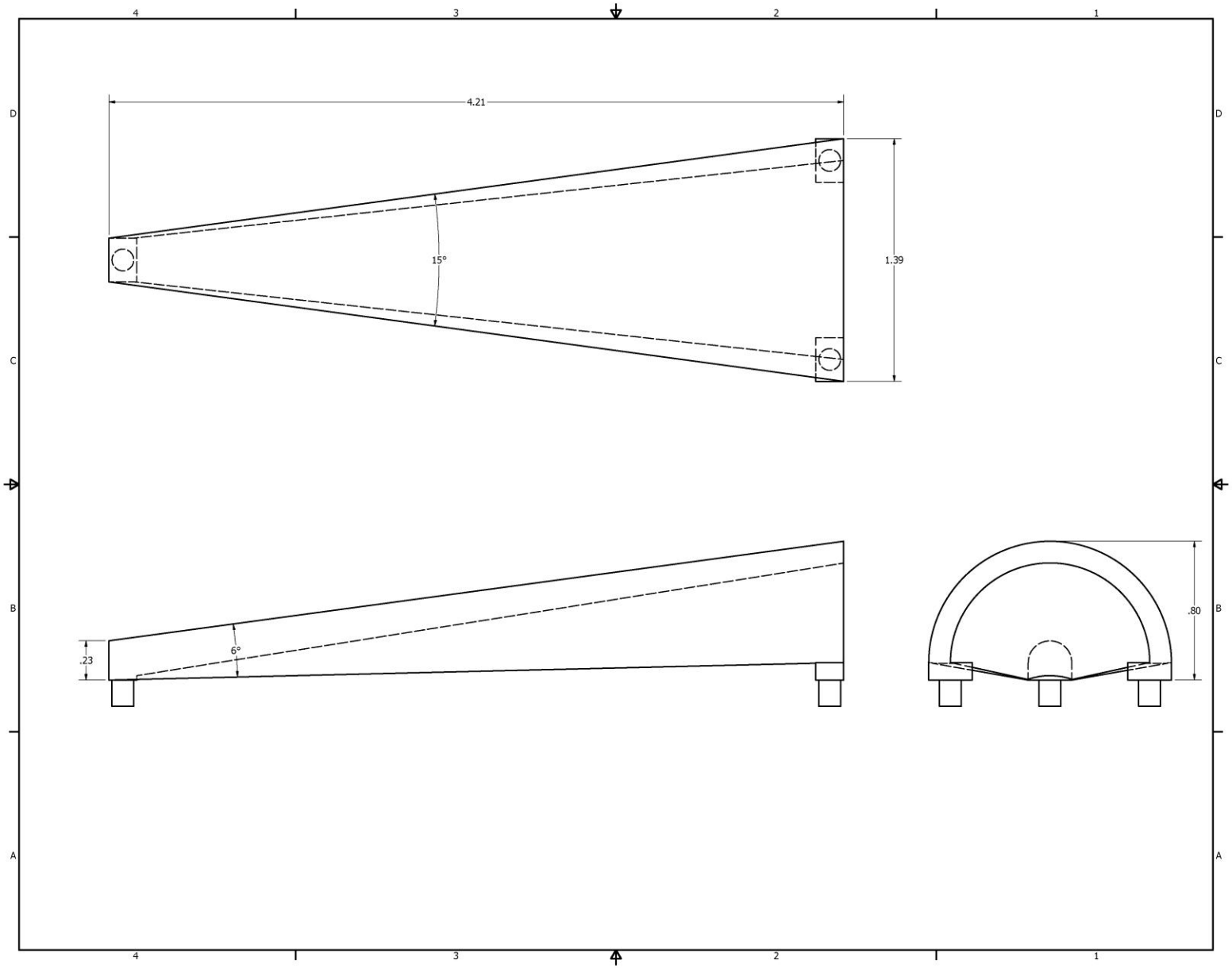
4.21
15°
1.39
.23
6°
.80

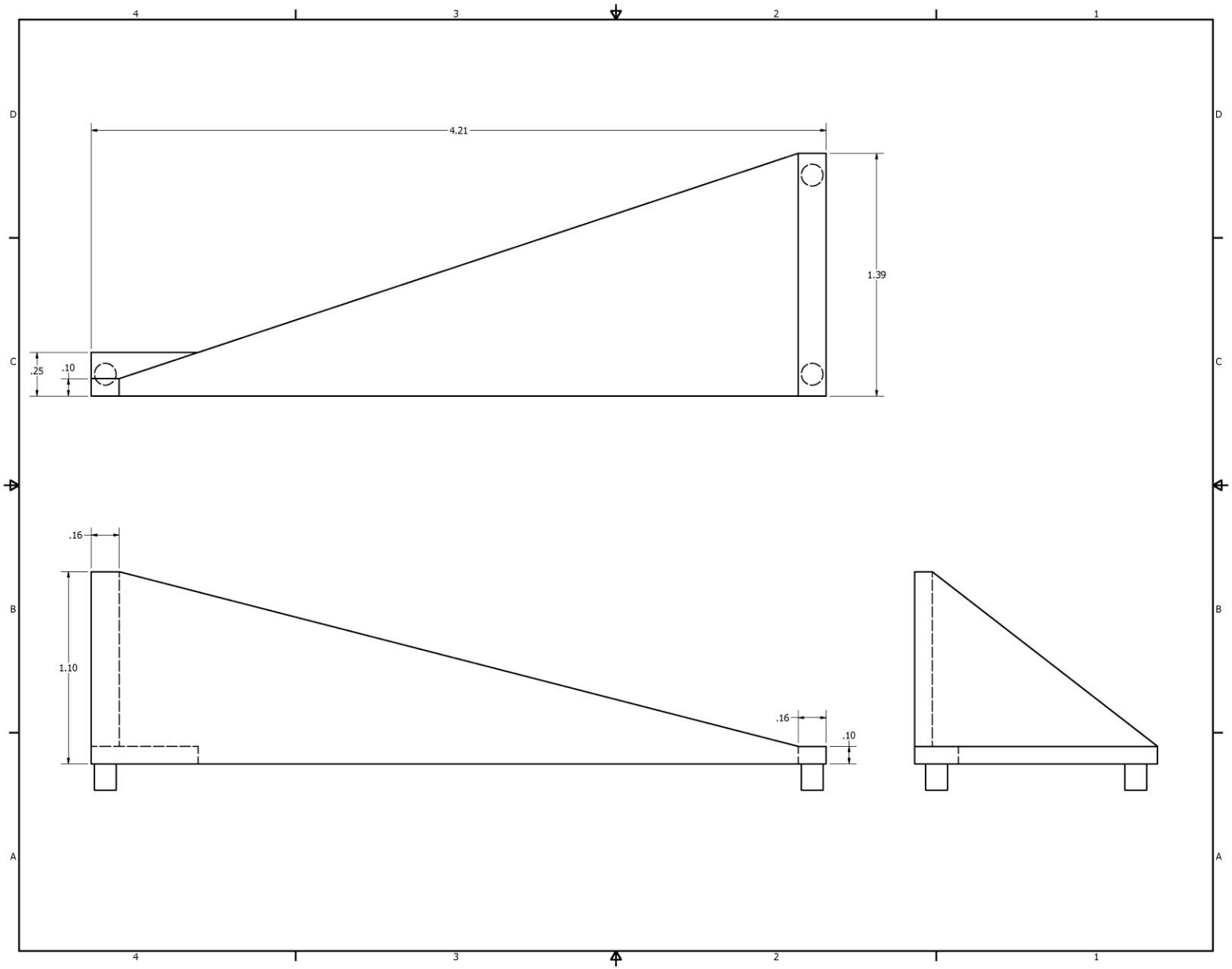
4.21
1.39
.25
.10
.16
1.10
.16
.10

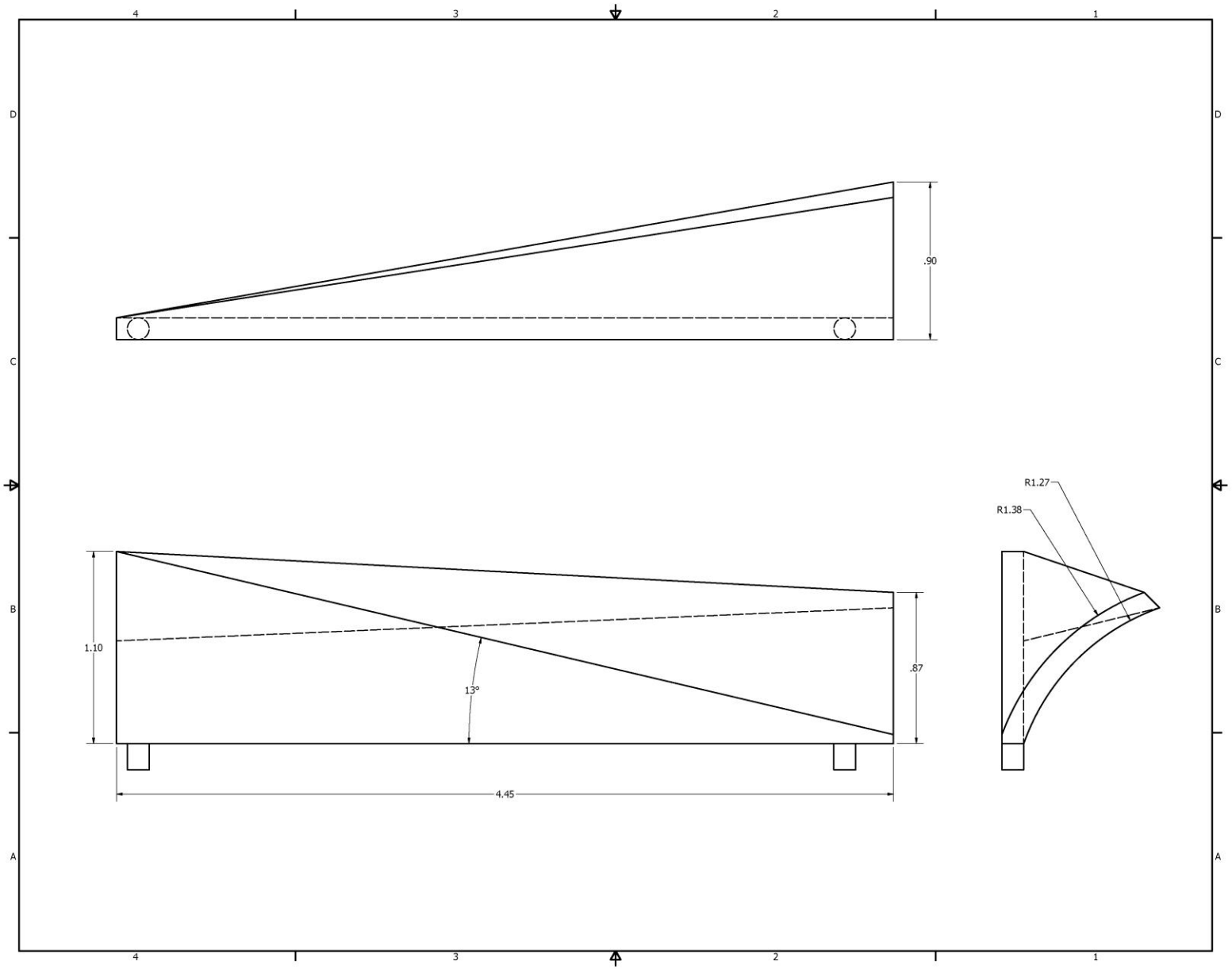
4
3
2
1
D
C
B
A
.90
1.10
13°
.87
4.45
R1.27
R1.38

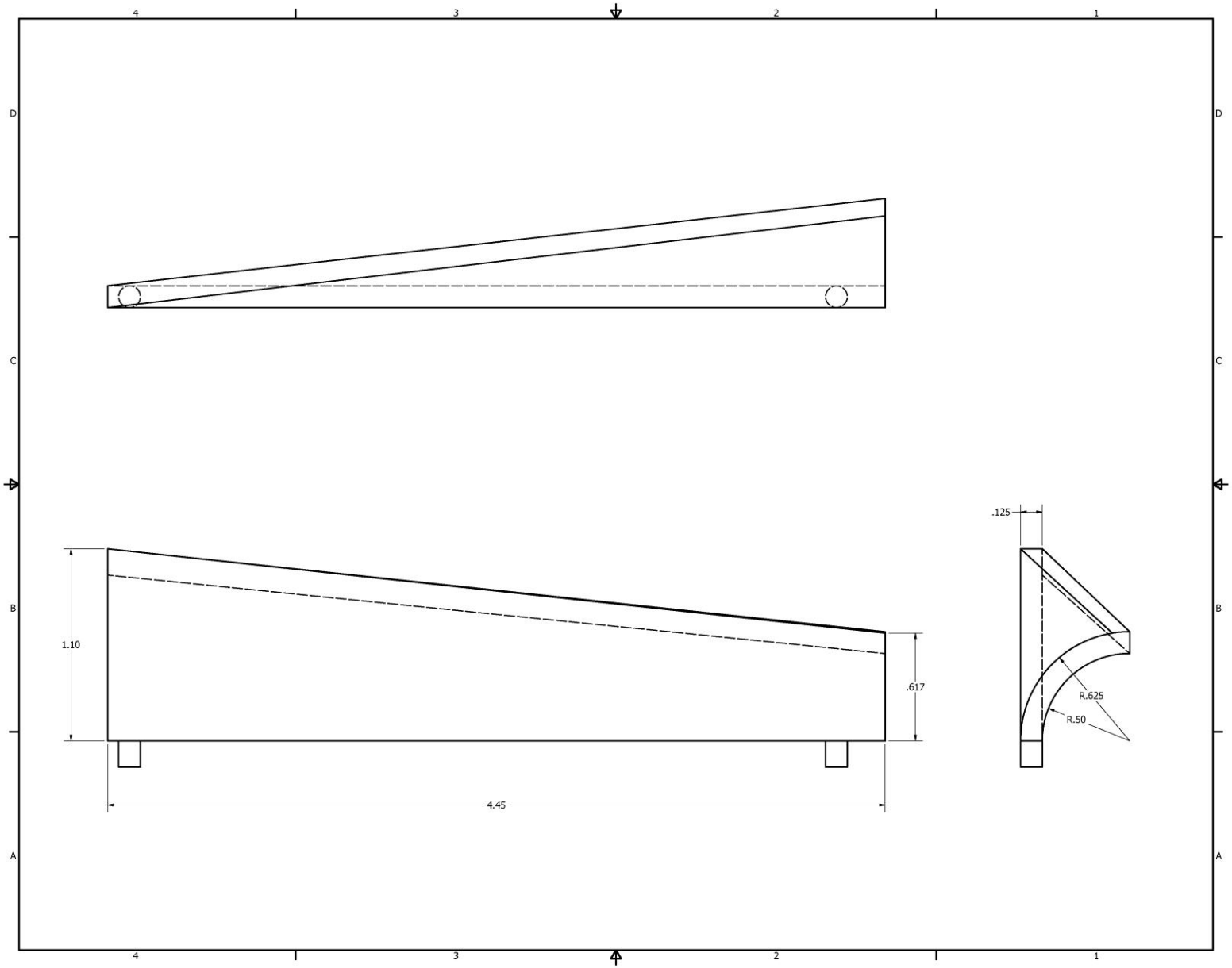
4
3
2
1
D
C
B
A
1.10
.617
4.45
.125
R.625
R.50

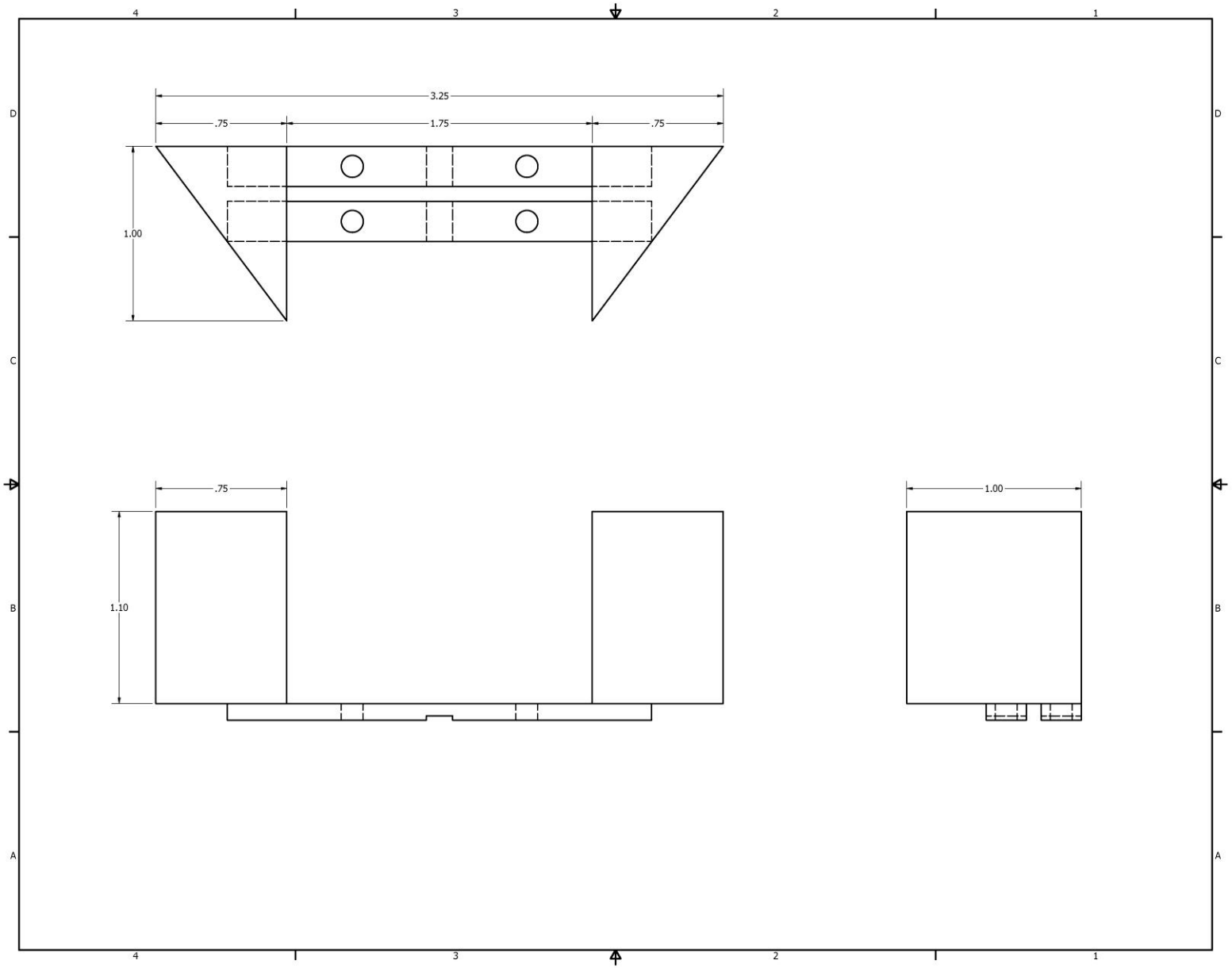
3.25
.75
1.75
.75
1.00
.75
1.10
1.00

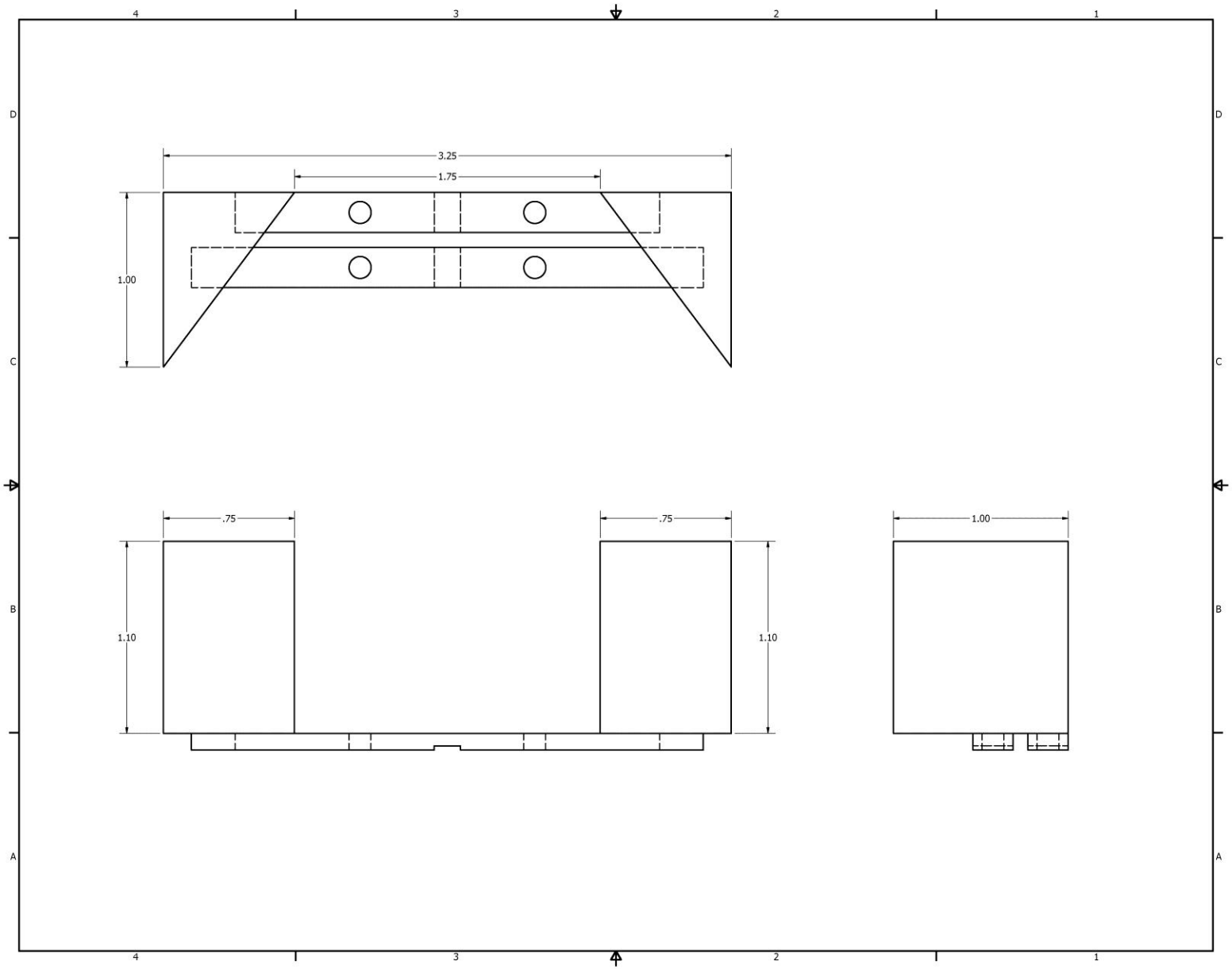
4
3
2
1
D
C
B
A
3.25
1.75
1.00
.75
.75
1.10
1.10
1.00

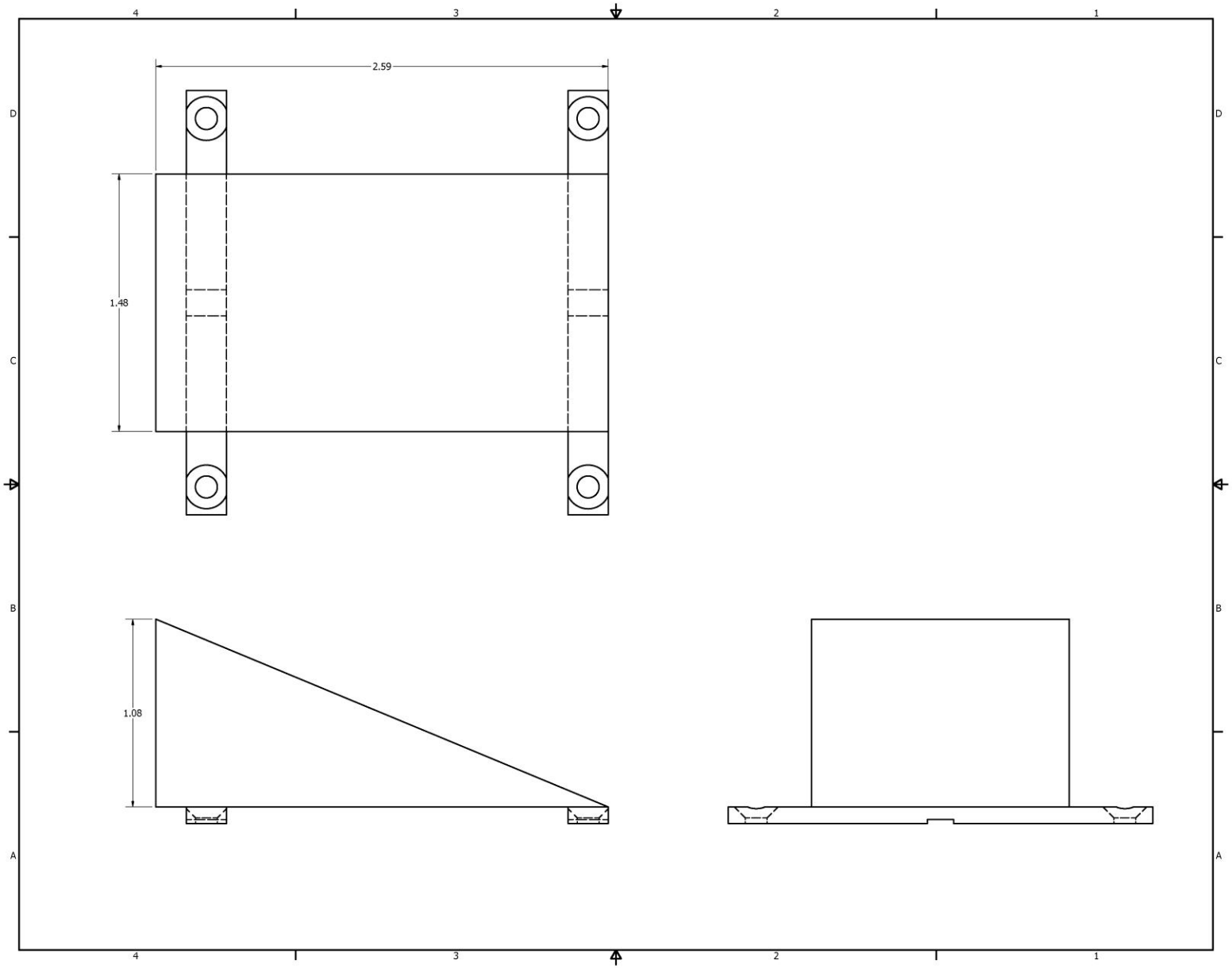
4
3
2
1
D
C
B
A
2.59
1.48
1.08

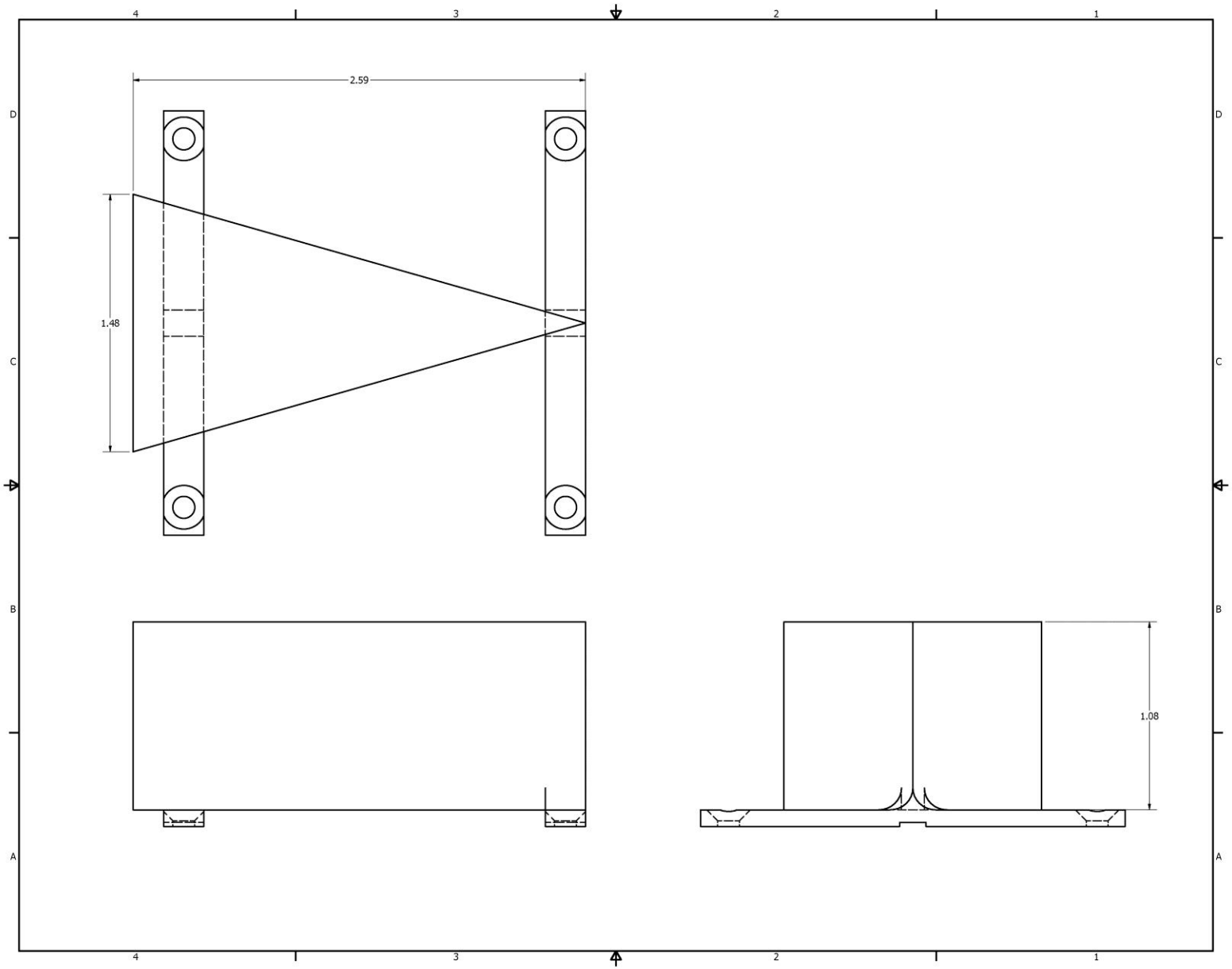
2.59
1.48
1.08

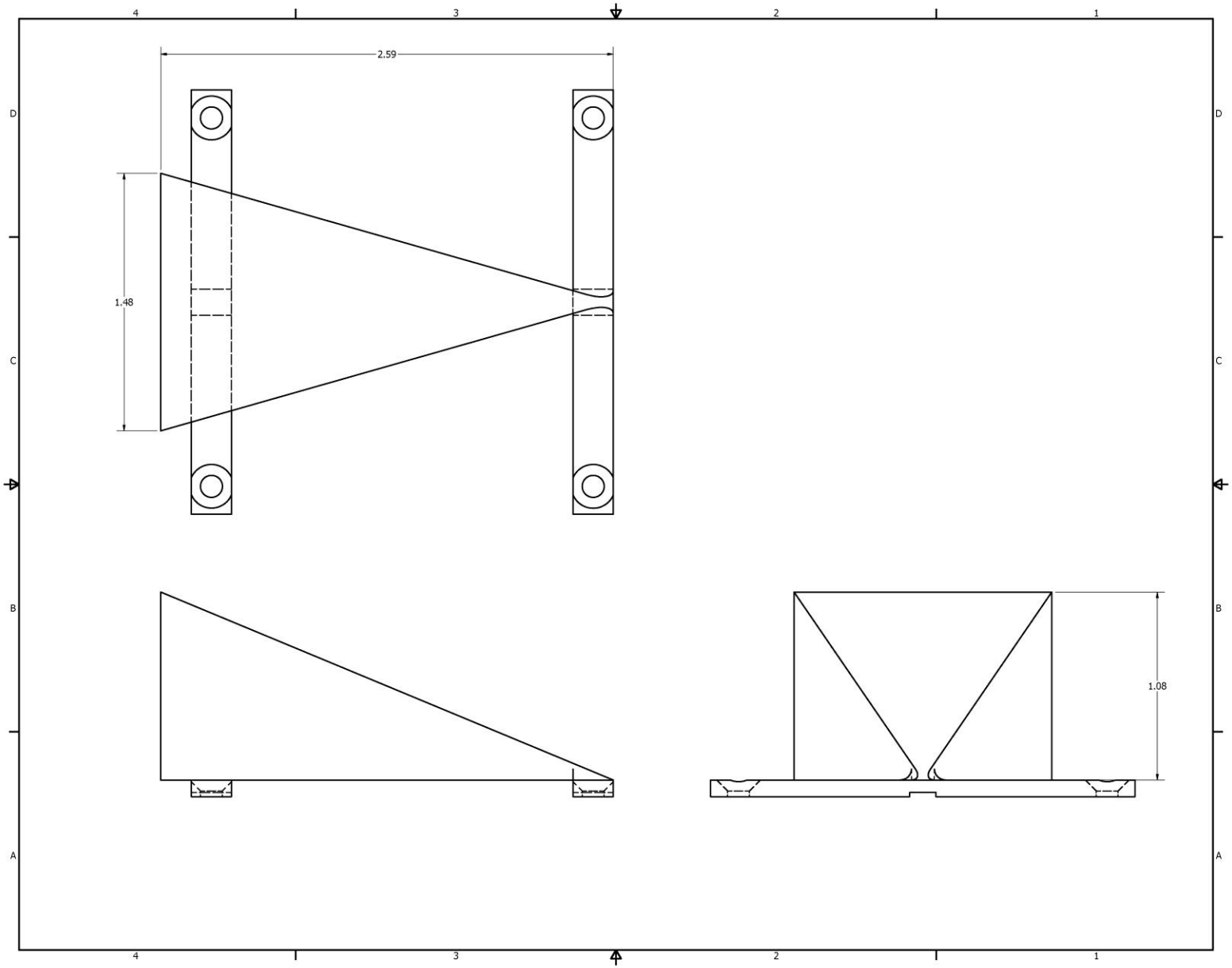
2.59
1.48
1.08

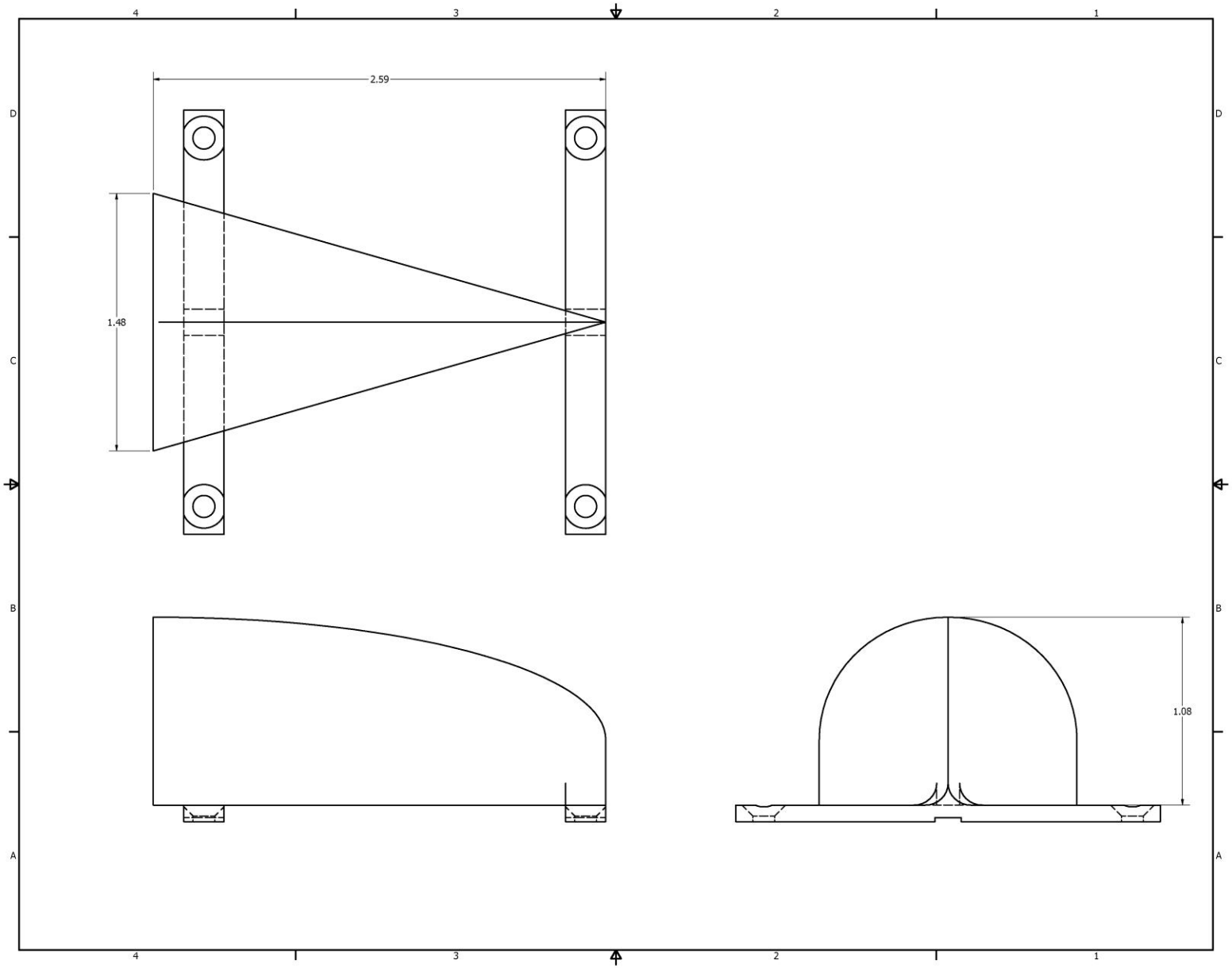
4
3
2
1
D
C
B
A
2.59
1.48
1.08

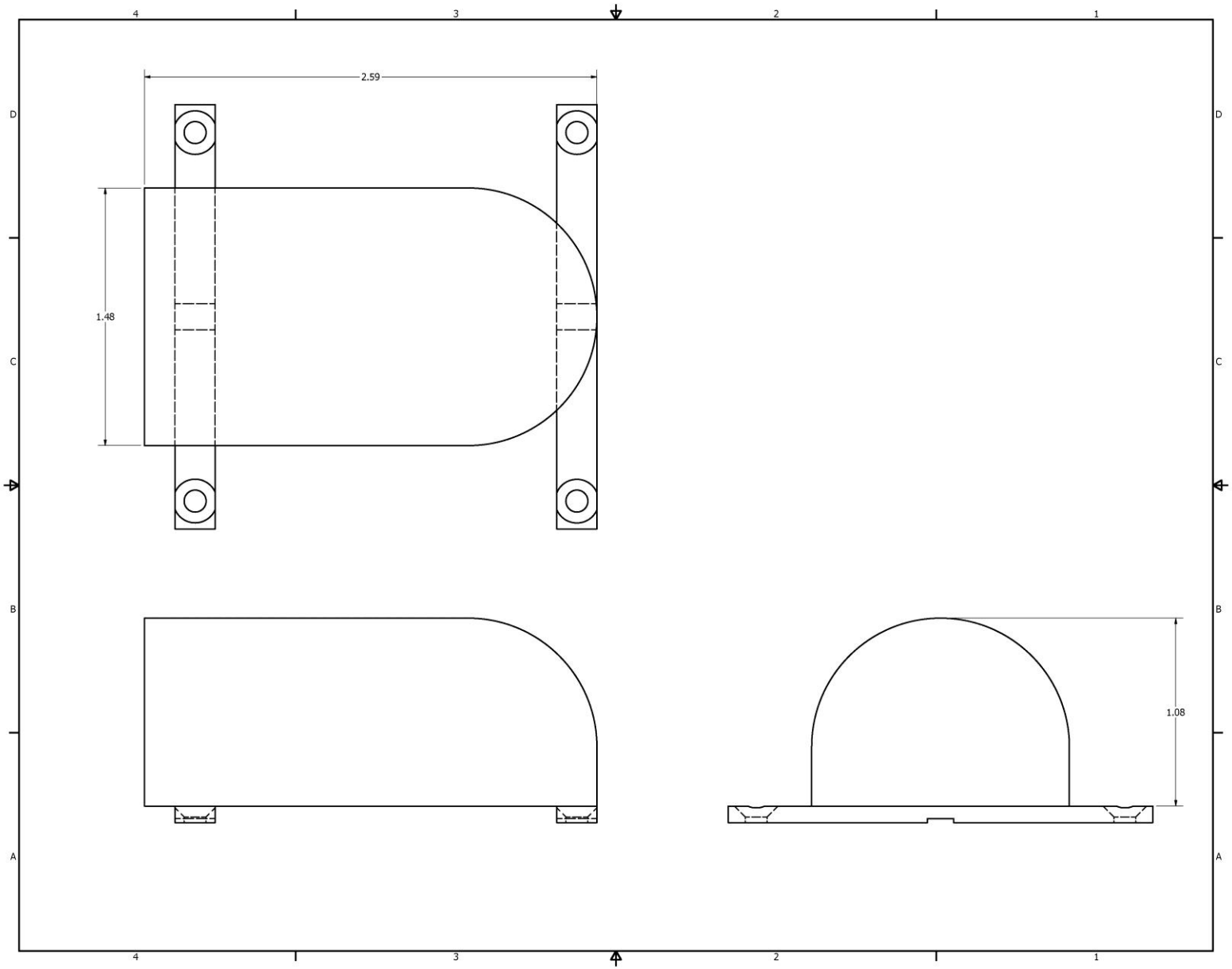
4
3
2
1
D
C
B
A
2.59
1.48
1.08

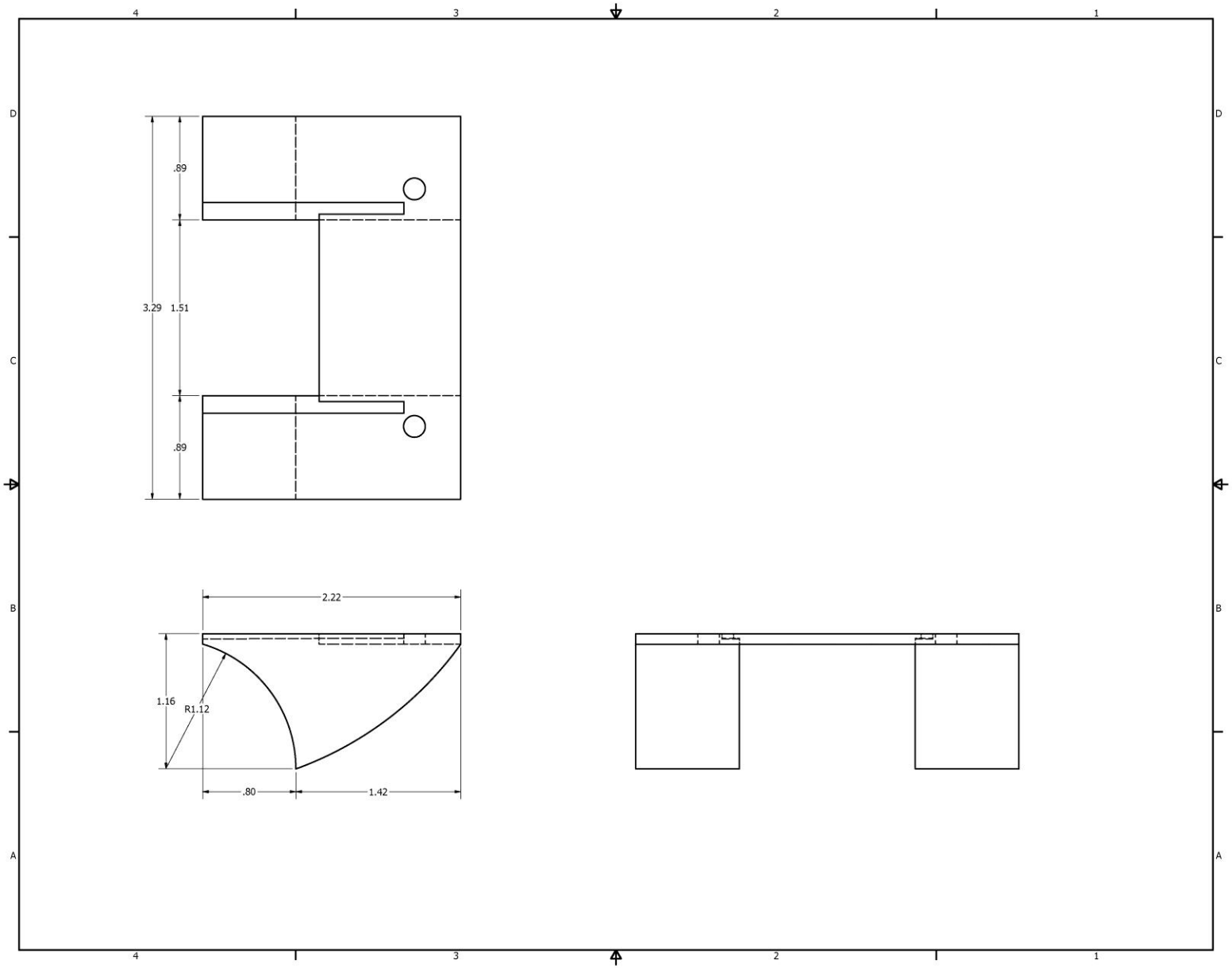
4
3
2
1
D
C
B
A
.89
3.29
1.51
.89
2.22
1.16
R1.12
.80
1.42

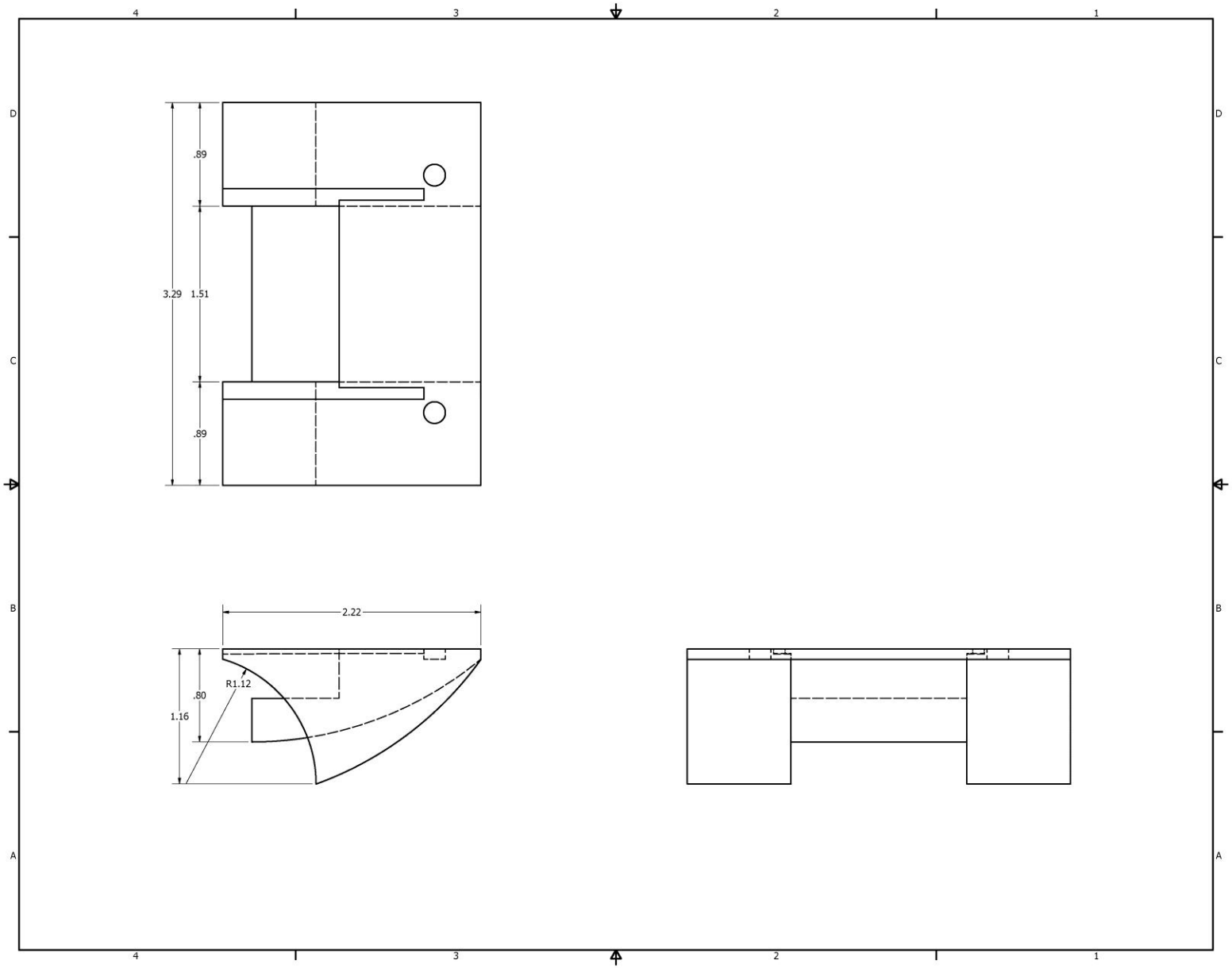
4
3
2
1
D
C
B
A
.89
3.29
1.51
.89
2.22
R1.12
.80
1.16

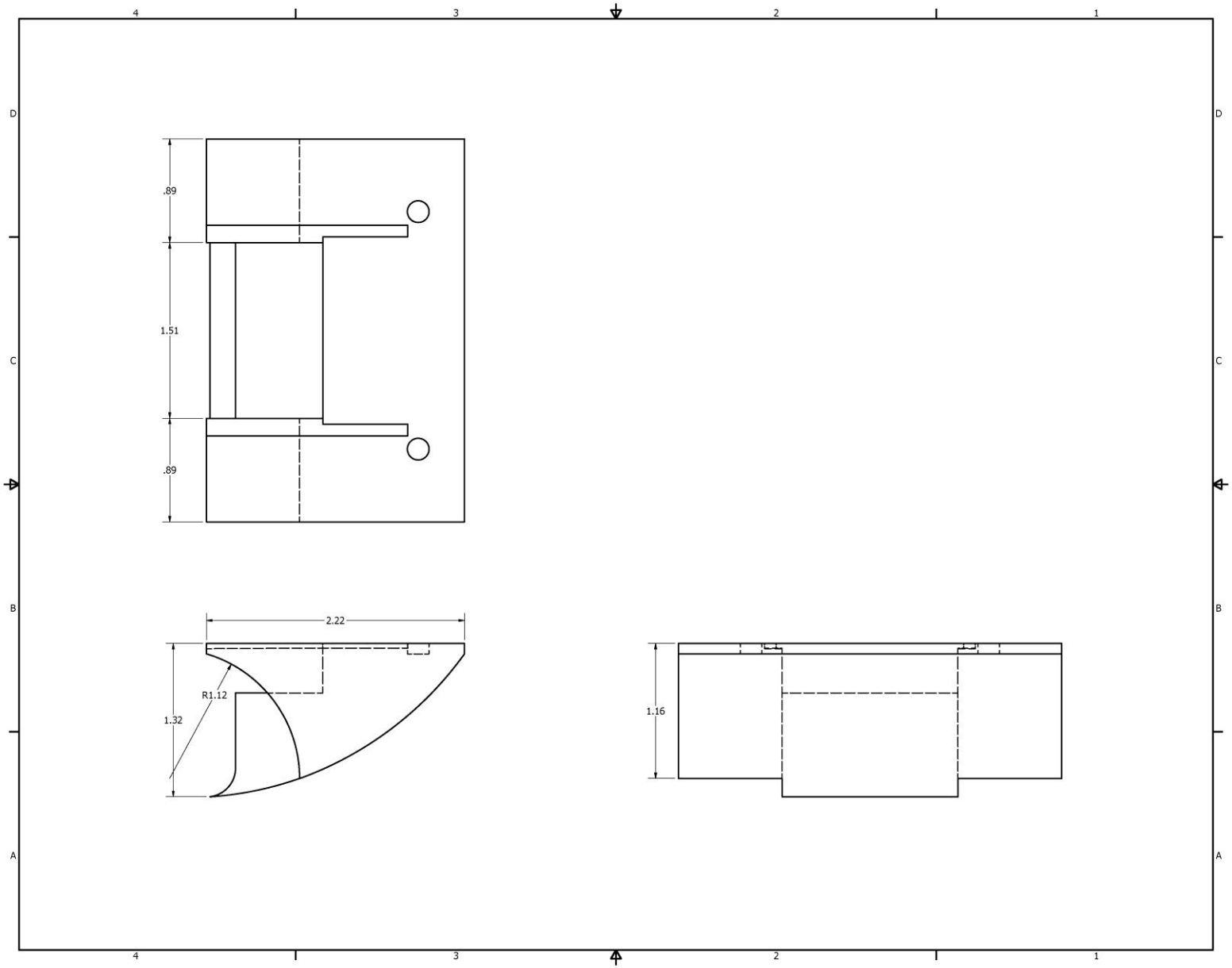
.89
1.51
.89
2.22
R1.12
1.32
1.16

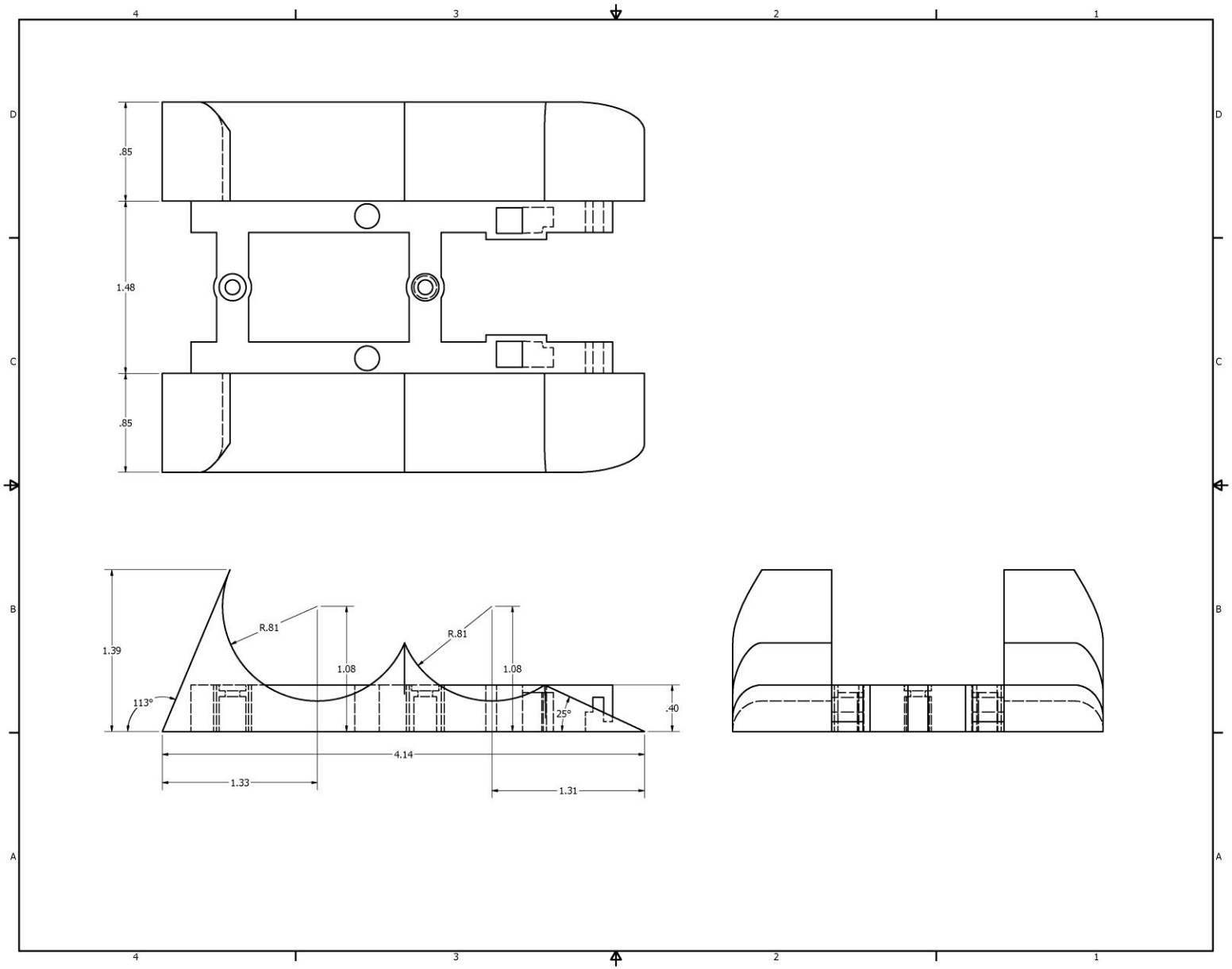
.85
1.48
.85
1.39
R.81
1.08
R.81
1.08
113°
25°
.40
4.14
1.33
1.31

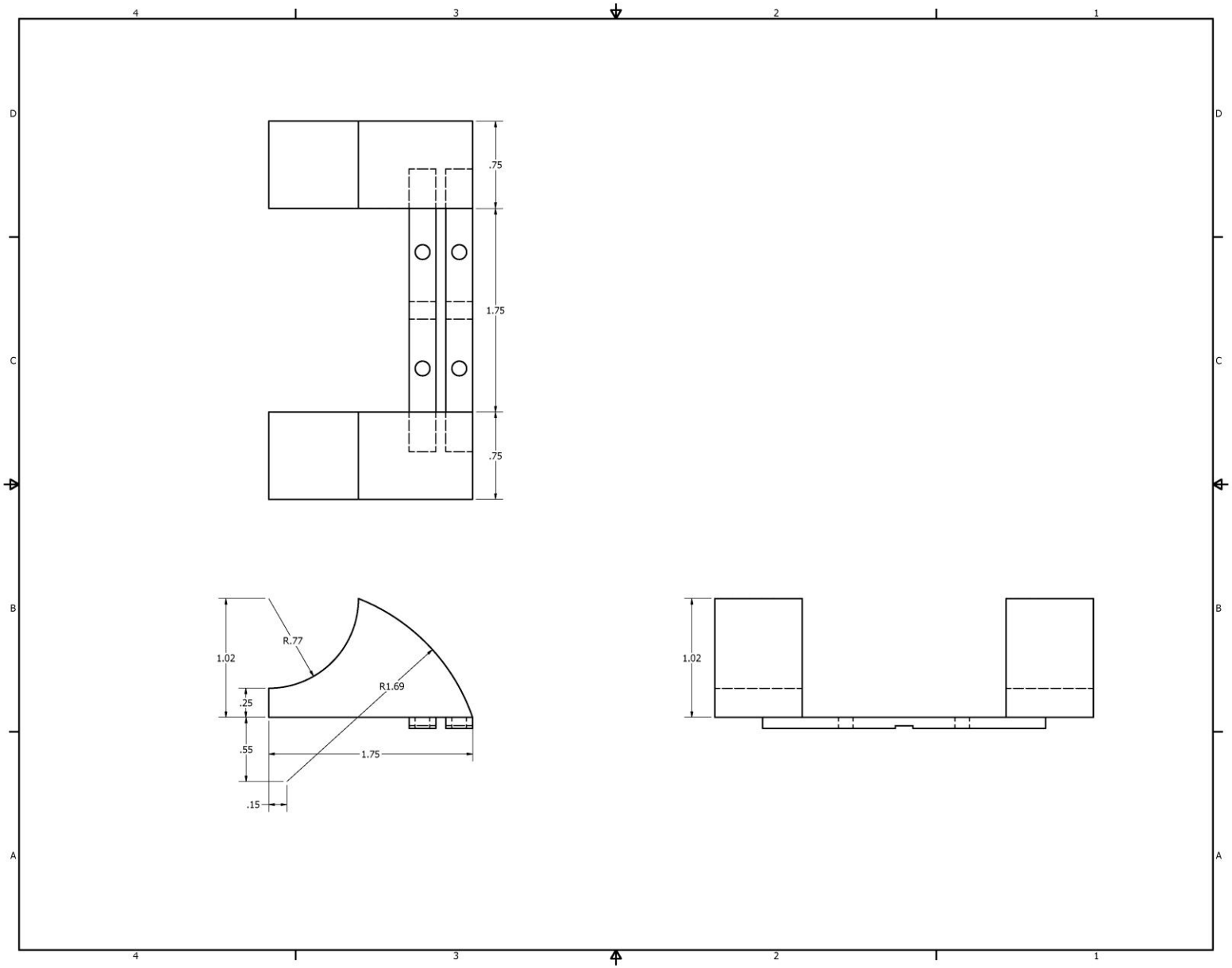
.75
1.75
.75
R.77
1.02
R1.69
.25
.55
1.75
.15
1.02

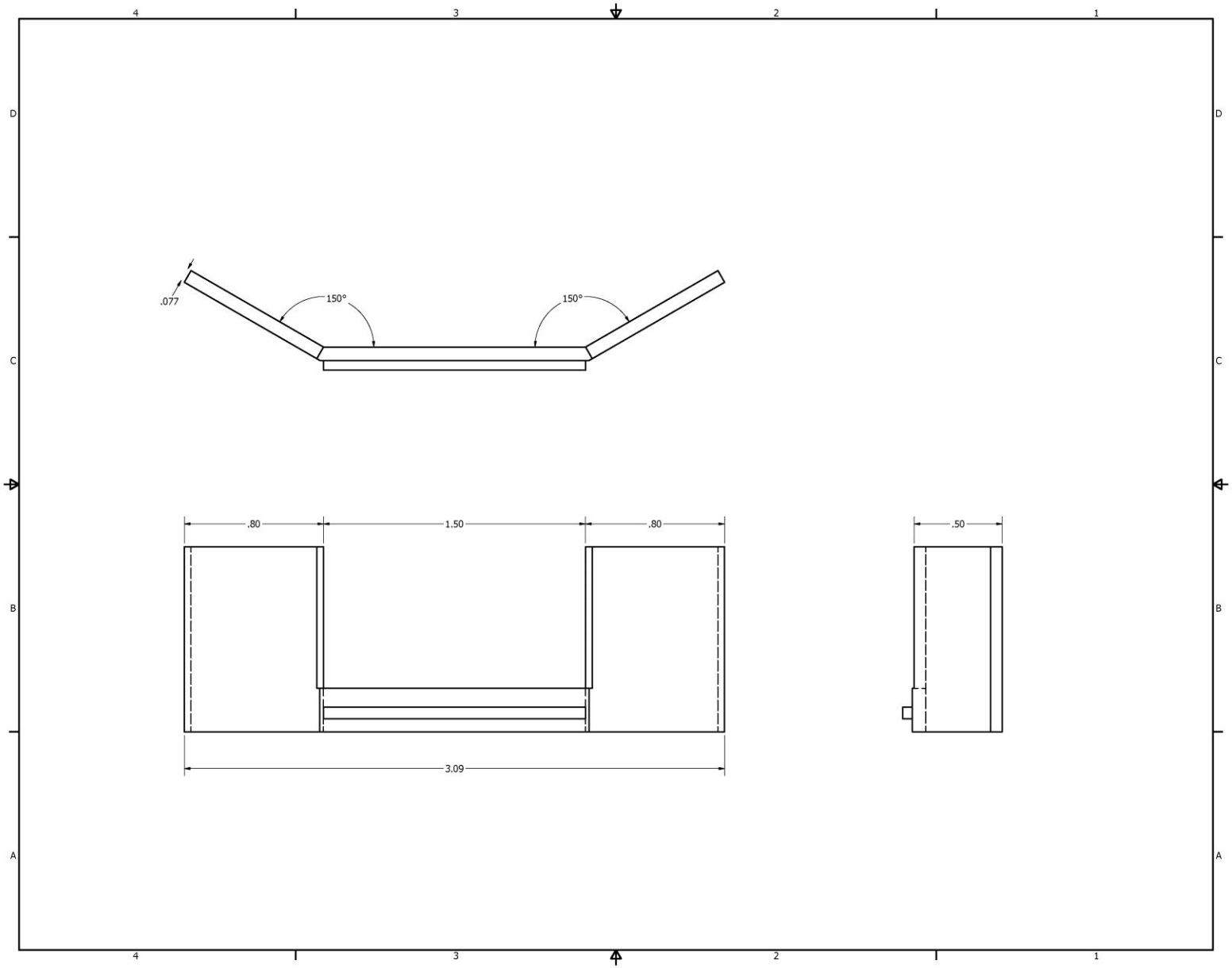
4
3
2
1
D
C
B
A
.077
150°
150°
.80
1.50
.80
.50
3.09

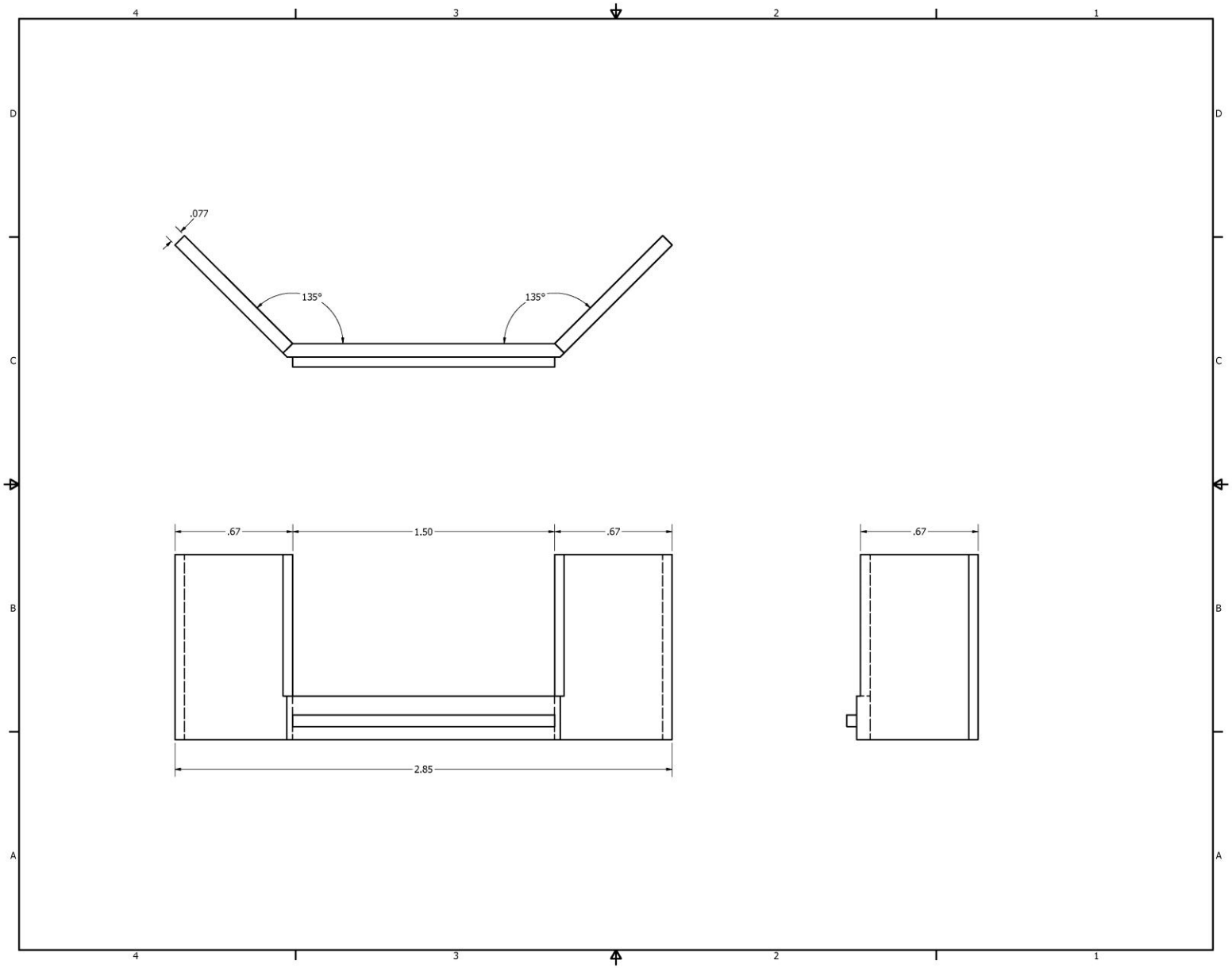
4
3
2
1
D
C
B
A
.077
135°
135°
.67
1.50
.67
2.85
.67

Appendix Section 6
Wind Tunnel Pictures

No devices 55 MPH

No devices 65 MPH

No devices 70 MPH

Side skirt, flat plate 55 MPH

Side skirt, flat plate 65 MPH

Side skirt, flat plate 70 MPH

Side skirt, flat plate, mid angle 55 MPH

Side skirt, flat plate, mid angle 65 MPH

Side skirt, flat plate, mid angle 70 MPH

Side skirt, flat plate, full angle 55 mph

Side skirt, flat plate, full angle 65 mph

Side skirt, flat plate, full angle 70 mph

Side skirt, curved plate 55 MPH

Side skirt, curved plate 65 MPH

Side skirt, curved plate 70 MPH

Side skirt, half trough 55 mph

Side skirt, half trough 65 mph

Side skirt, half trough 70 mph

Side skirt, trough 55 mph

Side skirt, trough 65 mph

Side skirt, trough 70 mph

Side skirt, lofted trough 55 mph

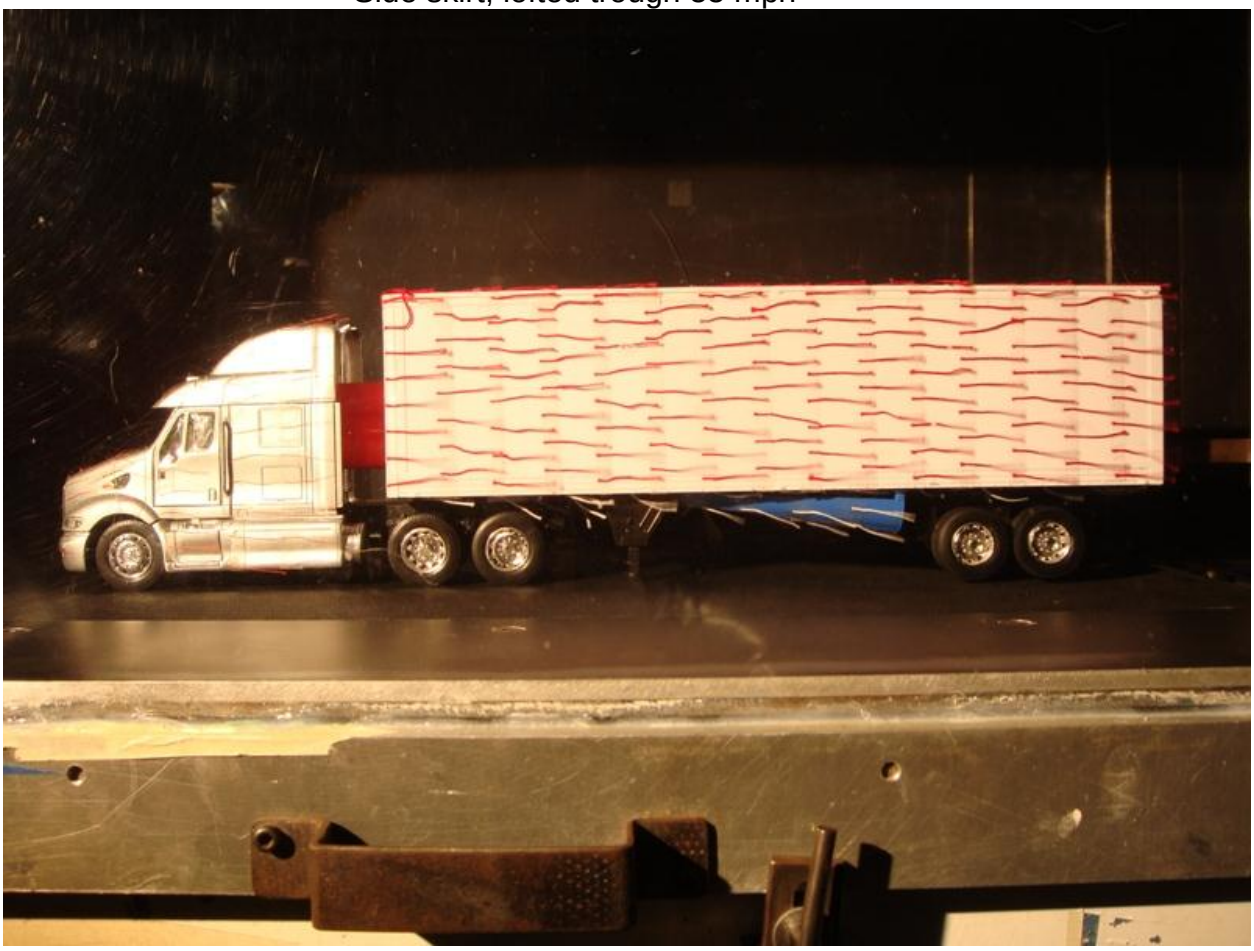

Side skirt, lofted trough 65 mph

Side skirt, lofted trough 70 mph

Side skirt, lofted horizontal to vertical plate 55 MPH

Side skirt, lofted horizontal to vertical plate 65 MPH

Side skirt, lofted horizontal to vertical plate 70 MPH

Side skirt, lofted arch with flat side, installed with arch facing rear wheels 55 mph

Side skirt, lofted arch with flat side, installed with arch facing rear wheels 65 mph

Side skirt, lofted arch with flat side, installed with arch facing rear wheels 70 mph

Side skirt, lofted arch with flat side, installed with arch facing front wheels 55 mph

Side skirt, lofted arch with flat side, installed with arch facing front wheels 65 mph

Side skirt, lofted arch with flat side, installed with arch facing front wheels 70 mph

Side skirt, lofted arch installed with arch facing rear wheels 55 mph

Side skirt, lofted arch installed with arch facing rear wheels 65 mph

Side skirt, lofted arch installed with arch facing rear wheels 70 mph

Side skirt, Lofted arch, installed with arch facing front wheels 55 mph

Side skirt, Lofted arch, installed with arch facing front wheels 65 mph

Side skirt, Lofted arch, installed with arch facing front wheels 70 mph

Front wheel diffuser 55 MPH

Front wheel diffuser 65 MPH

Front wheel diffuser 70 MPH

Front wheel nozzle 55 MPH

Front wheel nozzle 65 MPH

Front wheel nozzle 70 MPH

Rear wheel keel, horizontal wedge 55 mph

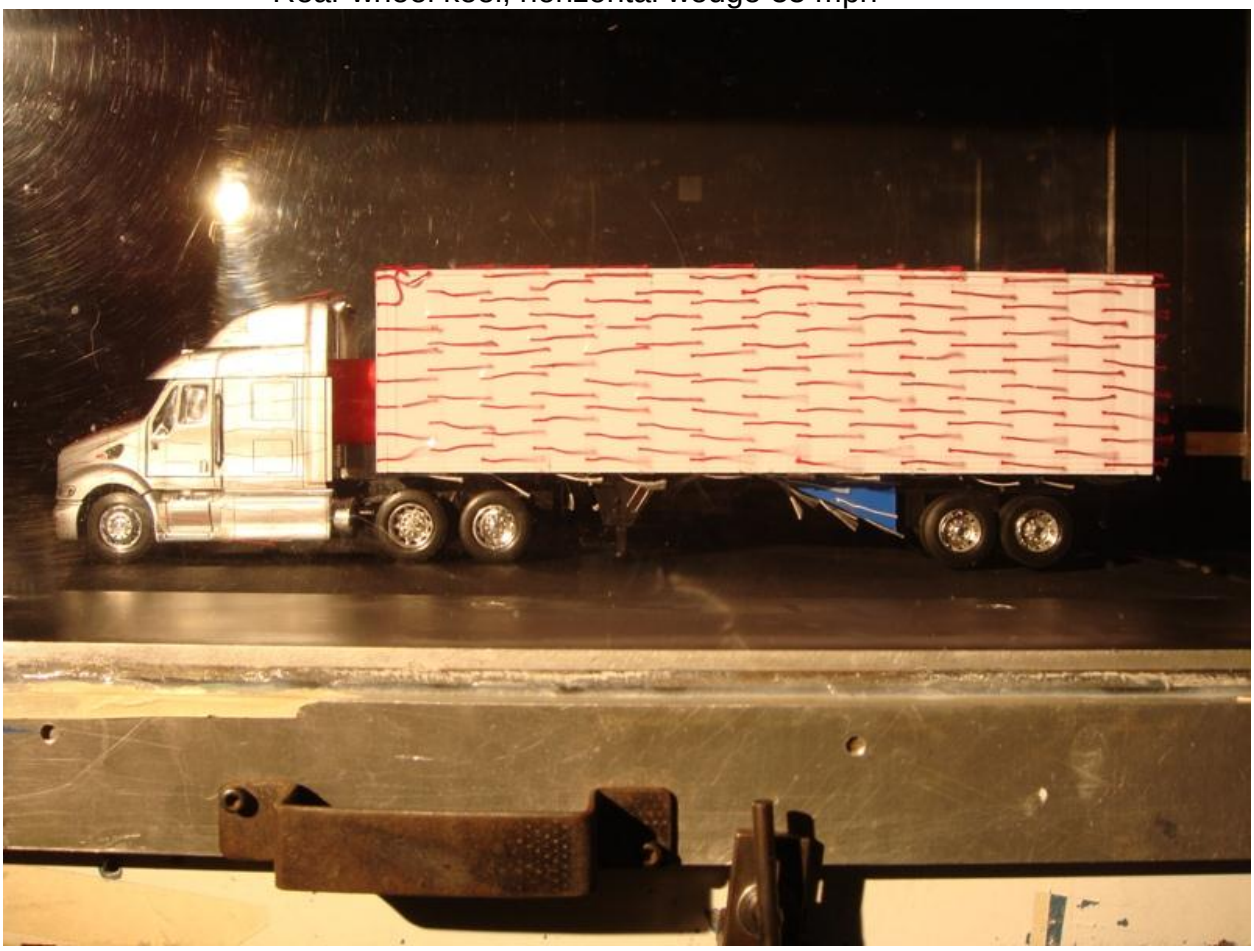

Rear wheel keel, horizontal wedge 65 mph

Rear wheel keel, horizontal wedge 70 mph

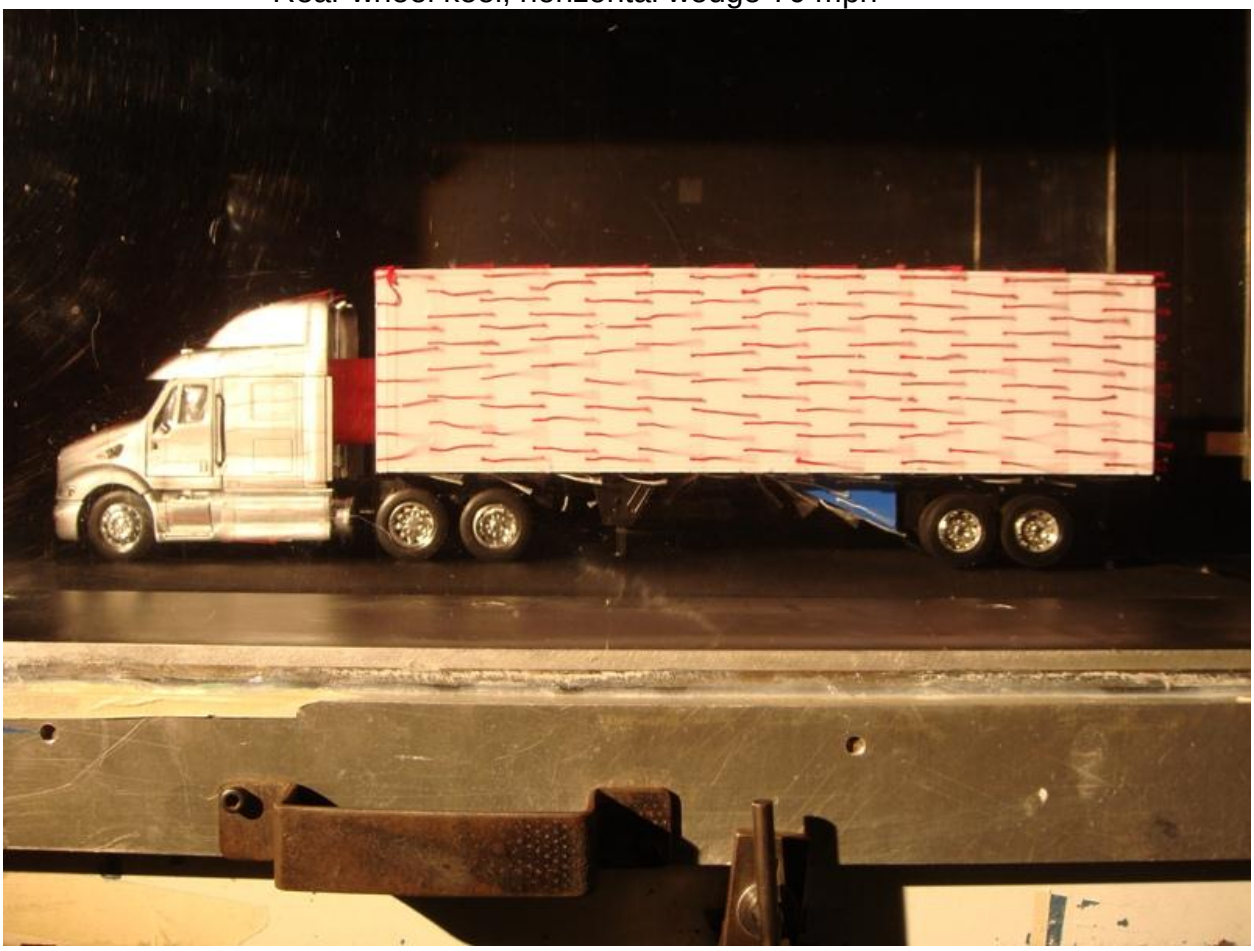

Rear wheel keel, vertical wedge 55 mph

Rear wheel keel, vertical wedge 65 mph

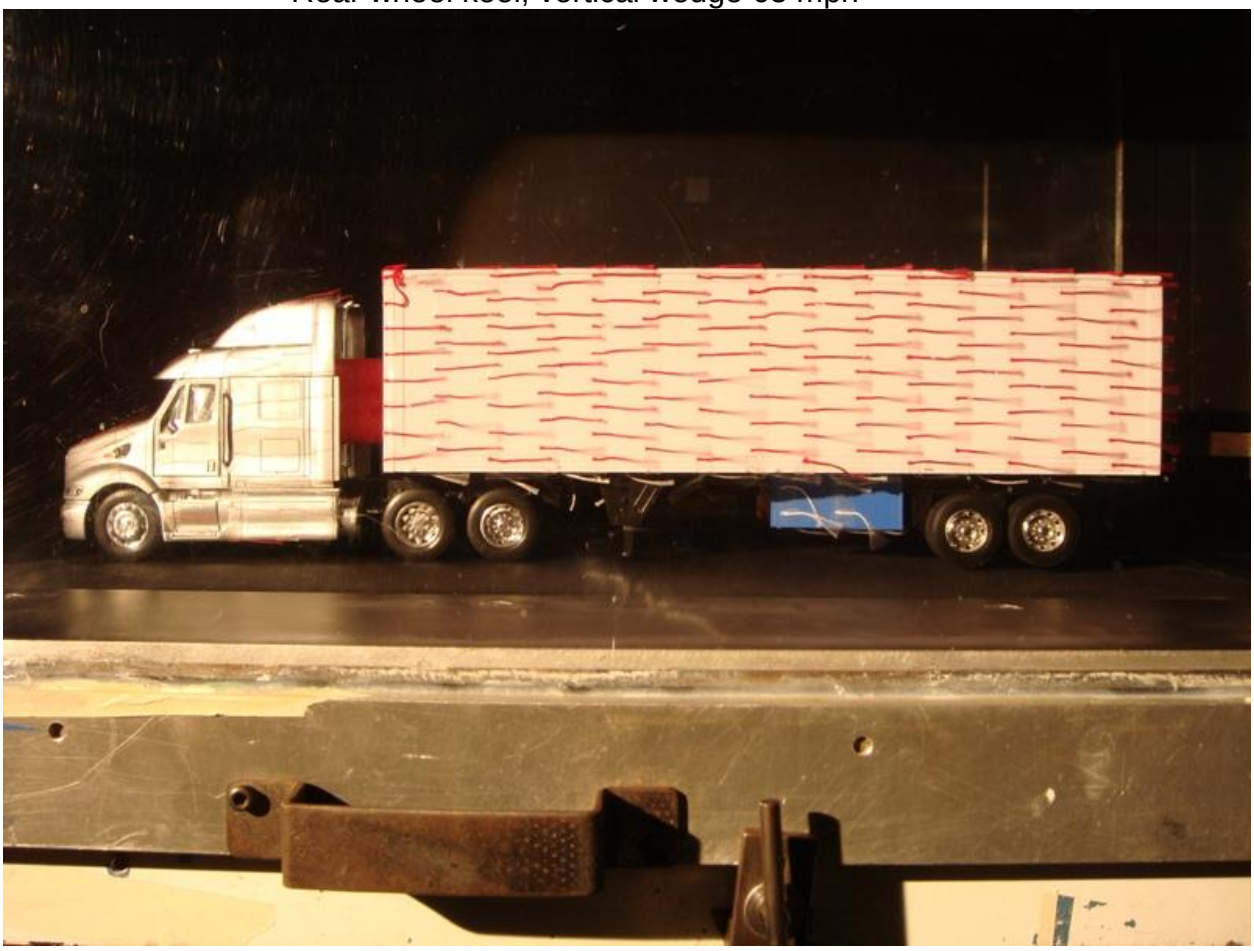

Rear wheel keel, vertical wedge 70 mph

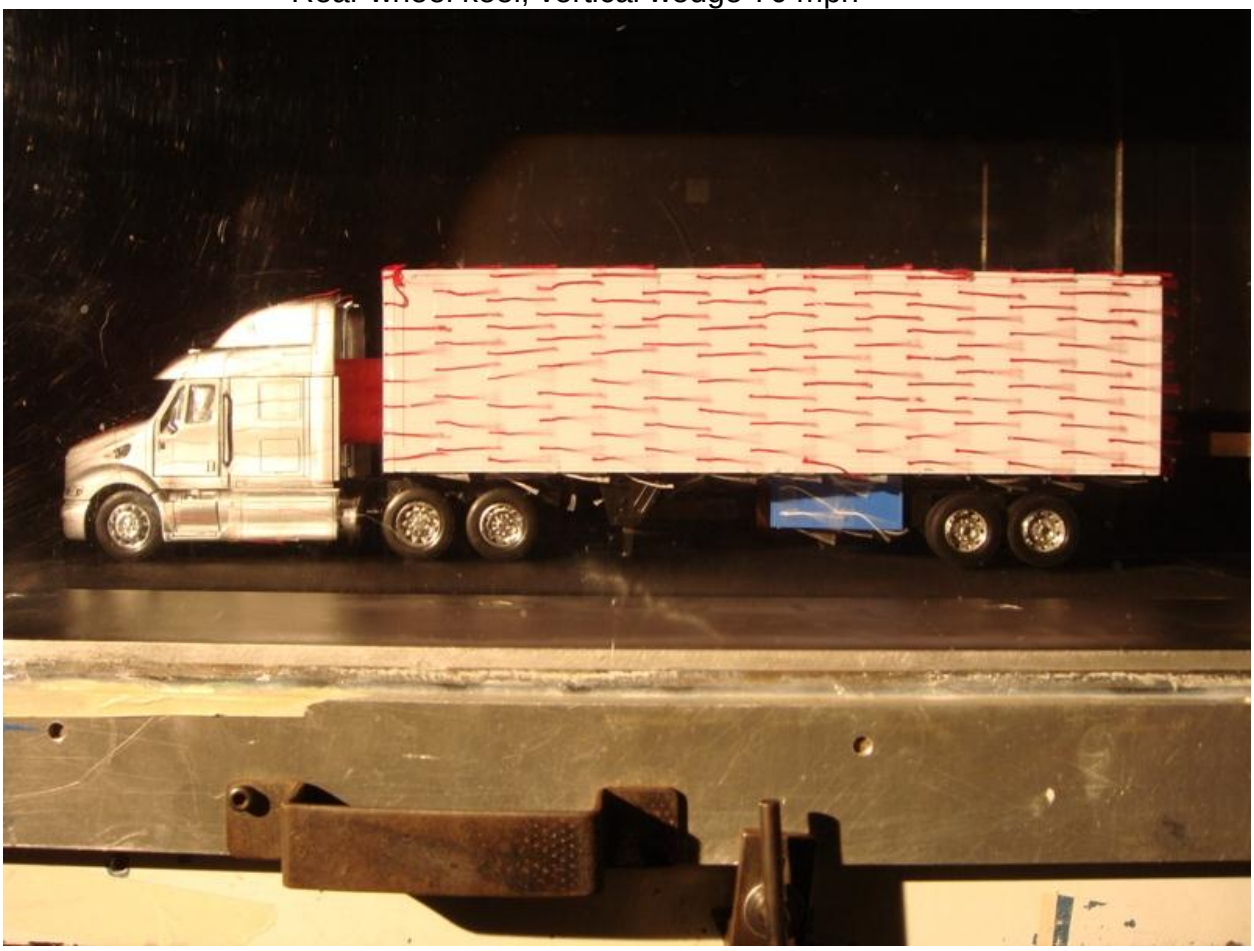

Rear wheel keel, combination horizontal and vertical wedge 55 mph

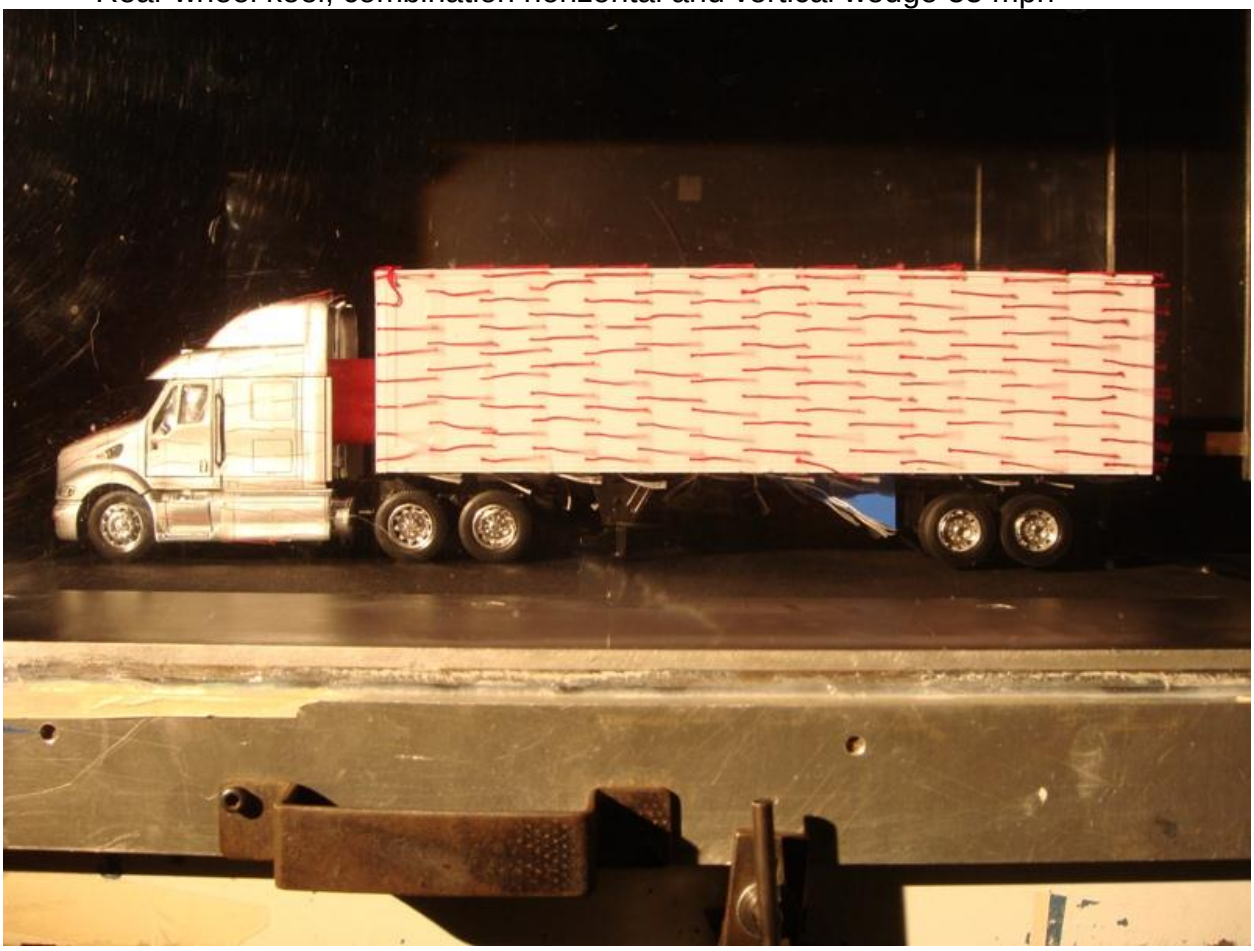

Rear wheel keel, combination horizontal and vertical wedge 65 mph

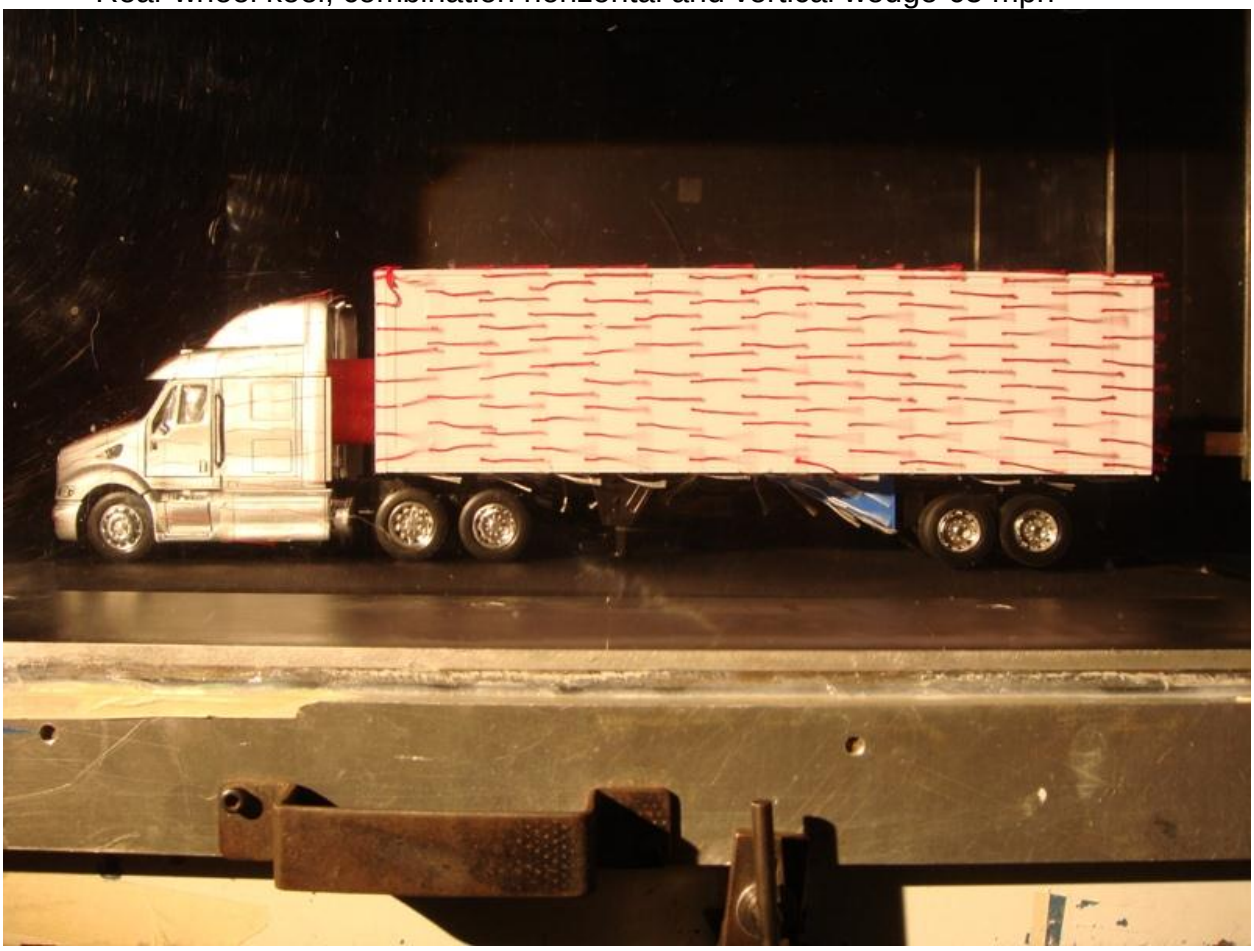

Rear wheel keel, combination horizontal and vertical wedge 70 mph

Rear wheel keel, bow wedge 55 MPH

Rear wheel keel, bow wedge 65 MPH

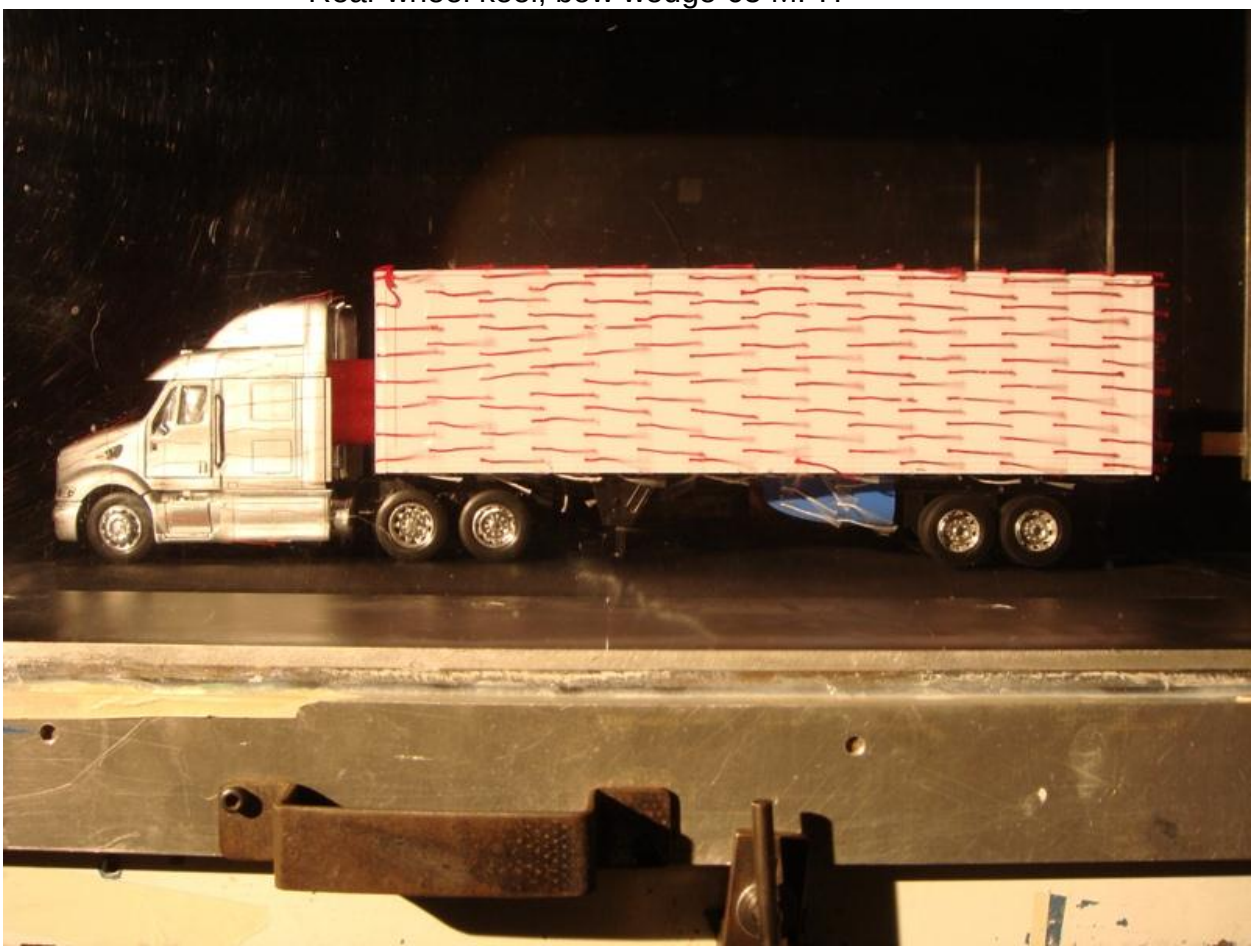

Rear wheel keel, bow wedge 70 MPH

Rear wheel keel, round wedge 55 MPH

Rear wheel keel, round wedge 65 MPH

Rear wheel keel, round wedge 70 MPH

Rear diffuser with no axle faring 55 MPH

Rear diffuser with no axle faring 65 MPH

Rear diffuser with no axle faring 70 MPH

Rear diffuser with half axle faring, rear view, 55 MPH with belt

Rear diffuser with half axle faring rear view 55 MPH

Rear diffuser with half axle faring 55 MPH

Rear diffuser with half axle faring, rear view 65 MPH with belt

Rear diffuser with half axle faring, rear view 65 MPH

Rear diffuser with half axle faring, rear view 70 MPH with belt

Rear diffuser with half axle faring, rear view 70 MPH

Rear diffuser with full axle faring, rear view 55 MPH

Rear diffuser with full axle faring, rear view 65 MPH

Rear diffuser with full axle faring, rear view 70 MPH with belt

Rear diffuser with full axle faring, rear view 70 MPH

Wheel well 55 mph

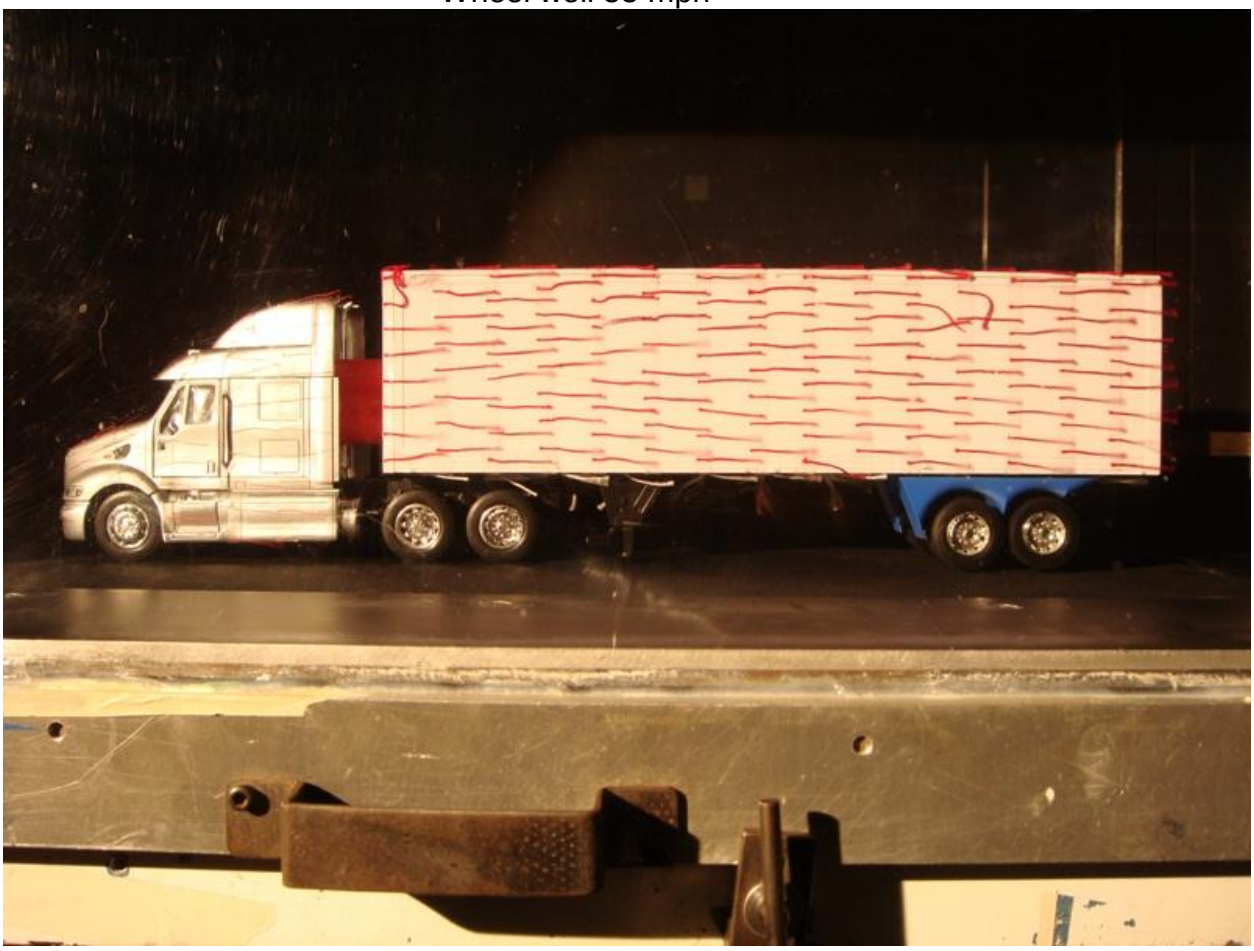

Wheel well 65 mph

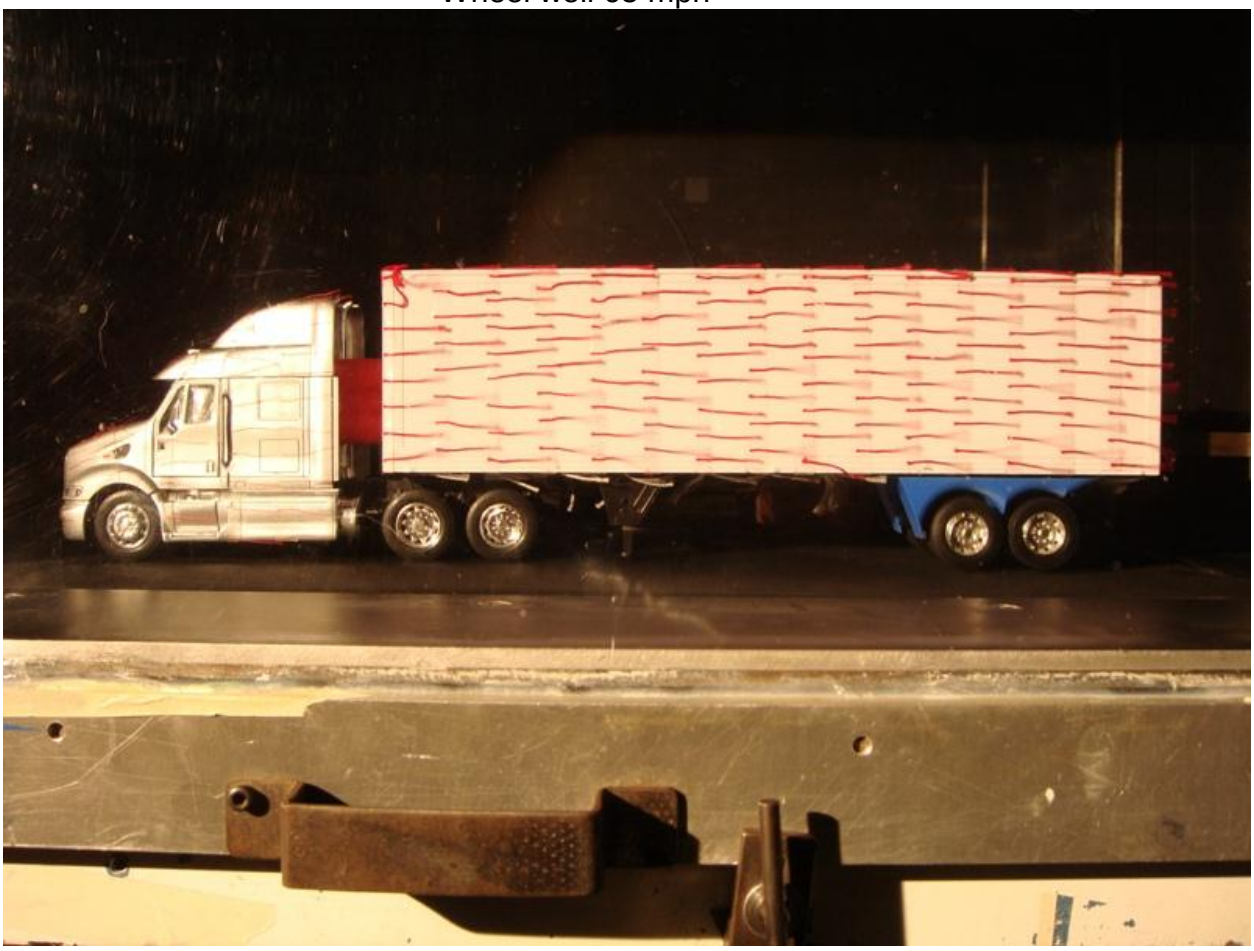

Wheel well 70 mph

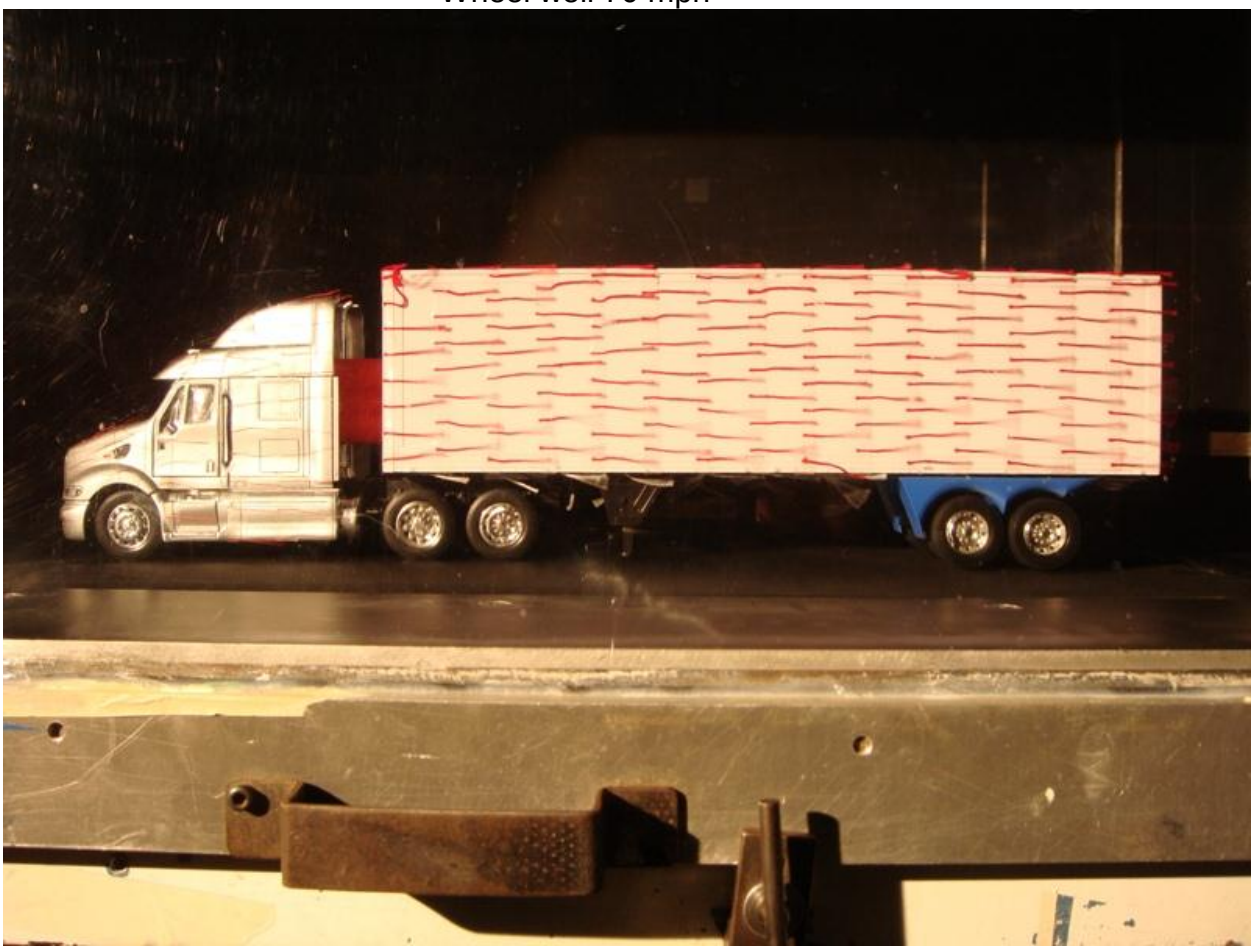

Diffusers behind and in front of rear wheels, rear view 55 mph

Diffusers behind and in front of rear wheels, rear view 55 mph with belt

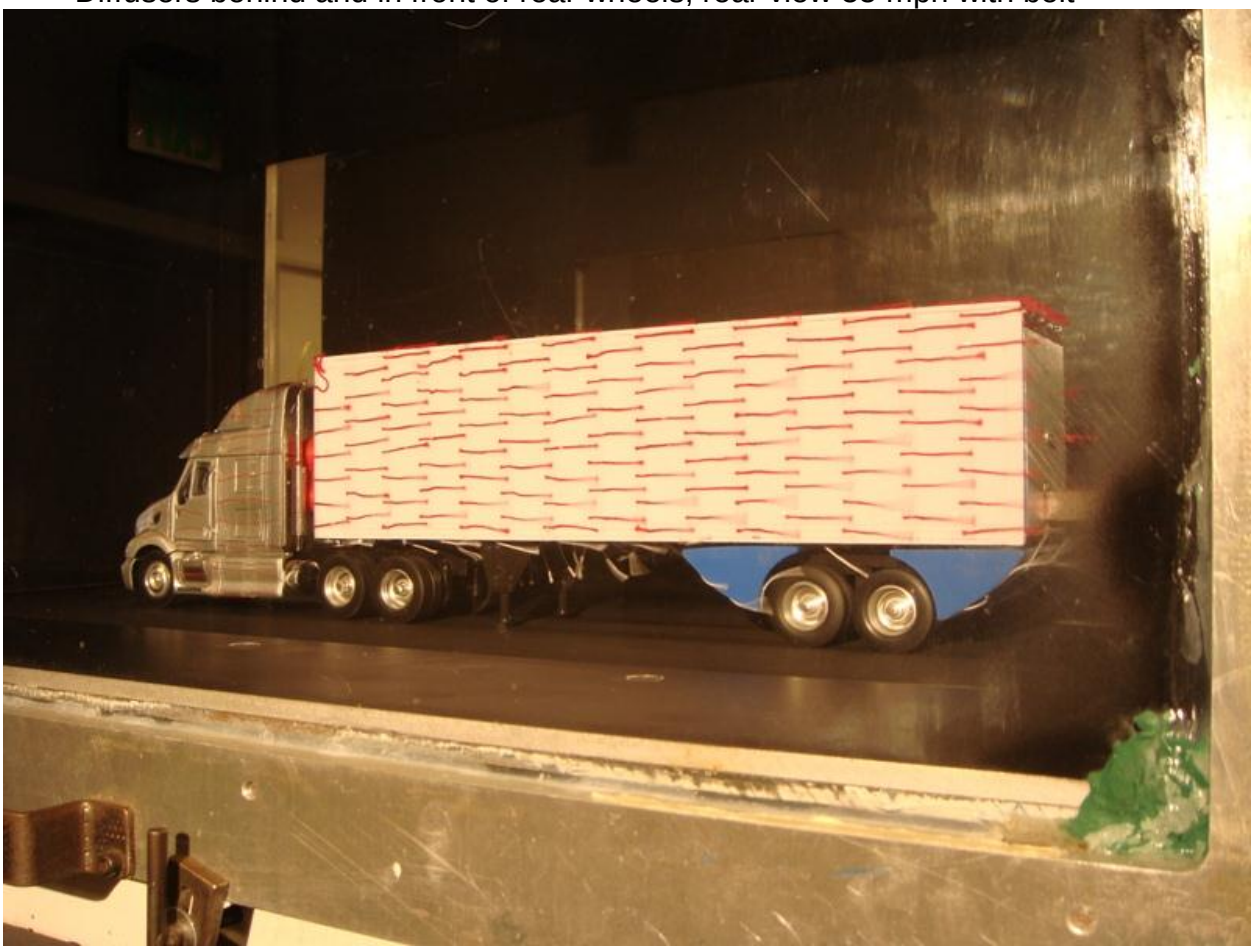

Diffusers behind and in front of rear wheels, front view 55 mph with belt

Diffusers behind and in front of rear wheels, front view 55 mph

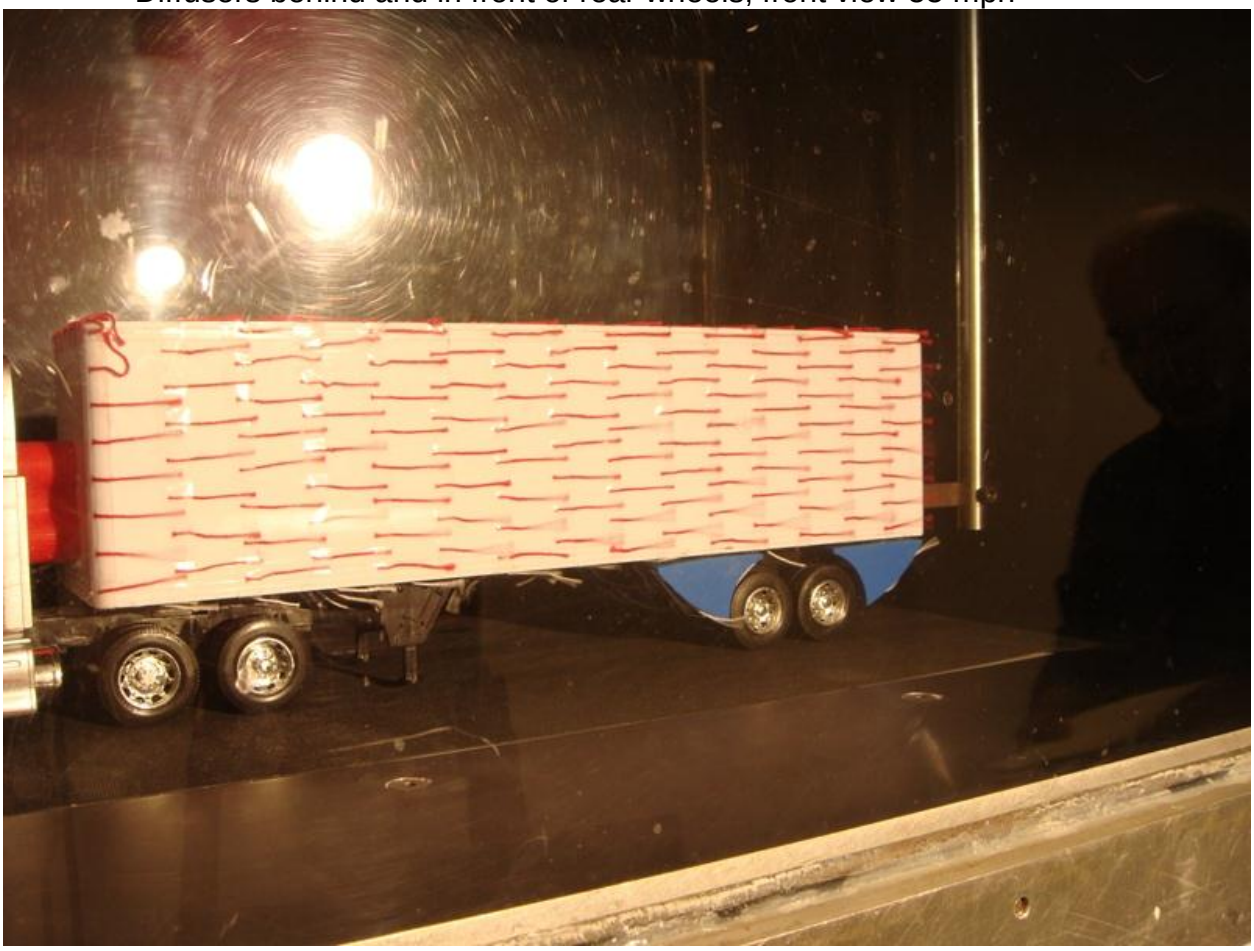

Diffusers behind and in front of rear wheels, rear view 65 mph

Diffusers behind and in front of rear wheels, rear view 65 mph with belt

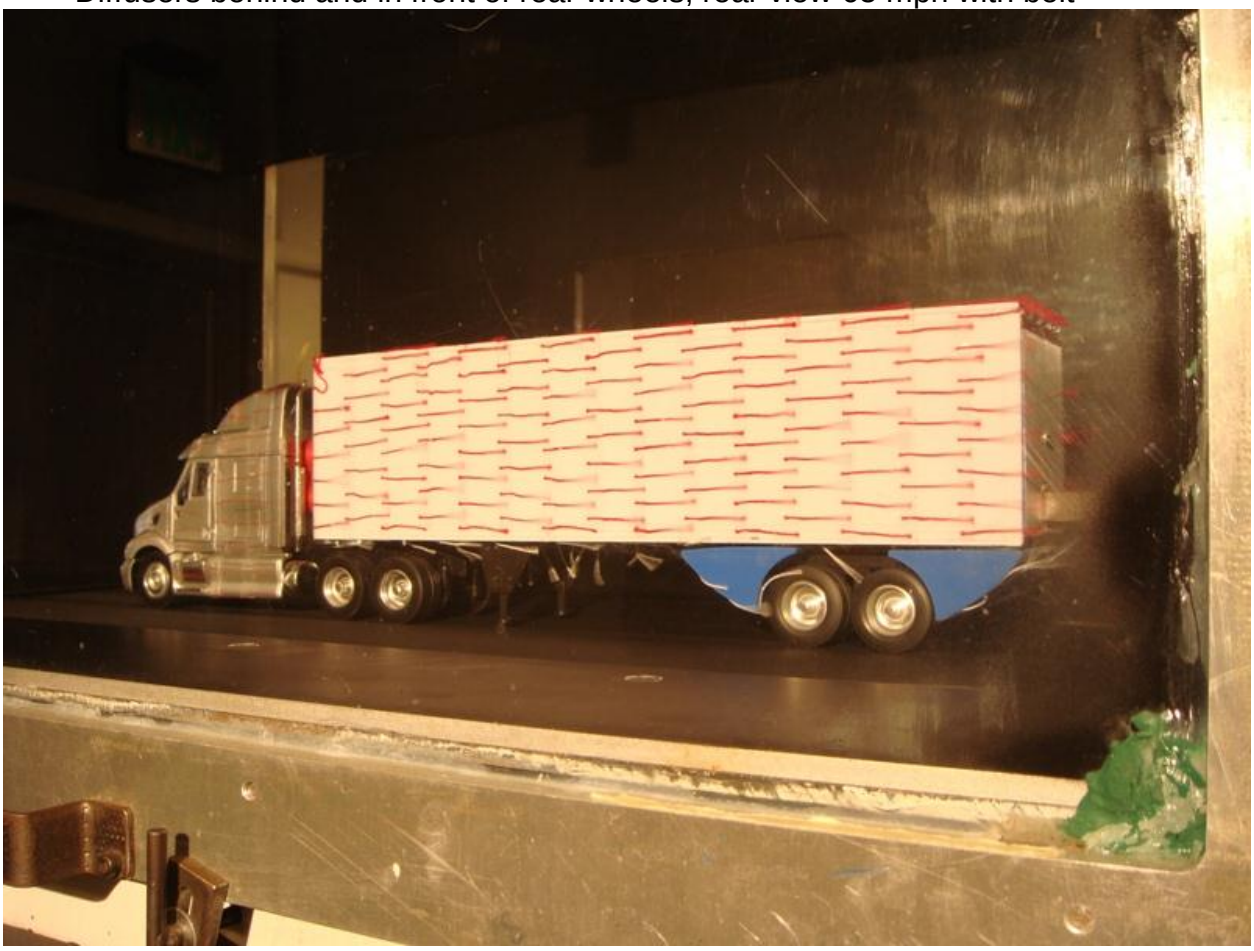

Diffusers behind and in front of rear wheels, front view 65 mph with belt

Diffusers behind and in front of rear wheels, front view #1 65 mph

Diffusers behind and in front of rear wheels, front view #1 65 mph

Diffusers behind and in front of rear wheels, rear view 70 mph

Diffusers behind and in front of rear wheels, rear view 70 mph with belt

Diffusers behind and in front of rear wheels, front view 70 mph with belt

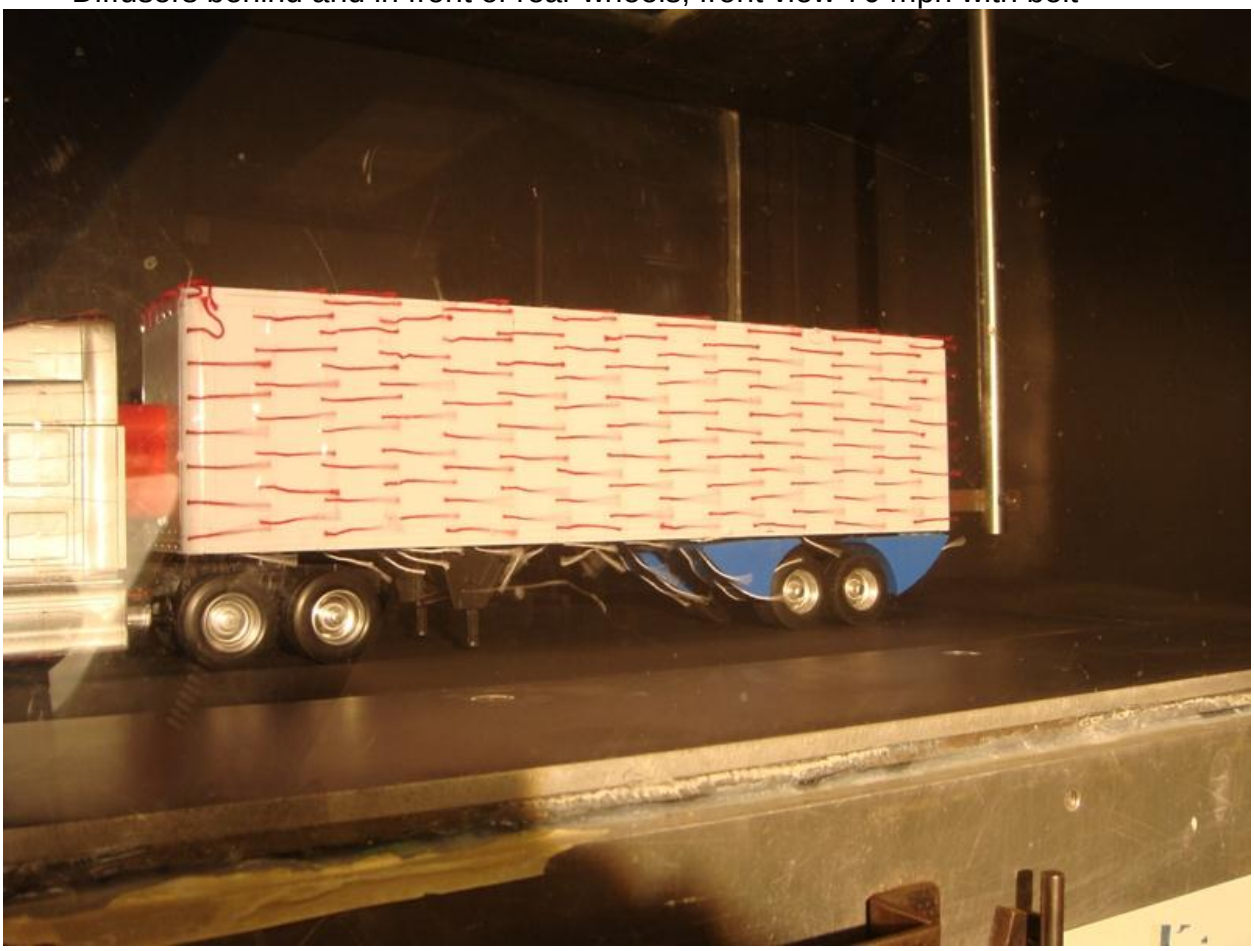

Diffusers behind and in front of rear wheels, front view 70 mph

Diffusers behind and in front of rear wheels, and lofted arch side skirt, rear view
55 MPH

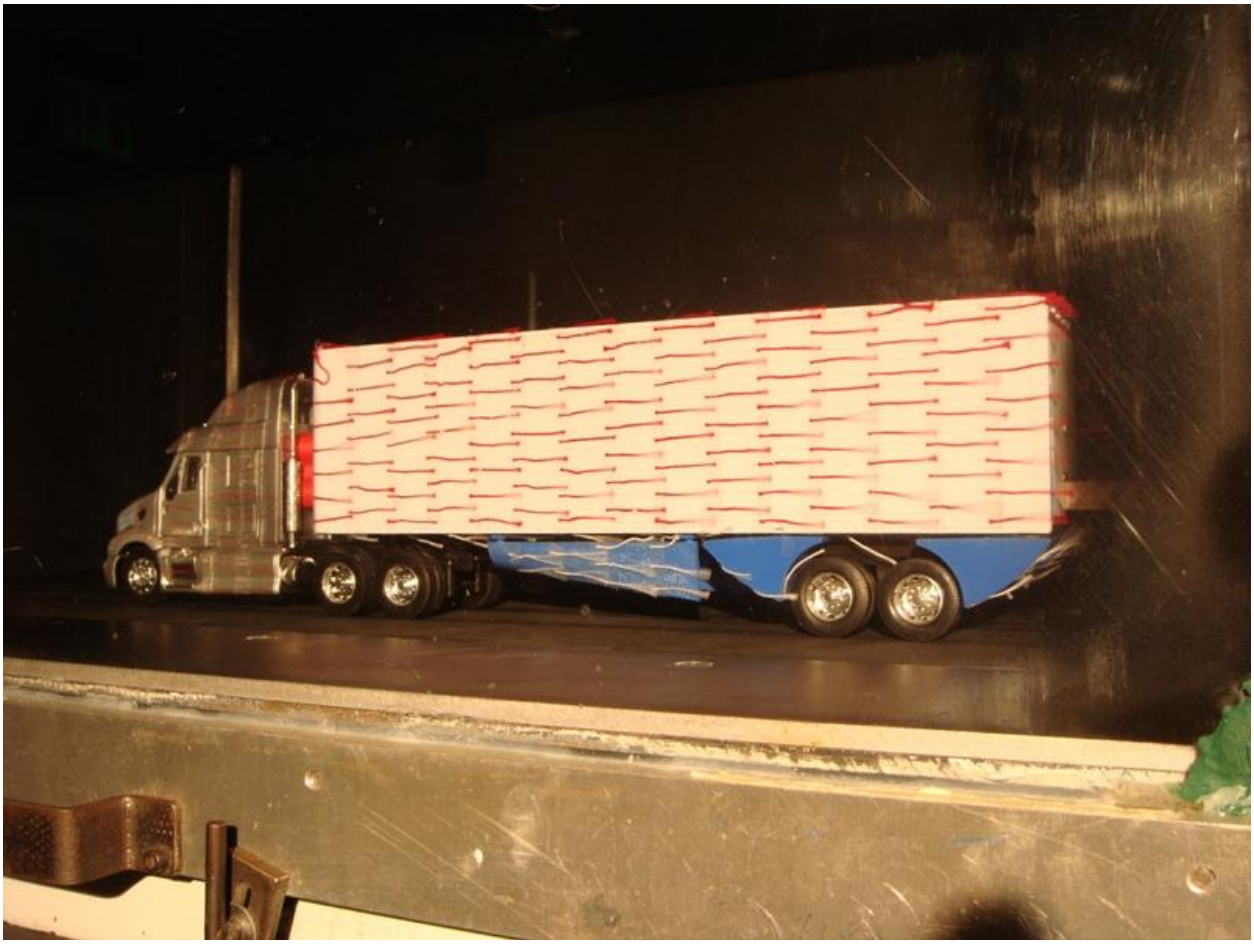

Diffusers behind and in front of rear wheels, and lofted arch side skirt, rear view
65 MPH

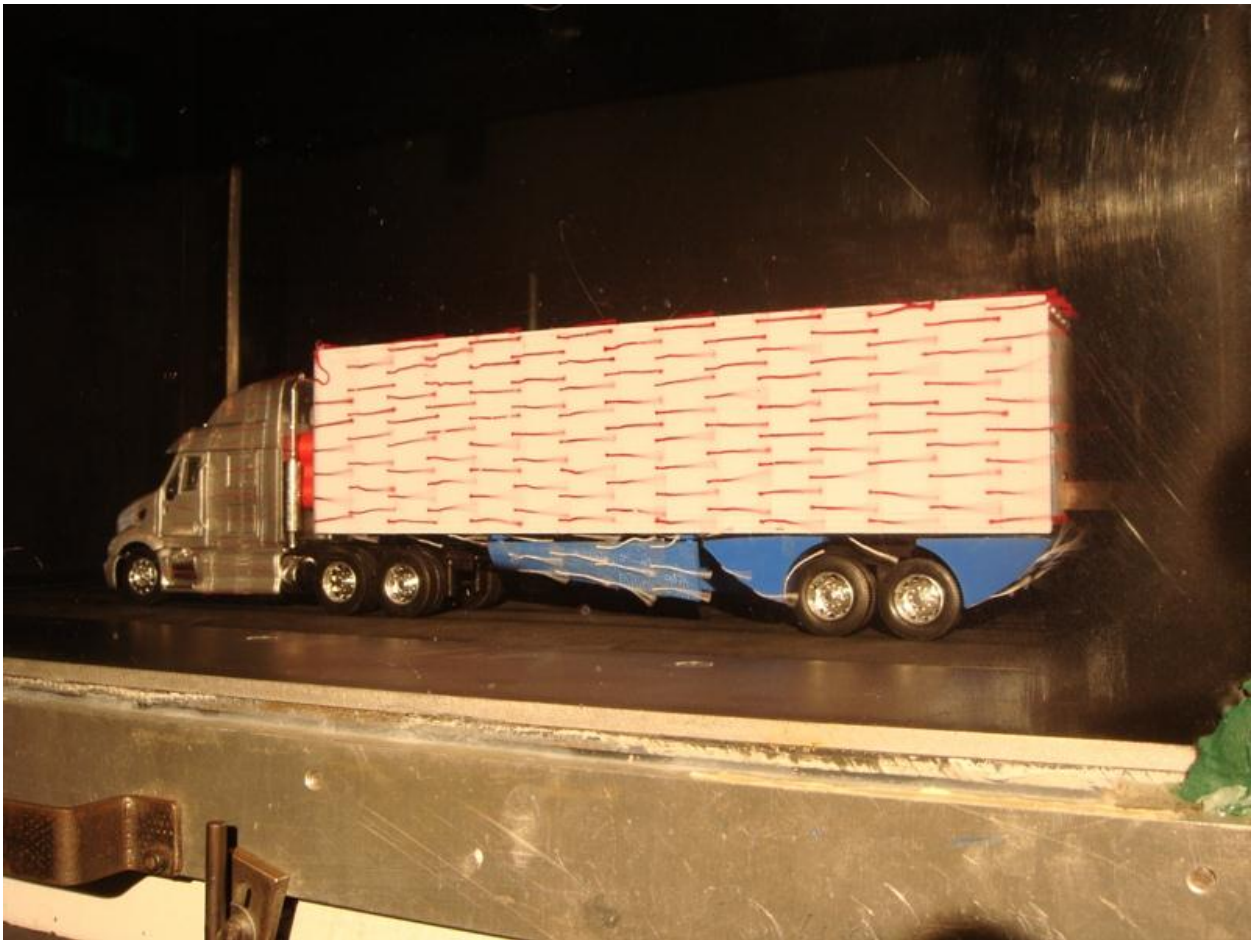

Diffusers behind and in front of rear wheels, and lofted arch side skirt, rear view
70 MPH

Diffusers behind and in front of rear wheels, and lofted arch side skirt, front view
70 MPH

Diffusers behind and in front of rear wheels, and lofted arch side skirt, rear view
70 MPH with belt

Diffusers behind and in front of rear wheels, and lofted arch side skirt, rear view
70 MPH with belt

Mudflap, mid angle 55 mph

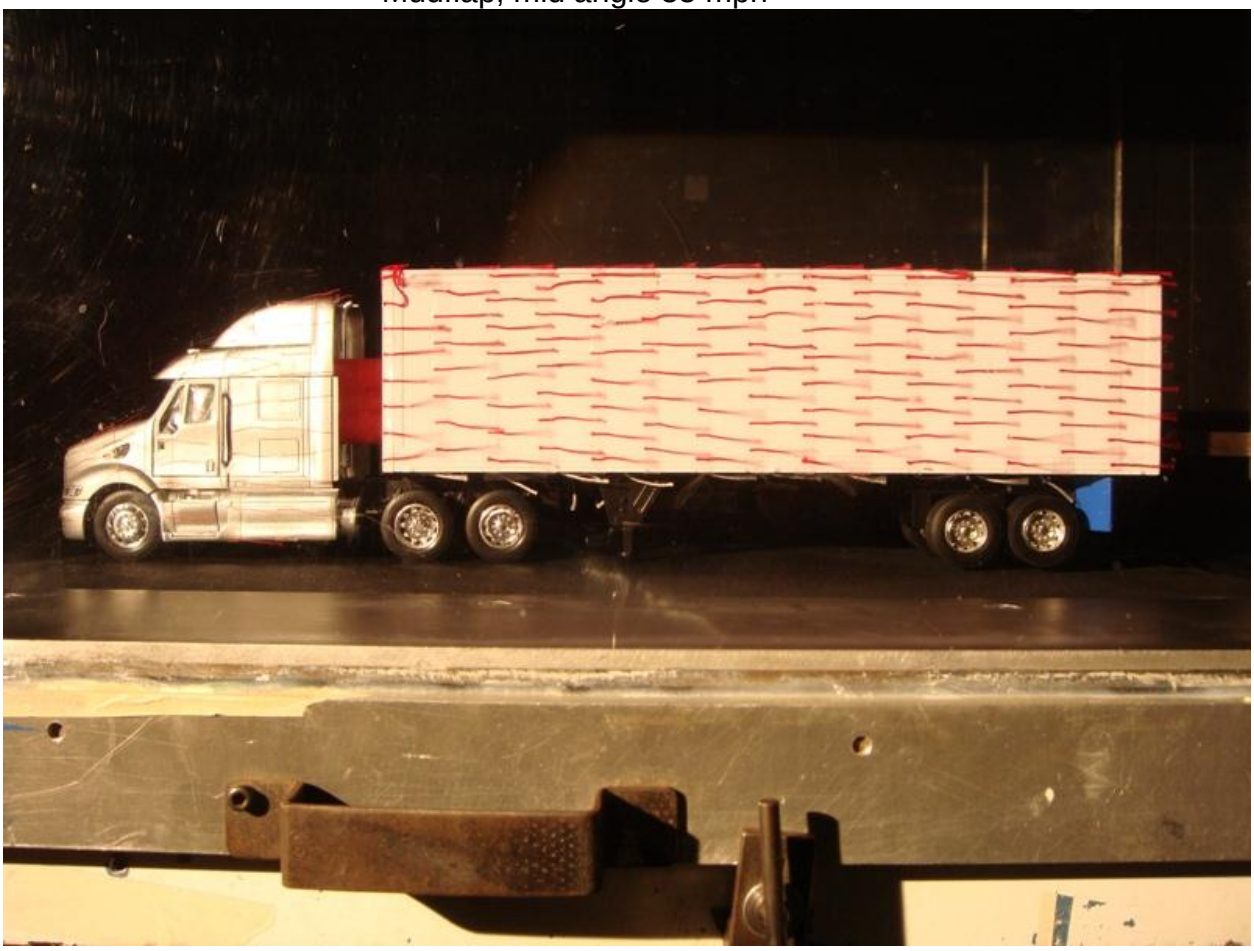

Mudflap, mid angle 65 mph

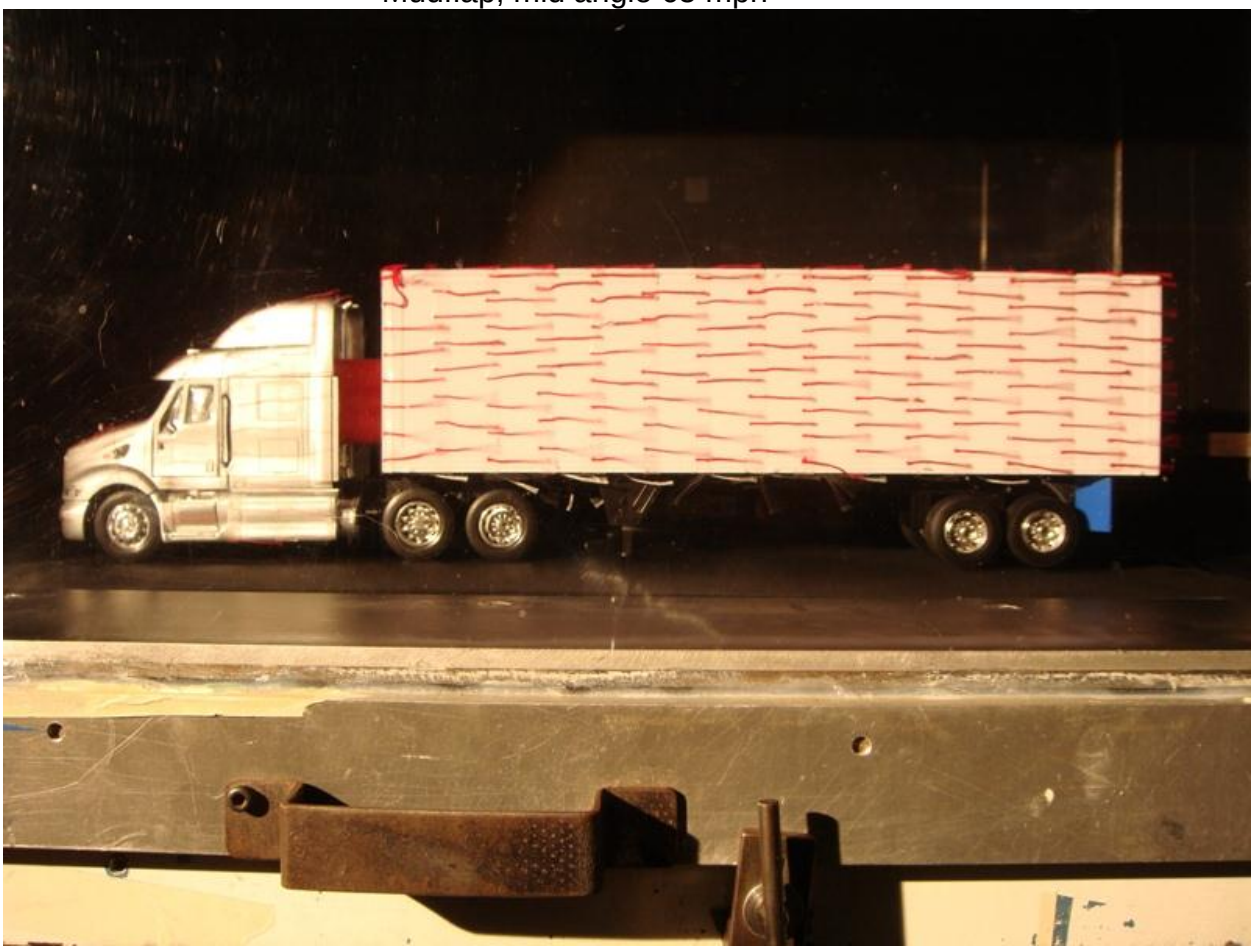

Mudflap, mid angle 70 mph

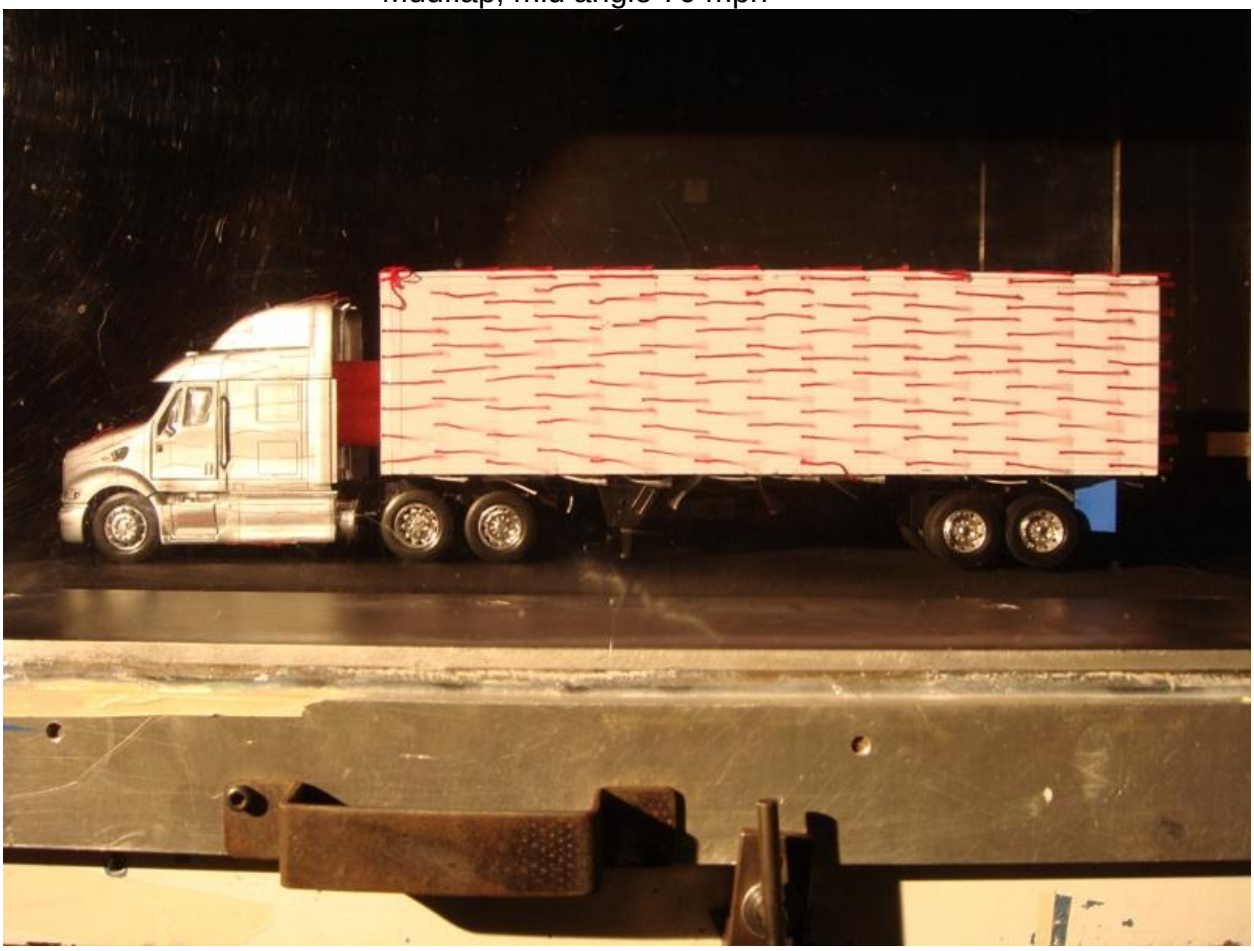

Mudflap, full angle 55 mph

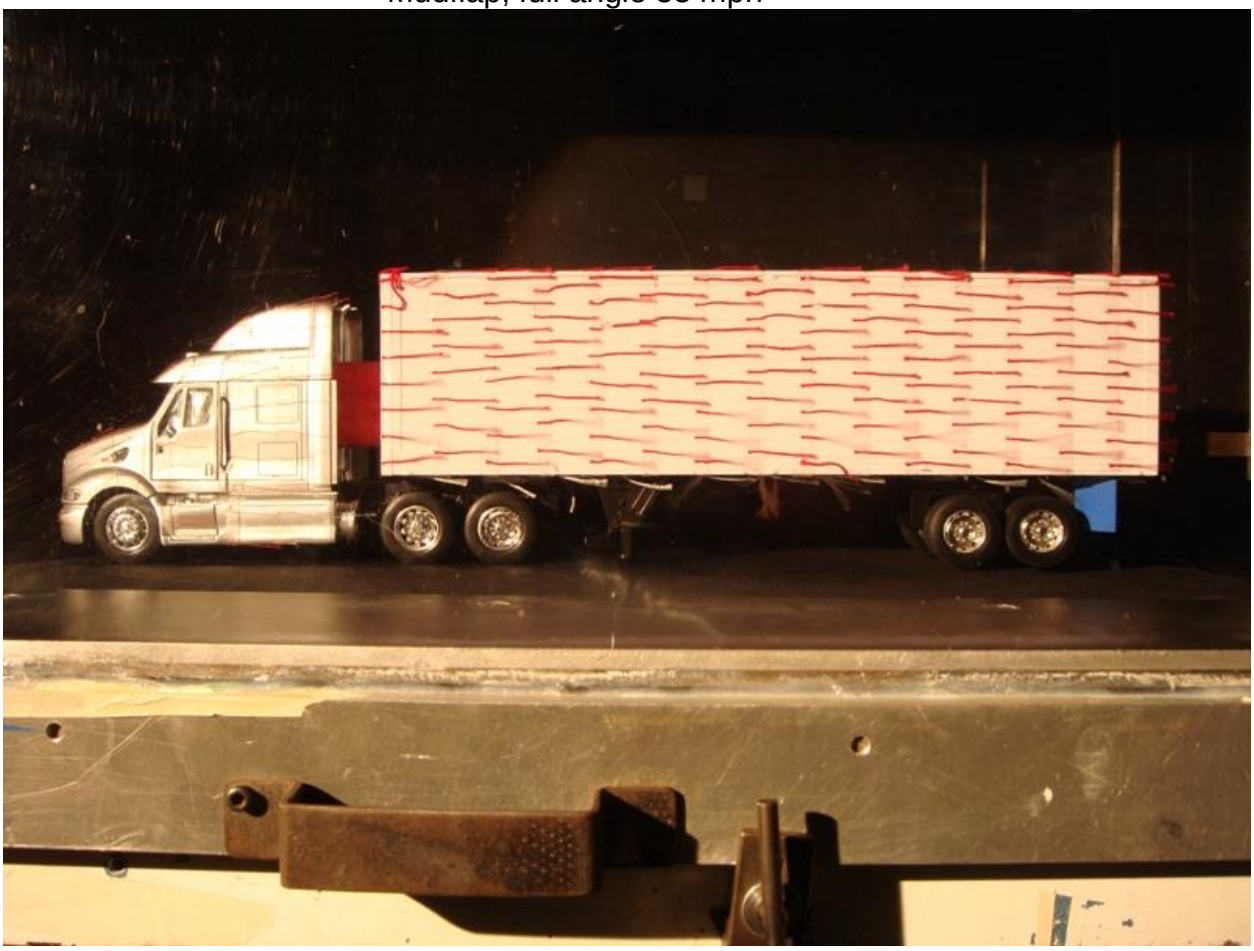

Mudflap, full angle 65 mph

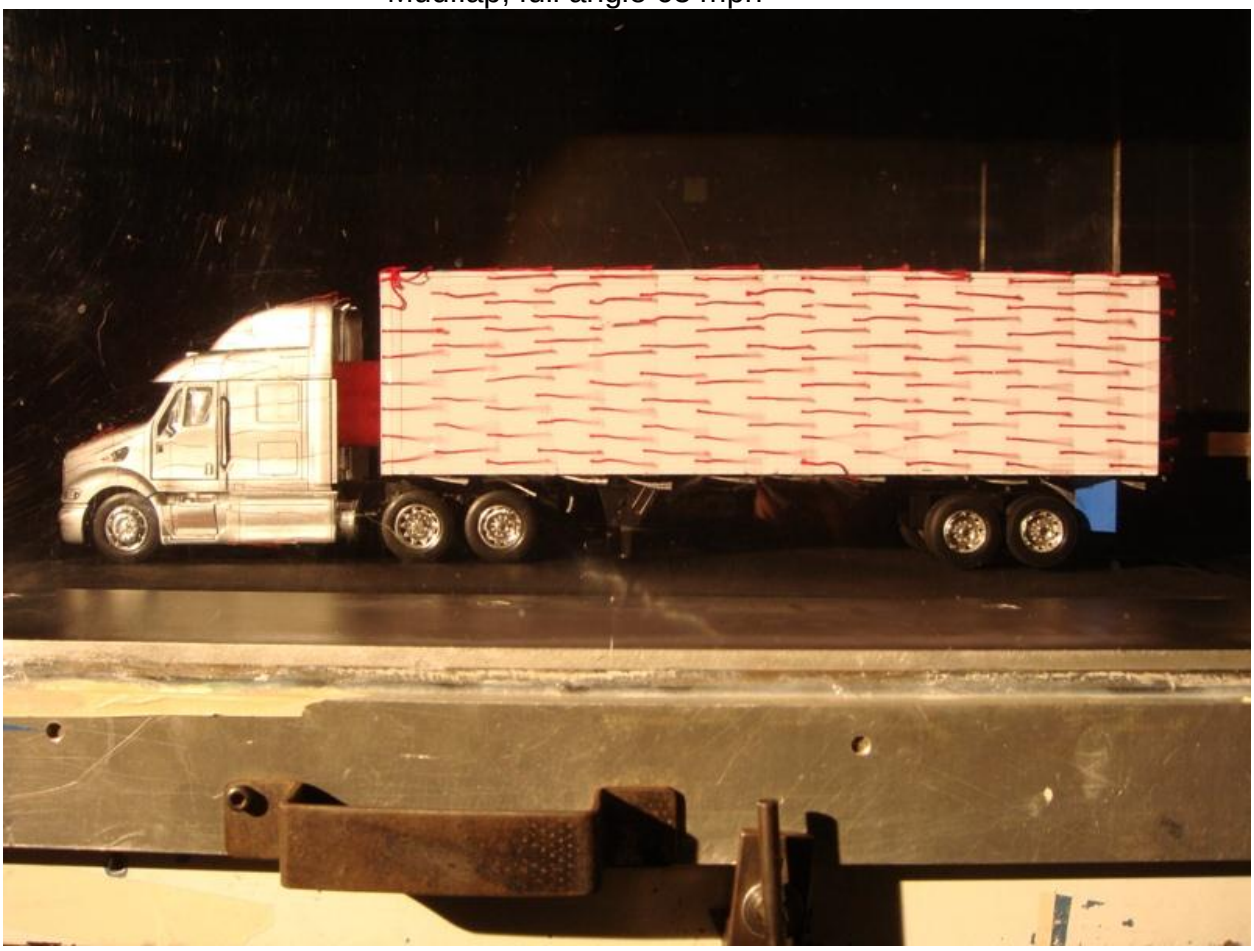

Mudflap, full angle 70 mph

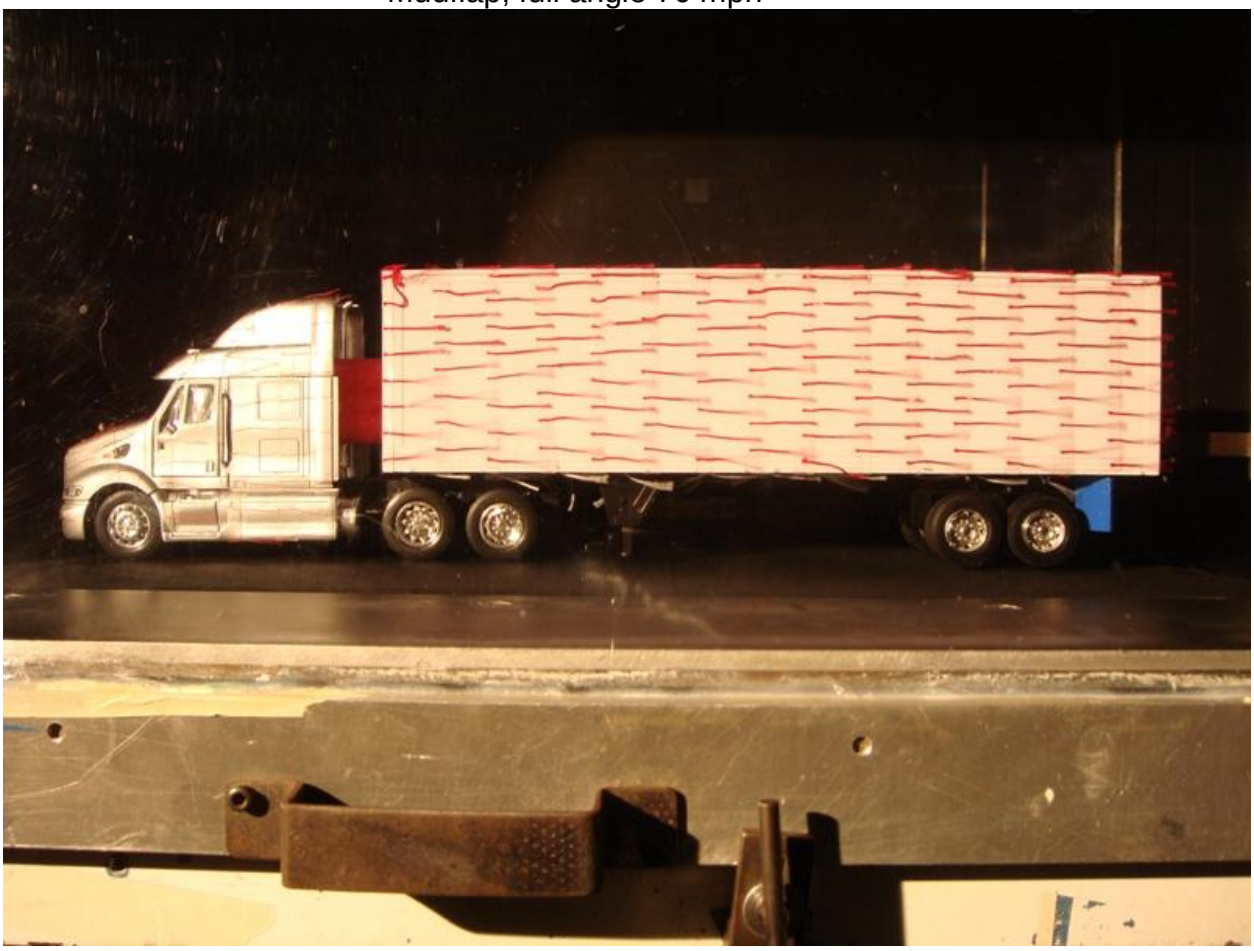

Vita

Nicolas Reed was born in Saginaw, Michigan. After graduating from Caro High School, Caro, Michigan, in 2000, he began pursuing an undergraduate degree at Michigan Technological University in Hougton, MI. He received a Bachelor of Science degree in Mechanical Engineering from Michigan Technological University in May 2004. Starting 2005, he was employed as a systems engineer with Aerospace Testing Alliance at Arnold Engineering Development Complex, a position he holds to this day. In June, 2006, he entered the Graduate School at The University of Tennessee Space Institute.

This thesis was typed by the author.